JAERI 1323

JAERI 1323

Improvements on Burnup Chain Model and Group Cross Section Library in the SRAC System

January 1992

日 本 原 子 力 研 究 所

Japan Atomic Energy Research Institute

JAERI レポートは，日本原子力研究所が研究成果編集委員会の審査を経て不定期に公刊している研究報告書です。

入手の問合わせは，日本原子力研究所技術情報部情報資料課（〒319－11 茨城県那珂郡東海村）あて，お申しこしください。なお，このほかに財団法人原子力弘済会資料センター（〒319－11 茨城県那珂郡東海村日本原子力研究所内）で複写による実費頒布をおこなっております。

JAERI reports are reviewed by the Board of Editors and issued irregularly.

Inquiries about availability of the reports should be addressed to Information Division Department of Technical Information, Japan Atomic Energy Research Institute, Tokai-mura, Naka-gun, Ibaraki-ken 319－11, Japan.

編集兼発行　日本原子力研究所
印　　刷　日立高速印刷㈱

Improvements on Burnup Chain Model and Group Cross Section Library in the SRAC System

Hiroshi AKIE, Keisuke OKUMURA, Hideki TAKANO,
Yukio ISHIGURO and Kunio KANEKO*

Department of Reactor Engineering
Tokai Research Establishment
Japan Atomic Energy Research Institute
Tokai-mura, Naka-gun, Ibaraki-ken 319-11, Japan

(Received April 15, 1991)

Abstract

Data and functions of the cell burnup calculation of the SRAC system were revised to improve mainly the accuracy of the burnup calculation of high conversion light water reactors (HCLWRs). New burnup chain models were developed in order to treat fission products (FPs) and actinide nuclides in detail. Group cross section library, SRACLIB-JENDL2, was generated based on JENDL-2 nuclear data file. In generating this library, emphasis was placed on FPs and actinides. Also revised were the data such as the average energy release per fission for various actinides. These improved data were verified by performing the burnup analysis of PWR spent fuels. Some new functions were added to the SRAC system for the convenience to yield macroscopic cross sections used in the core burnup process.

Keywords: SRAC System, Burnup Calculation, Fission Product, Actinide, High Conversion Light Water Reactor, Burnup Chain Model, Group Cross Section Library, JENDL-2

* The Japan Research Institute, Ltd.

SRACシステムの燃焼チェーンモデルと群定数ライブラリの改良

日本原子力研究所東海研究所原子炉工学部

秋江拓志・奥村啓介・高野秀機・石黒幸雄・金子邦男*

(1991年4月15日受理)

要　　旨

高転換軽水炉(HCLWR)の燃焼解析の精度向上を計るため，SRACシステムの格子燃焼計算に用いられるデータの改訂と機能の追加が行われた。核分裂生成核種(FP)とアクチナイド核種の燃焼を精度よく扱うために，新しい燃焼チェーンモデルが開発された。JENDL-2に基づく群定数ライブラリSRACLIB-JENDL 2が，FPとアクチナイド核種に重点をおいて作成された。核分裂当りの放出エネルギー等のデータも修正された。これら新しいデータの精度がPWR使用済み燃料の燃焼解析により検討された。さらに，炉心燃焼計算に用いられる巨視的断面積の作成の便のために，新たな機能がSRACの格子燃焼計算に追加された。

＊　株式会社日本総合研究所

Contents

1. Introduction ····· 1
2. Calculation Method and Cell Model ····· 3
2.1 Burnup Calculation in the SRAC System ····· 3
2.2 HCLWR Cell Model ····· 4
3. Chain Model and Data for Burnup Calculation ····· 6
3.1 Chain Model of Fission Product Nuclides ····· 6
3.1.1 Improved Model with 65 Explicit Nuclides ····· 6
3.1.2 Simple FP Chain Model ····· 7
3.2 Chain Model of Actinide Nuclides ····· 8
3.3 Revised Data for Burnup Calculation ····· 8
3.3.1 Fission Energies ····· 8
3.3.2 FP Yield Data ····· 9
3.3.3 Branching Ratio of Am–242 β Decay ····· 9
4. Production of Group Cross Section Library SRACLIB–JENDL2 ····· 28
4.1 Production of Group Cross Section Library ····· 28
4.2 Nuclear Data Uncertainties of FPs and Minor Actinides ····· 29
4.3 Self Shielding Effect of FPs ····· 30
4.4 Resonance Interference Effect Between FPs and Actinides ····· 30
5. Burnup Analysis of PWR Spent Fuel ····· 43
6. New Functions of the Burnup Calculation ····· 55
6.1 Fission Gas Release ····· 55
6.2 Constant Flux Burnup ····· 55
6.3 Cell Parameter Change during Burnup ····· 56
7. Conclusion ····· 59
Acknowledgements ····· 59
References ····· 60
Appendix I Input Instructions for SRAC Cell Burnup Calculation ····· 62
Appendix II Chain Model and Data Library ····· 64
Appendix III Table of Isotopes Contained in SRACLIB–JENDL2 ····· 67

目　　次

1. まえがき …… 1
2. 計算法と格子モデル …… 3
2.1 SRAC システムにおける燃焼計算 …… 3
2.2 HCLWR 格子モデル …… 4
3. 燃焼計算のためのチェーンモデルとデータ …… 6
3.1 核分裂生成核種のチェーンモデル …… 6
3.1.1 65 核種を扱う新モデル …… 6
3.1.2 簡便 FP チェーンモデル …… 7
3.2 アクチナイド核種のチェーンモデル …… 8
3.3 燃焼データの改訂 …… 8
3.3.1 核分裂当りの発生エネルギー …… 8
3.3.2 FP 生成率データ …… 9
3.3.3 Am-242 の β 崩壊の分岐比 …… 9
4. 群定数ライブラリ SRACLIB-JENDL 2 の作成 …… 28
4.1 群定数ライブラリの作成 …… 28
4.2 FP 核種及びマイナーアクチナイド核種の核データの不確かさ …… 29
4.3 FP 核種の自己遮蔽効果 …… 30
4.4 FP 核種とアクチナイド核種の共鳴相互干渉効果 …… 30
5. PWR 使用済み燃料の燃焼解析 …… 43
6. 燃焼計算に追加された新機能 …… 55
6.1 FP ガス放出 …… 55
6.2 中性子束レベル一定燃焼 …… 55
6.3 燃焼期間中の格子パラメータ変化 …… 56
7. まとめ …… 59
謝　辞 …… 59
参考文献 …… 60
付録 I　SRAC 格子燃焼計算の入力 …… 62
付録 II　燃焼チェーンデータ …… 64
付録 III　SRACLIB-JENDL 2 に含まれる核種の表 …… 67

List of Tables

Table 1 Specifications of fuel cell model
Table 2 Contribution of nuclides to burnup reactivity loss[6)]
Table 3 FP yield in % per fission from major actinides
(Cumulative yield from precursor FPs of the same mass number, total=200%)
Table 4 Fission energies of major actinides
Table 5 Comparison of thermal capture cross sections and capture resonance integrals (barns)

List of Figures

Fig. 1 HCLWR cell model.

Fig. 2 Contribution of nuclides to the burnup reactivity change of the HCLWR of Vm/Vf=1.1.

Fig. 3 Fission product (FP) burnup chain model by Iijima et al.

Fig. 4 Fractional absorption rates of FPs at 50GWd/t (Vm/Vf=0.6).

Fig. 5 Capture cross sections of the pseudo nuclides in Iijima's chain.

Fig. 6 Burnup reactivity changes of the cell of Vm/Vf=0.6 calculated by Iijima's chain with different pseudo cross sections.

Fig. 7 Pseudo cross sections for Iijima's chain (45FP) and the chain by Takano et al. (65 FP).

Fig. 8 Burnup chain model for FPs by Takano et al. with 65 explicit and 1 pseudo nuclide.

Fig. 9 Capture cross sections of pseudo FPs in Takano's chain.

Fig. 10 Burnup reactivity changes by Takano's chain with different cross sections of pseudo FP (Vm/Vf=0.6).

Fig. 11 Absorption fractions of FPs at each burnup in the conventional PWR.

Fig. 12 Absorption fractions of FPs at each burnup in the MOX fueled PWR.

Fig. 13 Absorption fractions of FPs at each burnup in the HCLWR of Vm/Vf=1.1.

Fig. 14 Simple FP chain model for design calculations (R56, R86, R96, and R16 denote pseudo FP nuclides created by the fission reactions of U-235, U-238, Pu-239 and Pu-241, respectively).

Fig. 15 Burnup dependence of infinite multiplication factor (k_∞) and conversion ratio (CR) for the cell of Vm/Vf=0.6 by Takano's and the simplified FP chains.

Fig. 16 Burnup dependence of infinite multiplication factor (k_∞) and conversion ratio (CR) for the cell of Vm/Vf=2.0 by Takano's and the simplified FP chains.

Fig. 17 Void reactivity changes at 50GWd/t by Takano's and the simplified chain for the cell of Vm/Vf=0.6.

Fig. 18 Void reactivity changes at 50GWd/t by Takano's and the simplified chain for the cell of Vm/Vf=2.0.

Fig. 19 Actinide burnup chain model in the original SRAC system.

Fig. 20 Burnup reactivity changes in the cell of Vm/Vf=1.1 and the effect of higher actinides.

Fig. 21 Actinide chain model for HCLWR burnup calculation.

Fig. 22 Actinide chain for burnup of TRU nuclides and Th based fuel.

Fig. 23 Burnup reactivity changes by different fission energies (Vm/Vf=1.1).

Fig. 24 Absorption fraction of FPs at 50GWd/t by new and original FP yield data (Vm/Vf=1.1).

Fig. 25 Burnup dependence of Ag-109 number density calculated by new and original FP yield for the cell of Vm/Vf=1.1.

Fig. 26 Pu-242 number densities calculated with and without Am-242 EC chain (Vm/Vf=1.1, 7% fissile Pu).

Fig. 27 Capture cross sections of Xe-131 in the thermal energy range calculated with original and new SRACTLIB code ('point cross section' denotes energy pointwise cross section).

Fig. 28 Comparison of capture cross sections of Ru-103 among the four nuclear data files.

Fig. 29 Comparison of capture cross sections of Eu-155 among the four nuclear data files.
Fig. 30 Comparison of (a) capture and (b) fission cross sections of Am-243 among the nuclear data files.
Fig. 31 Contribution of individual nuclides to total absorption at the burnup state of 50 GWd/t.
Fig. 32 Burnup dependence of the ratios of the multiplication factors calculated with the other files compared to those with JENDL-2.
Fig. 33 Comparison of fractional absorptions for minor actinides at burnup state of 50 GWd/t.
Fig. 34 Contributions of fission products to the total absorption rate with and without self shielding effect (Vm/Vf=0.74, 50GWd/t).
Fig. 35 Comparison of inifinite dilute and shielded group cross sections of Xe-131 for the cell of Vm/Vf=0.74 at 50GWd/t.
Fig. 36 Comparison of inifinite dilute and shielded group cross sections of Cs-133 for the cell of Vm/Vf=0.74 at 50GWd/t.
Fig. 37 The effect of resonance shielding for fission products on the multiplication factors.
Fig. 38 Comparison of resonance capture cross sections for U-238 and Sm-150.
Fig. 39 Neutron flux calculated with PEACO at the burnup state of 50GWd/t.
Fig. 40 Capture reaction rate of Sm-150 calculated with the ultra fine group method at 50GWd/t in the 17.6 to 22.6eV energy group.
Fig. 41 Comparison of resonance capture cross sections for U-238 and Ag-109.
Fig. 42 Capture cross section of Ag-109 and neutron spectrum calculated by the ultra fine group method.
Fig. 43 Infinite dilute cross section and effective cross section weighted by the ultra fine group neutron spectrum for Ag-109.
Fig. 44 Fractional absorption rate of FPs calculated with the table-look-up method and ultra fine group method (PEACO) for the cell of Vm/Vf=0.74 at 50GWd/t.
Fig. 45-1 Fractions of U-234 to initial uranium atoms in the PWR spent fuels (Calculation /Experiment (C/E) values).
Fig. 45-2 Fractions of U-235 to initial uranium atoms in the PWR spent fuels (C/E values).
Fig. 45-3 Fractions of U-236 to initial uranium atoms in the PWR spent fuels (C/E values).
Fig. 45-4 Fractions of U-238 to initial uranium atoms in the PWR spent fuels (C/E values).
Fig. 45-5 Fractions of Pu-238 to initial uranium atoms in the PWR spent fuels (C/E values).
Fig. 45-6 Fractions of Pu-239 to initial uranium atoms in the PWR spent fuels (C/E values).
Fig. 45-7 Fractions of Pu-240 to initial uranium atoms in the PWR spent fuels (C/E values).
Fig. 45-8 Fractions of Pu-241 to initial uranium atoms in the PWR spent fuels (C/E values).
Fig. 45-9 Fractions of Pu-242 to initial uranium atoms in the PWR spent fuels (C/E values).
Fig. 45-10 Fractions of Pu to initial uranium atoms in the PWR spent fuels (C/E values).
Fig. 46-1 Weight ratios of Np-237/initial uranium in the PWR spent fuels (C/E values).
Fig. 46-2 Weight ratios of Am-241/initial uranium in the PWR spent fuels (C/E values).
Fig. 46-3 Weight ratios of Am-242m/initial uranium in the PWR spent fuels (C/E values).
Fig. 46-4 Weight ratios of Am-243/initial uranium in the PWR spent fuels (C/E values).
Fig. 46-5 Weight ratios of Cm-242/initial uranium in the PWR spent fuels(C/E values).
Fig. 46-6 Weight ratios of Cm-244/initial uranium in the PWR spent fuels (C/E values).
Fig. 47-1 Cs-134 atoms/initial uranium in the spent fuels of PWR (C/E values).
Fig. 47-2 Nd-143 atoms/initial uranium in the spent fuels of PWR (C/E values).
Fig. 47-3 Nd-145 atoms/initial uranium in the spent fuels of PWR (C/E values).

Fig. 47-4 Nd-148 atoms/initial uranium in the spent fuels of PWR (C/E values).
Fig. 47-5 Eu-154 atoms/initial uranium in the spent fuels of PWR (C/E values).
Fig. 48 Difference of effective multiplication factors (k_{eff}s) with and without fission gas release effect.
Fig. 49 Production of Pu isotopes in the blanket cell calculated with fixed power and fixed flux conditions (Vm/Vf=1.1). For the fixed flux cases, linear heat rating is an initial value.

1. Introduction

The high conversion light water reactor (HCLWR) concept has received considerable attention over several years because of its potential for beter fuel utilization relative to current LWRs. In comparison with current LWRs, HCLWRs with tighter pitch lattice have the two design features of (i) reduced volume ratio of water to fuel (Vm/Vf) and (ii) higher plutonium enrichment. These features bring the following neutronics characteristics of HCLWRs:

- The neutron spectrum in the core is intermediate between conventional LWRs and FBRs. Hence, HCLWRs are peculiar in the sense that the intermediate energy range is very important; more than 40% of the fission reactions and 70% of the capture reactions take place at the resonance energy region ($1eV \leqq E \leqq 10keV$). When the studies of HCLWRs started, neutronic designs were performed mainly on the basis of cell codes which have been developed for calculation of thermal reactors. In those days, most of these codes could not accurately treat resonance self and mutual shielding.
- The reactivity loss by burnup is much less than current LWRs because of higher conversion ratio. For this reason, higher accuracy is needed in the burnup calculation of HCLWRs than in current LWRs for the prediction of discharged burnup, cycle duration, etc.
- The burnup reactivity loss in HCLWRs is dominated by fission product (FP) accumulation. The order of relative importance of each FP nuclide in HCLWRs is considerably different from one in conventional LWRs. Additionally, higher burnup rate for plutonium fuel results in higher production rate of minor actinide nuclides*, such as americium and curium. These FPs and minor actinides do not always need to be treated in detail in burnup calculation of conventional LWRs. The contribution of various isotopes related to the reactivity loss should be accurately evaluated in the burnup calculation of HCLWRs.

The concept of HCLWRs has been investigated at Japan Atomic Energy Research Institute (JAERI) since 1984. The code system SRAC[1] has been mainly used in the neutronics calculations in this investigation. The SRAC system has been originally developed for calculation of thermal reactors. Because of its precise resonance calculation method, the SRAC system has advantageous features to be applied to HCLWRs[2], where the various reactions in the resonance energy range are dominant. However, some improvements were still needed particularly in the burnup calculation, because the accuracy of burnup calculation in HCLWRs was identified as a much more important problem than in current LWRs for the reasons above mentioned.

A brief description is first made of the SRAC burnup calculation method in Chapter 2, and also of the HCLWR cell model that is used in the burnup calculations in this report.

In order to accurately treat FPs and actinides in burnup calculation, improvements have been made for burnup chain model, which describes generation, transmutation and disintegration of nuclides during burnup. The burnup chain models of FPs and actinides initially used in the burnup calculation of HCLWRs were those which had been prepared for burnup of thermal reactors. A new detailed FP chain model (Takano's model) has been developed that contains 65 explicit nuclides and one pseudo FP. Furthermore, the actinide chain model has been improved so as to include minor actinides, such as Am-241, Am-243, Cm-244, etc.

A simplified FP chain model has been also proposed for design calculations, because a number of data I/O for cross sections are necessary in the calculation with the detailed chain model. The simple model uses 10 explicit FPs and 4 pseudo nuclides. The accuracy of the model was investigated by

*: In this report, 'minor actinides' is used for the isotopes of americium, curium and neptunium.

comparing with Takano's chain model.

Such data as FP yield per fission, fission energies, etc. have been revised. These revised data, together with the new chain data for FPs and actinides, have been compiled into a file for burnup (burnup library) in the SRAC system. The revision of the chain models and the burnup data are described in Chapter 3.

New group cross sections were needed for the burnup calculation of minor actinides and FPs. In the original SRAC data libraries, SRACLIB–ENDFB4 and SRACLIB–JENDL1/2, all the necessary cross section data for FPs and minor actinides are not contained. Thus, group cross sections were produced for these nuclides based on JENDL–2 and ENDF/B–V nuclear data files, and the new group cross section libraries SRACLIB–JENDL2 and SRACLIB–ENDFB5 were generated. The SRAC system has been equipped with these new libraries. Chapter 4 describes the production of the group cross section libraries.

The validity of the chain models and data library are studied on burnup characteristics of typical HCLWR cells in Chapters 3 and 4, and also on a burnup analysis of spent fuels of PWR in Chapter 5.

Beside the improvements in the data, some new functions, such as the burnup calculation model under constant flux, have been added in the burnup routine of the SRAC system. They are described in Chapter 6.

2. Calculation Method and Cell Model

In the SRAC cell calculations, microscopic effective cross sections of each component nuclide are usually obtained by the table-look-up method based on the NR approximation. The effective cross sections thus obtained are used for calculating the cell neutron spectrum of mutigroup structure by the collision probability method. This spectrum is then used to obtain the effective one group microscopic cross sections for a burnup calculation.

In the energy range from the thermal-cut-off energy (it can be selected from the energy group boundaries between 0.414eV and 3.93eV) to 130.1eV, the precise resonance calculation method, PEACO routine[3], can be used, which numerically calculates neutron spectrum in various types of heterogeneous cells on a hyperfine group structure based on the collision probability method. In this case, the effective few group cross sections in this energy region are replaced by those obtained by the PEACO calculations.

Because of the importance of the resonance treatment in HCLWRs, the PEACO method is always used in the cell calculations in this report. Here, the thermal-cut-off energy is selected as 3.93eV.

2.1 Burnup Calculation in the SRAC System

The SRAC system installs a burnup routine which solves the following differential equation expressing the chain relationship of nuclides by nuclear reactions:

$$\frac{dN_n(t)}{dt} = -A_n(t)N_n(t) + Y_n(t) + \sum_j G_{j,n-1\to n}(t)N_{n-1}(t) ,$$

where

$N_n(t)$: concentration of nuclide n at some location at time t,
$A_n(t)$: specific loss rate of nuclide n at time t,
$Y_n(t)$: direct yield rate from fission to nuclide n,
$G_{j,n-1\to n}(t)$: specific generation rate from precursor nuclide $n-1$ to n along chain j.

The one group microscopic cross sections obtained in the SRAC cell calculation are used to calculate the coefficients A_n, Y_n and $G_{j,n-1\to n}$. This equation is usually solved by the numerical method, such as the Runge-Kutta method. In the SRAC system, the solution of analytical integration is used for this equation. This is the method adopted in the CITATION code[4] to avoid accumulation of numerical error that might occur in the numerical calculations. In the analytical solution, the coefficients A_n, Y_n and $G_{j,n-1\to n}$ are assumed to be constant neglecting the time dependence of one group microscopic cross sections and neutron flux. The one group microscopic cross sections actually change with the change of atomic number densities. Hence, in the burnup calculation of the SRAC system, the burnup period under consideration must be divided into several burnup steps (up to 15 steps) to update the one group microscopic cross sections. The number of burnup steps and the periods of each burnup step are specified by user as shown in Appendix I. Furthermore, a burnup calculation is usually made under the assumption of fixed power. This means that neutron flux is time dependent. In the SRAC burnup routine, a burnup step is automatically divided into several sub-steps so as to be able to assume a time-independent neutron flux during each sub-step.

The SRAC burnup routine is called at each burnup step after a cell calculation. The burnup routine calculates the change of nuclide densities during a burnup step under a given power level. The new densities are returned to the cell calculation routine for the next burnup step. This process is called "cell burnup". The core burnup process using the COREBN code[1], where there are spatial distributions of

neutron flux, power density, fuel burnup rate, etc., utilizes the tabulated sets of the macroscopic cross sections prepared beforehand by the cell burnup calculations. For the core burnup process, hence, the cell burnup calculations should be performed for possible range of burnup, material temperatures and various fuel compositions. All the necessary data for many daughter nuclides and their chains are stored in the burnup library (Appendix Ⅱ), so that the input data for the cell burnup calculation are minimized as seen in Appendix Ⅰ.

2.2 HCLWR Cell Model

A series of burnup calculations have been made on an HCLWR cell model for the study of HCLWR burnup characteristics. As shown in Fig.1, the model is a hexagonal pin cell with fuel, cladding and moderator. The moderator/fuel volume ratio (Vm/Vf) ranges from 0.6 to 2.0. The specifications of the cells are shown in Table 1. The cells of the Vm/Vf=0.6, 1.1, 1.4 and 2.0 are the same as the ones in the NEACRP HCLWR cell burnup benchmarks[5]. The case of Vm/Vf=0.74 is one of the cell models used in the HCLWR design studies at JAERI.

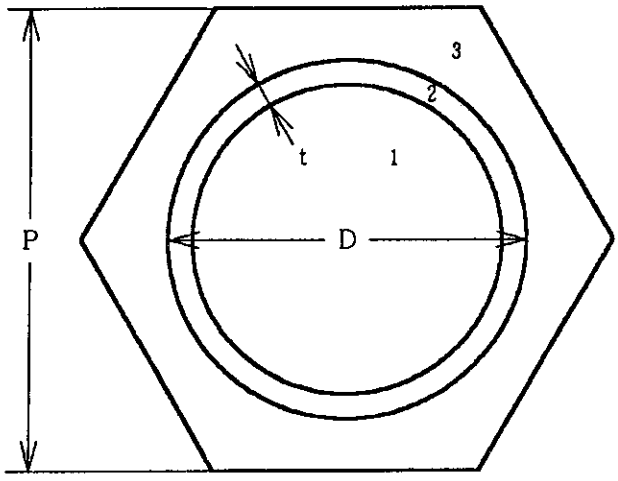

1. PuO_2 + UO_2
2. Stainless steel or Zr
3. H_2O

Fig. 1 HCLWR cell model.

Table1 Specifications of fuel cell model

Moderator/fuel volume ratio (Vm/Vf)	0.6	0.74	1.1	1.4	2.0
Cell pitch P(cm)	1.088	1.149	1.220	1.293	1.428
Fuel(PuO_2+depleted UO_2)					
Pu fis. (%)	8.0	8.0	7.0	7.0	4.0
Temperature (K)	900	900	900	900	900
Cladding	SS★	SS	Zr	Zr	Zr
Outer diameter D (cm)	0.95	0.95	0.95	0.95	0.95
Thickness t (cm)	0.065	0.04	0.065	0.065	0.065
Temperature (K)	600	600	600	600	600
Moderator (H_2O)					
Temperature (K)	600	600	600	600	600
Linear heat rate (W/cm)	160	180	160	160	160

★: Stainless steel

3. Chain Model and Data for Burnup Calculation

In this chapter, the revision of the burnup chain model and the burnup data, such as fission energies and FP yield data, are described. The chain description data, the nuclide data such as fission energy and decay constant, and FP yield data are compiled together in a file(Appendix Ⅱ). This file is called the burnup library in the SRAC system.

3.1 Chain Model of Fission Product Nuclides

3.3.1 Improved Model with 65 Explicit Nuclides

In HCLWRs, about 60% of burnup reactivity loss is caused by the accumulation of FPs, as described in Fig.2 and Table 2[6]. So the treatment of FP nuclides is one of the most important problems in the burnup calculation of HCLWRs. There have been several FP burnup chain models prepared in the SRAC system. On the basis of Garrison and Roos model[7], SRAC has the simplest one which treats Xe-135, Sm-149 and 3 lumped FP groups. However, this model is effective only for the cases where the accumulation of FPs is not important, e.g. low burnup rate calculations or burnup calculations of the U-235 high enriched fuels as used in research reactors. An accurate model with 45 explicit nuclides is also available in the SRAC system, which were proposed by Iijima et al. for BWR burnup calculations[8]. The other FPs than 45 explicit nuclides are lumped into one pseudo FP in this chain model. The chain scheme of this model is shown in Fig.3. Based on this Iijima's chain, a new FP chain model suitable for the burnup calculation of HCLWRs was investigated by Takano et al.[9]

In the case where Iijima's chain is used in a burnup calculation of HCLWRs, there are two problems concerned with the pseudo FP. One is that the pseudo FP has large absorption fraction, and the other is that the pseudo FP includes several nuclides with large resonance cross section.

Figure 4 shows the order of importance for fractional absorption rates of individual FP nuclides to total absorption. These absorption rates were calculated for the cell with Vm/Vf=0.6 by using Iijima's chain. It can be seen that the order of the pseudo FP nuclide is very high and the absorption rate becomes 0.75% of total absorption, or nearly 10% of the absorption of all FPs at 50GWd/t. Considering nuclear data uncertainty of the pseudo cross section, it is supposed to considerably affect the burnup characteristics of HCLWRs, because of this large absorption fraction of the pseudo nuclide.

In Fig. 5, the three types of the capture cross sections for the pseudo FP are compared. In this figure, the pseudo cross section used in the original SRAC is denoted by PSD and was generated so as to conserve the resonance integral of 10.6 barns and 2200m/s cross section of 2.60 barns recommended by Iijima et al.[8]. The cross sections denoted by JENDL-2 and ENDF/B-V were produced on the basis of the FP data of JENDL-2 and ENDF/B-V, respectively, based on the burnup calculation of the DCHAIN code[10], which solves the buildup and decay of 1170 nuclides. By this calculation, the concentrations of dominant 155 nuclides were obtained by the DCHAIN code, where the neutron spectrum of a typical HCLWR core calculated with the SRAC system was assumed.

Figure 6 compares the burnup reactivity loss of the cell with Vm/Vf=0.6 calculated by using Iijima's chain with the three different pseudo cross sections. The calculation with the PSD cross section underestimates the reactivity loss by about 0.7%, compared with the result by the JENDL-2 pseudo FP at the burnup of 50GWd/t. It is also observed at the 50GWd/t burnup that there is a difference of 0.3% $\Delta k/k$ between the results by the pseudo cross sections of PSD and ENDF/B-V. It should be also noted that the resonance integral for the ENDF/B-V pseudo cross section is 10.7 barns and is almost equal to that of the PSD cross section.

Figure 7 shows the group cross sections of the pseudo nuclide of Iijima's chain (denoted by '45 FP') calculated from 155 explicit nuclides based on JENDL-2. It can be seen there are several resonances due to FP nuclides such as Zr-93, Mo-95, In-115, etc. in this pseudo cross section. As shown in Table 3, the fission yields for these nuclides depend on the fissile nuclides. It is therefore difficult to define the pseudo FP cross section that is independent on fissile nuclide. Additionally, shielding effect of these resonances is supposed to be strongly dependent on neutron spectrum (i. e. reactor type).

For these reasons, a new FP chain model was proposed that the pseudo cross section has small absorption fraction in the total FP absorption and has little dependence both on fissile nuclide and on neutron spectrum. The new model (Takano's chain) explicitly treats 65 FP nuclides and one pseudo nuclide as shown in Fig. 8. In Fig. 7, the pseudo cross section of Takano's chain is also shown as '65 FP'. The pseudo resonance integral for Takano's model is 4.1 barns. The effect of data discrepancy on the burnup reactivity loss was investigated with the pseudo cross sections of Takano's chain based on the JENDL-2 and ENDF/B-V data (Fig.9). In Fig.10, the burnup reactivity loss is compared for the case of Vm/Vf=0.6. It will be seen that the effect of data discrepancy is very small.

Figures 11~13 show typical results of burnup calculation obtained with Takano's chain. These figures show the burnup dependent absorption fractions of FPs in a conventional PWR (Fig.11), MOX fueled PWR (Fig.12) and the HCLWR of Vm/Vf=1.1 (Fig.13). The importance of individual nuclide in the various reactors can be observed. In all these cores, the absorption fraction of pseudo FP is small. This means that Takano's FP chain can be applied to various types of reactor with small error from the pseudo FP cross section.

3.1.2 Simple FP Chain Model

In the core burnup calculations with the COREBN code, a number of cell burnup calculations are needed for every burnup materials in a core configuration (fuels with different enrichments, blanket, etc.). Detailed chains such as Iijima's or Takano's model require long computational time, large computer memory size and particularly a number of data I/O for cross sections of nuclides in the cell burnup calculations with the SRAC system. These models are not always suitable for such a design calculation with the COREBN code.

A simplified chain model was proposed in 1987 for core design purpose of HCLWRs, based on Takano's 65 nuclide chain and the burnup calculation by the DCHAIN code. The chain model treats explicitly the following 10 nuclides:

(1) Xe-131 and Cs-133; these have large absorption fraction and significant self shielding effect.
(2) Rh-103, Xe-135 and Sm-149; these have large absorption cross section in thermal energy range.
(3) Ru-101, Pd-105 and Sm-151; fractional absorptions of these nuclides strongly depend on Vm/Vf value.
(4) Pm-147; this has large absorption rate, and its atomic number density slowly increases with burnup.
(5) Sm-150; this is needed to construct samarium chain with the explicit isotopes of Sm-149 and Sm-151 above.

As mentioned in Section 3.1.1, the nuclides with the large dependence of the fission yield on fissile nuclides will be included in a pseudo FP. It is therefore better to define fissile dependent pseudo FP cross sections by using individual FP concentration yielded from the fission reactions of U-235, U-238, Pu-239 or Pu -241. Thus, four different pseudo nuclides were generated. The fission yield data for these pseudo FP were adjusted for the burnup and void reactivity changes calculated with Takano's model. Moreover, the fission yield data for Sm-149 were adjusted in the same way because Sm-149 has many precursors as seen in Fig. 8. The chain model is shown in Fig.14.

Figures 15 and 16 show burnup dependence of infinite multiplication factor(k_∞) and conversion ratio for the cells of Vm/Vf=0.6 and 2.0, respectively. Furthermore, moderator void reactivity changes were calculated for the both cells at 50GWd/t (Figs.17 and 18). In these figures, the lines denoted by 'Takano'

show the results by Takano's chain and 'Simple' means the results by the simple chain. These figures show that the results obtained by the simple chain agree very well with those by Takano's chain in the range of Vm/Vf=0.6~2.0. The largest discrepancies in k_∞ is about 0.2% and 0.1%, respectively for the cells with Vm/Vf=0.6 and 2.0, and the discrepancies of 0.15% and 0.2% are found in conversion ratio. The differences of void reactivities for these cells are less than 0.15% and 0.8% Δk/k, respectively.

3.2 Chain Model of Actinide Nuclides

The actinide chain model used in the original SRAC system was a very simple one that treats two chains; one consists of nuclides from Th-232 to U-236 and the other from U-238 to Pu-242 (Fig.19)[1]. But this model is not suitable for the burnup calculation of HCLWR cells, where Pu fuel is burnt up to high burnup stage and a large amount of minor actinide nuclides are produced. In order to examine the effect of these nuclides, isotopes of americium, curium and neptunium were added to the original chain one by one, and the corresponding cell burnup calculations were made for typical HCLWR cells.

Figure 20[11] shows burnup reactivity loss in the cell of Vm/Vf=1.1 calculated by using these chains. In the figure, the model used in the original SRAC system is shown by "without Np, Am and Cm". It is observed that the contributions of Am-241 and Am-243 on the burnup reactivity loss are very large to be about 1% and 1.5% Δk/k, respectively at 50GWd/t. In the measure of burnup, the effect of Am-241 and Am-243 is almost equal to reducing 10GWd/t. Curium-244, another higher isotope than Am-241 and Am-243, is of secondary importance. Based on this analysis, a new chain model that contains nuclides from U-238 to Cm-244 was made up as shown in Fig.21. The chain from Th-232 through uranium isotopes is kept as the original chain, because no Th-232 and little U-235 are contained in the HCLWR fuel. This model has been used in the recent burnup calculation of HCLWRs together with Takano's FP chain.

In recent years, generation and transmutation of trans-uranic (TRU) nuclides in fast and thermal reactors has been paid attention, especially in the investigations of TRU burner reactor. In order to analyse the burnup behavior (generation and transmutation) of these TRU nuclides, a more detailed chain was also considered in the SRAC system. Namely, the following nuclides were added to the actinide chain in Fig.21:

- -Np-237; the most important TRU nuclide.
- -Pu-238; the isotope of plutonium which is mainly generated from Np-237.
- -Cm-242; TRU nuclide and the precursor of Pu-238.
- -Cm-245; TRU nuclide which has large fission cross section.
- -U-232 and Th-228; these are not trans-uranic nuclides, but have the γ active daughter nuclides such as Bi-212 and Tl-208 and are important in the burnup calculation of Th based fuel.

The model is shown in Fig. 22.

3.3 Revised Data for Burnup Calculation

3.3.1 Fission Energies

In the preliminary results of the NEACRP HCLWR benchmark calculation, which were reported in 1987, it was shown that the SRAC system gave larger burnup reactivity loss than the other calculation codes. It was also pointed out in the preliminary report that the reason of this larger reactivity loss was the smaller energy release per fission for actinides. New fission energies were therefore taken from JNDC (Japanese Nuclear Data Committee) FP nuclear data library[12], in order to correct this burnup behavior given by the SRAC system.

Table 4 compares the original and new fission energies for major actinides. It can be seen that the differences are 4.4% for U-235 and 5.2% for Pu-239, respectively. The larger fission energies mean the

smaller decreasing rate of fissionable nuclides under the condition of a fixed power level, and therefore mean the smaller reactivity loss. In other words, the larger fission energies cause the larger energy release gigawatt-days per tonne heavy metal.

Both the burnup reactivity losses by the original and new fission energies are shown in Fig. 23, for the cell of Vm/Vf=1.1. The difference is about 0.6% k/k at 50GWd/t, or about 5% of burnup.

3.3.2 FP Yield Data

The SRAC burnup libraries had adopted FP yield data from the first version of JNDC FP library. Recently, the second version of JNDC FP library for 1227 nuclides has been compiled and published in the form of tables and figures[13]. The new library contains not only revised FP yield data, but also FP yield data from several fissionable nuclides such as Np-237, Pu-242, etc., which were not included in the first version.

The effect of the difference in FP yield data on burnup reactivity loss is very small. For the cell of Vm/Vf=1.1, the effect is less than 0.1% Δk/k at 50GWd/t. But, there can be seen some differences in fractional absorptions of individual nuclide, especially of Ag-109 as shown in Fig. 24. Figure 25 compares the difference of number densities of Ag-109 calculated with the original and new fission yield data.

3.3.3 Branching Ratio of Am-242 β Decay

Americium-242 has the short half life of about 16 hours and changes into Cm-242 and Pu-242 by β^- decay and electron capture (EC), respectively. The branching ratio of EC to total β decay of Am-242 is about 17%. The effect of the EC on Pu-242 generation was investigated by using the actinide chain model of 24 nuclides (Fig. 22), because the Am-242 (denoted by Am242g in Fig.22) EC chain was not originally included in this chain model.

The results of burnup calculations (for the cell of Vm/Vf=1.1 and 7% fissile Pu enrichment) show the effect is only 0.13% Δk/k at 50GWd/t, as compared with the case where the EC branch is neglected. The difference is caused mainly from the number density of Pu-242 generated. The difference in the number density of Pu-242 is fairly large to be about 8% (Fig. 26). In order to correctly estimate the number density of Pu-242, the EC branch of Am-242 is contained in the latest actinide chain model.

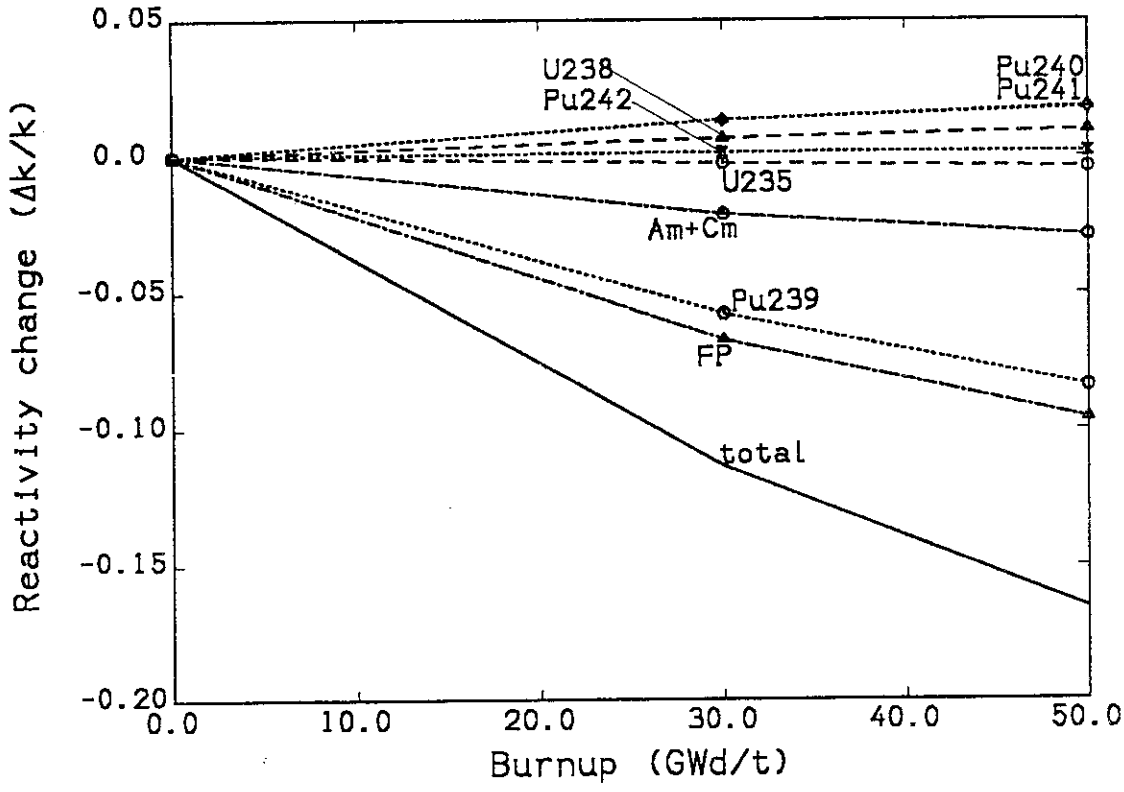

Fig. 2 Contribution of nuclides to the burnup reactivity change of the HCLWR of Vm/Vf=1.1.

Table2 Contribution of nuclides to burnup reactivity loss[6]

	LWR	HCLWR
Contribution		
Uranium isotopes	86.9%	0.8%
Plutonium isotojes	−20.6%	26.0%
Other actinides	1.8%	16.5%
Fission products	31.9%	56.7%

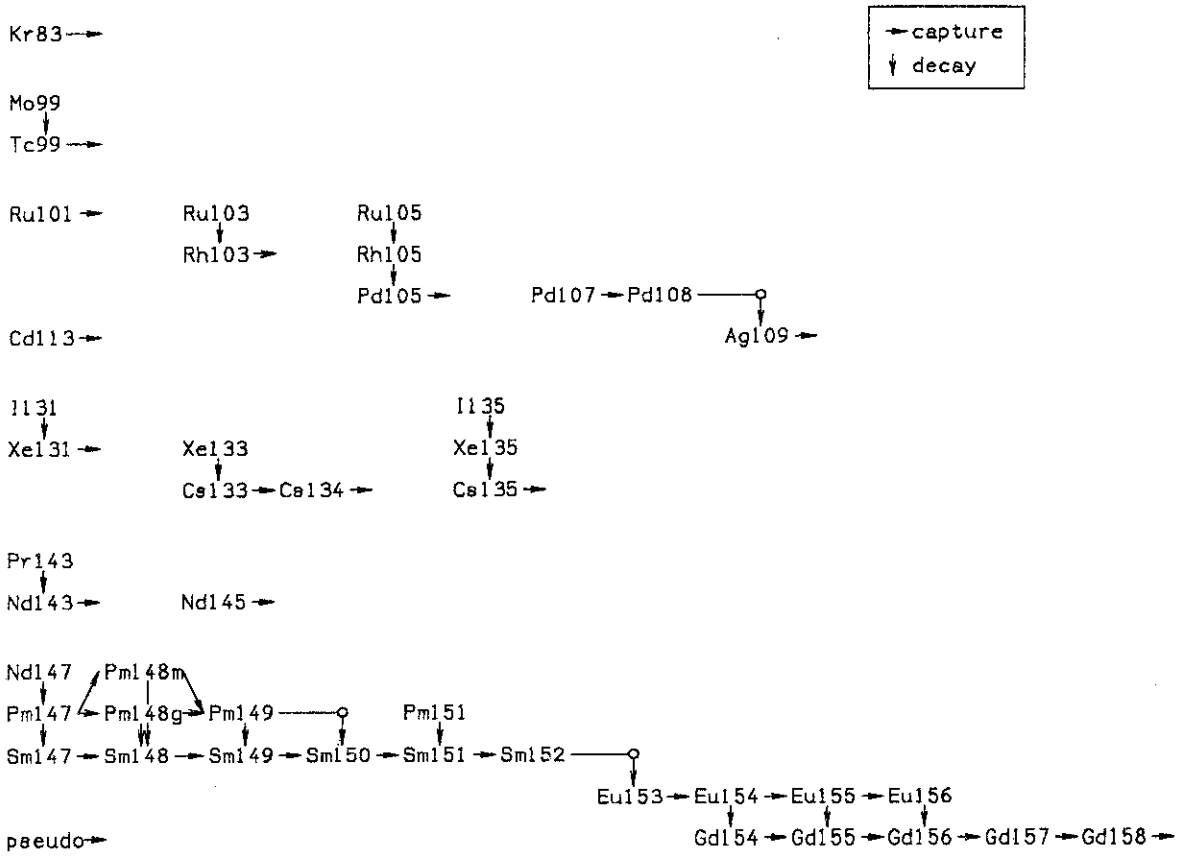

Fig. 3 Fission product (FP) burnup chain model by Iijima et al.

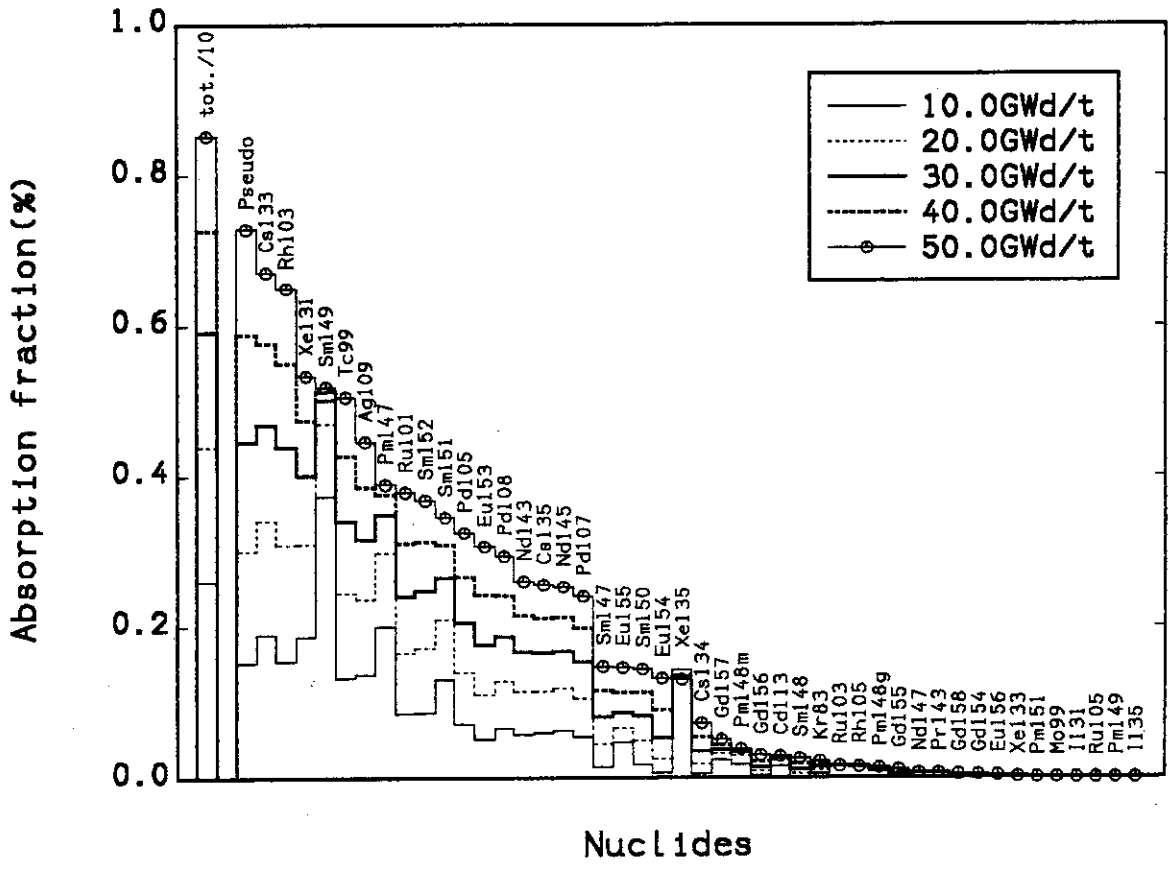

Fig. 4 Fractional absorption rates of FPs at 50GWd/t (Vm/Vf=0.6).

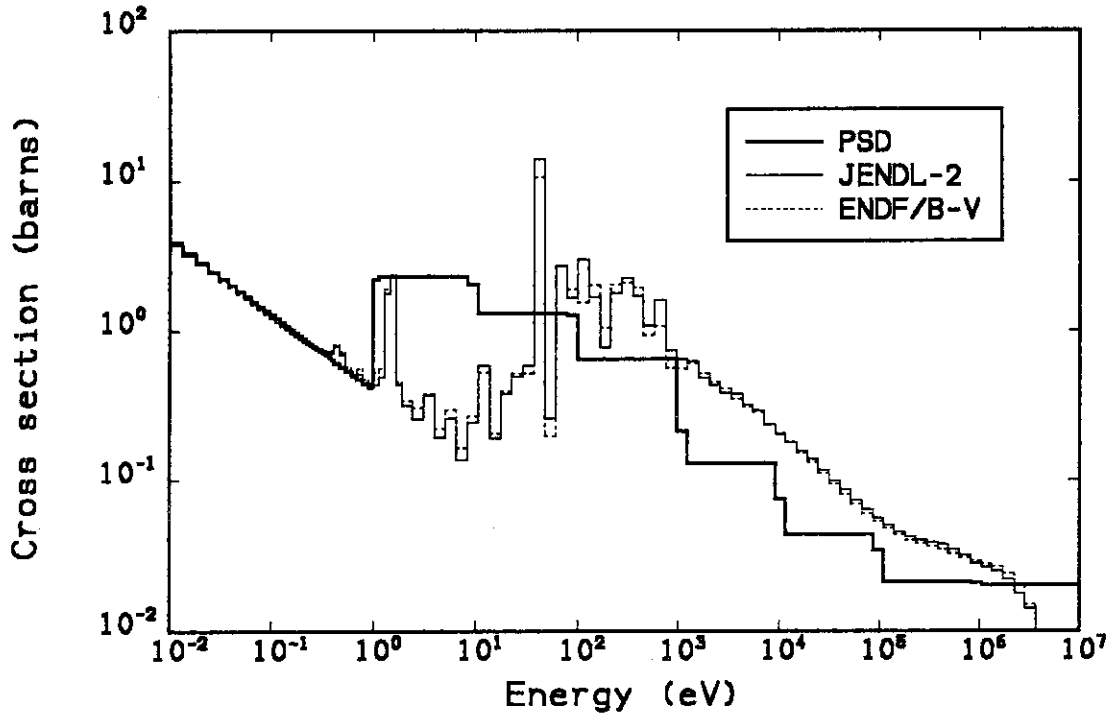

Fig. 5 Capture cross sections of the pseudo nuclides in Iijima's chain.

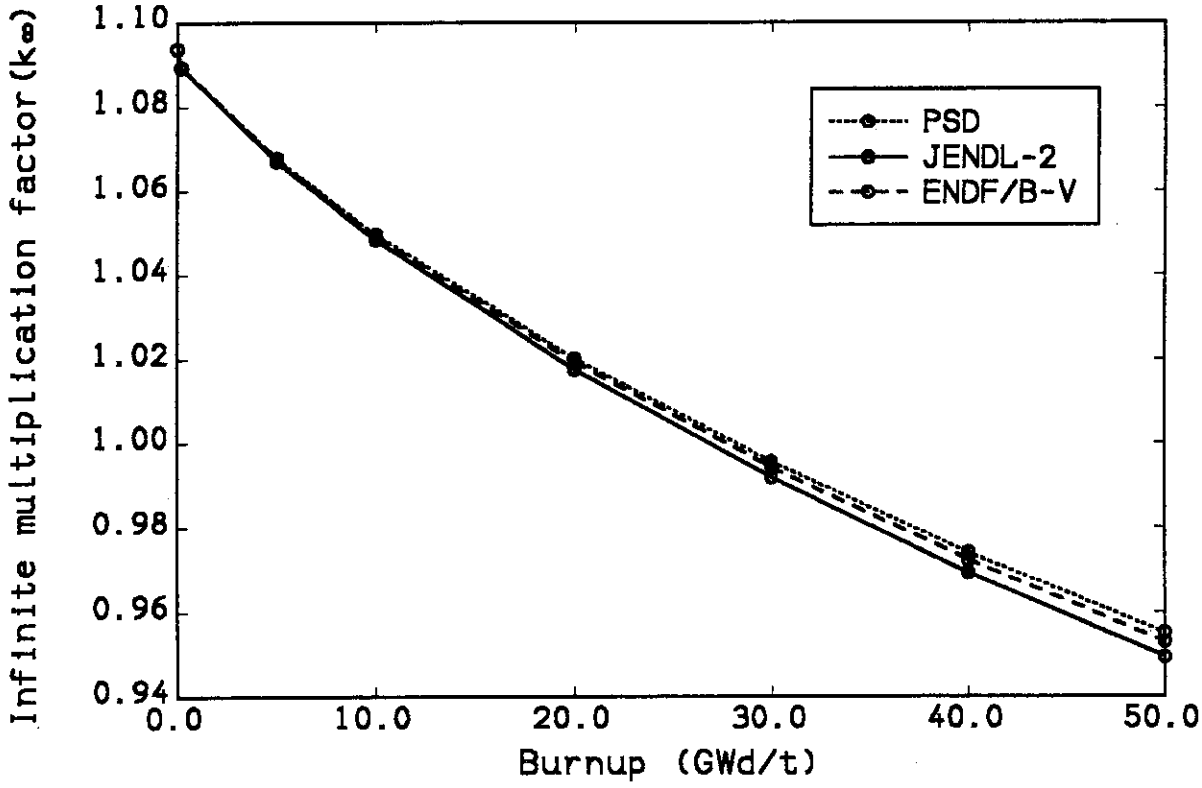

Fig. 6 Burnup reactivity changes of the cell of Vm/Vf=0.6 calculated by Iijima's chain with different pseudo cross sections.

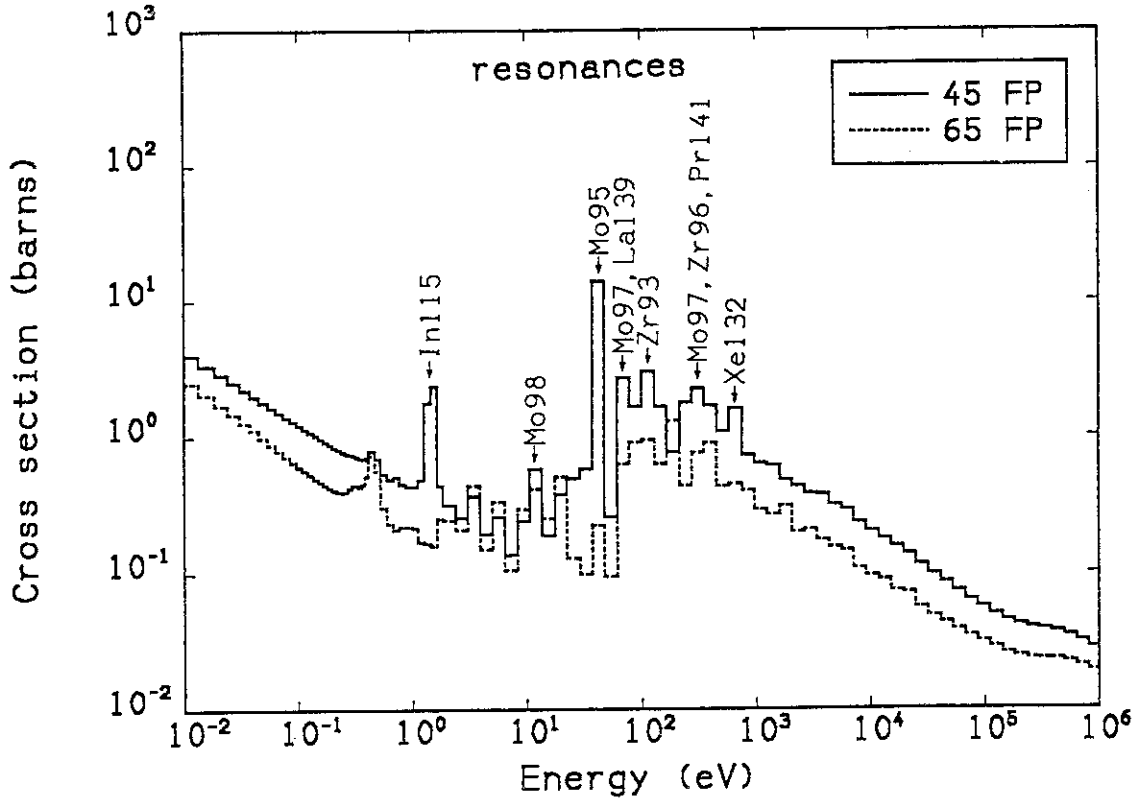

Fig. 7 Pseudo cross sections for Iijima's chain (45FP) and the chain by Takano et al. (65 FP).

Table3 FP yield in % per fission from major actinides (Cumulative yield from precursor FPs of the same mass number, total=200%)

	Th-232	U-233	U-235	U-238	Pu-239	Pu-241
Zr-93	6.756	7.015	6.390	5.001	3.896	3.094
Mo-95	5.375	6.191	6.496	5.107	4.895	4.075
Mo-97	4.492	5.496	6.008	5.575	5.445	4.912
In-115	0.069	0.012	0.011	0.034	0.036	0.042

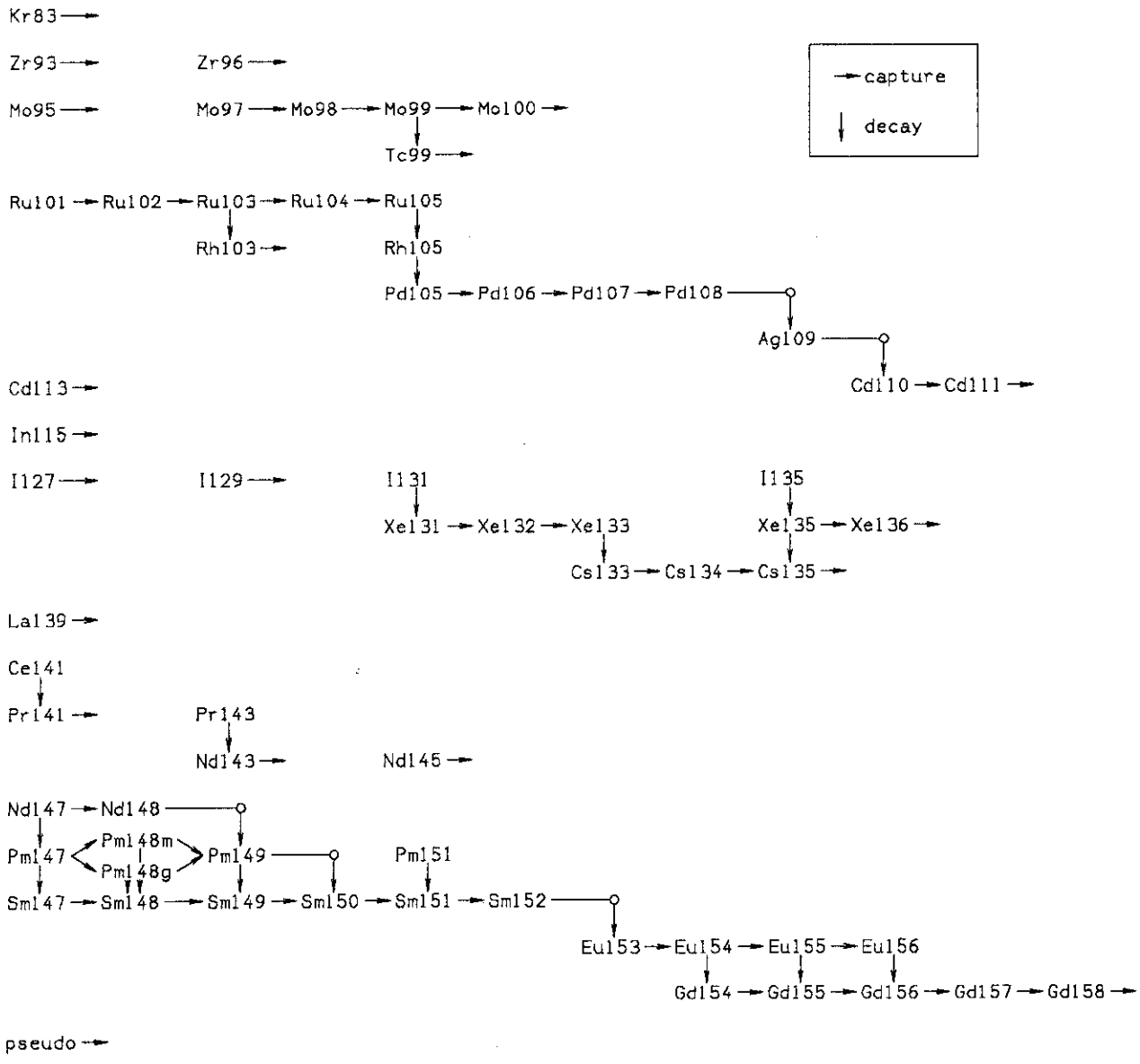

Fig. 8 Burnup chain model for FPs by Takano et al. with 65 explicit and 1 pseudo nuclide.

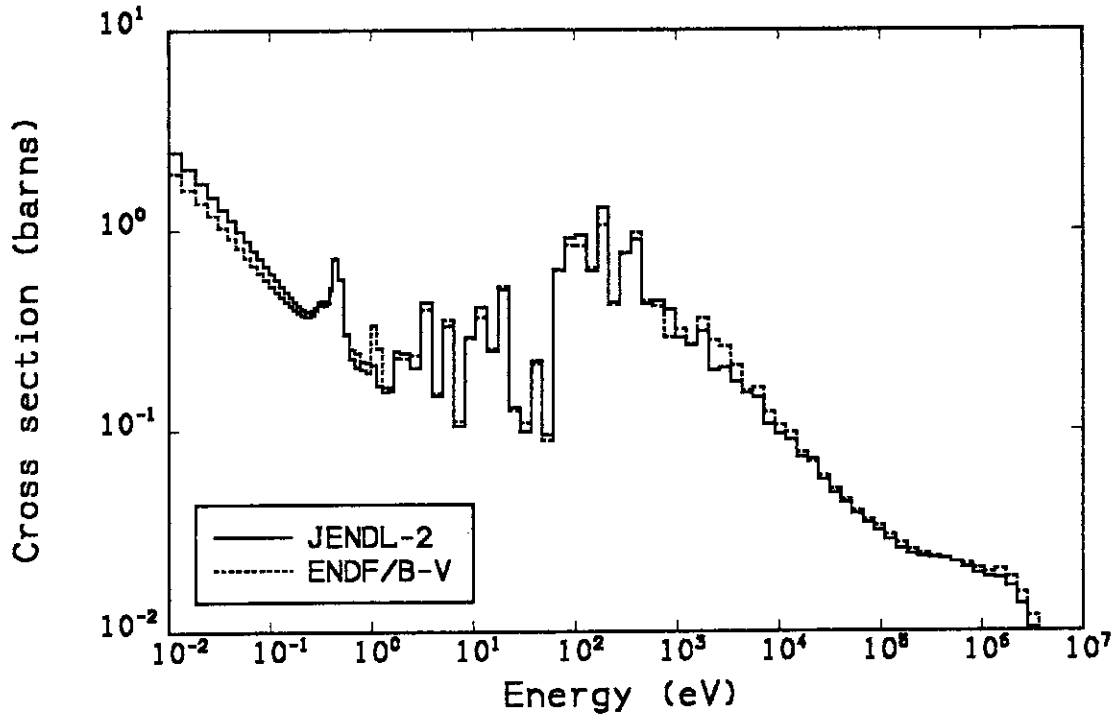

Fig. 9 Capture cross sections of pseudo FPs in Takano's chain.

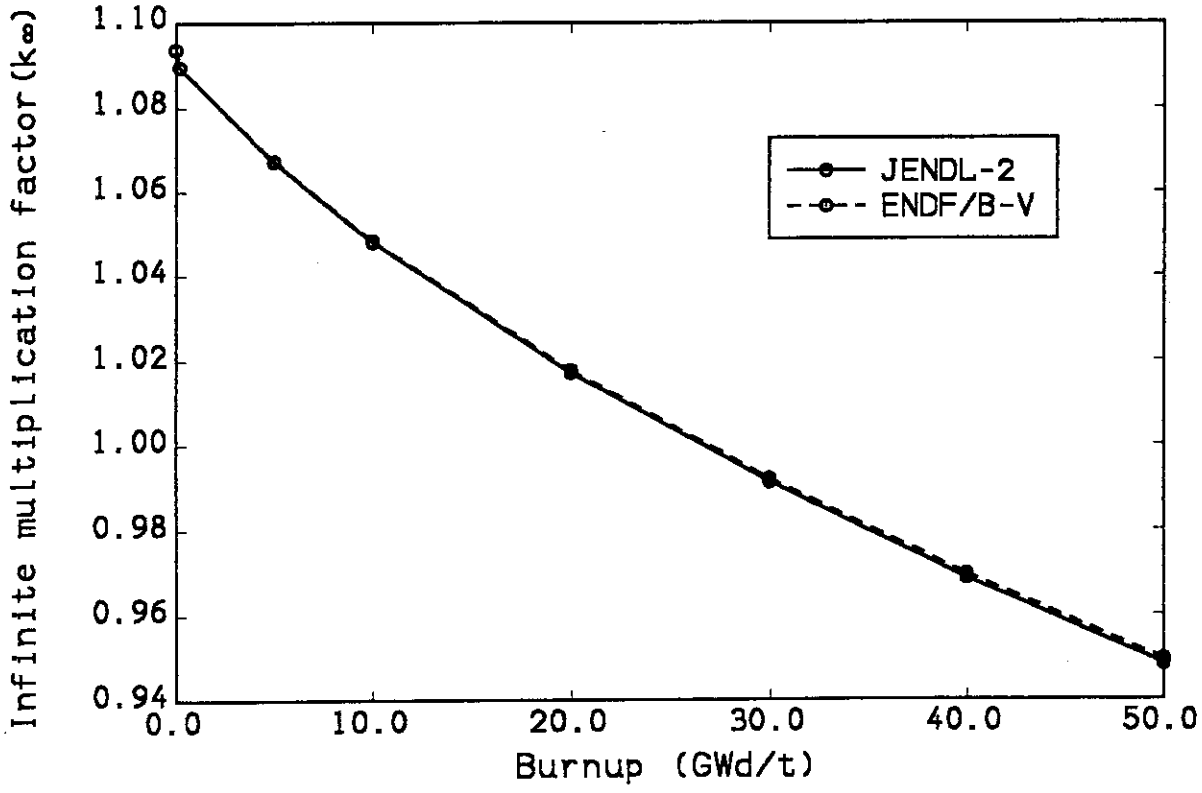

Fig. 10 Burnup reactivity changes by Takano's chain with different cross sections of pseudo FP (Vm/Vf=0.6).

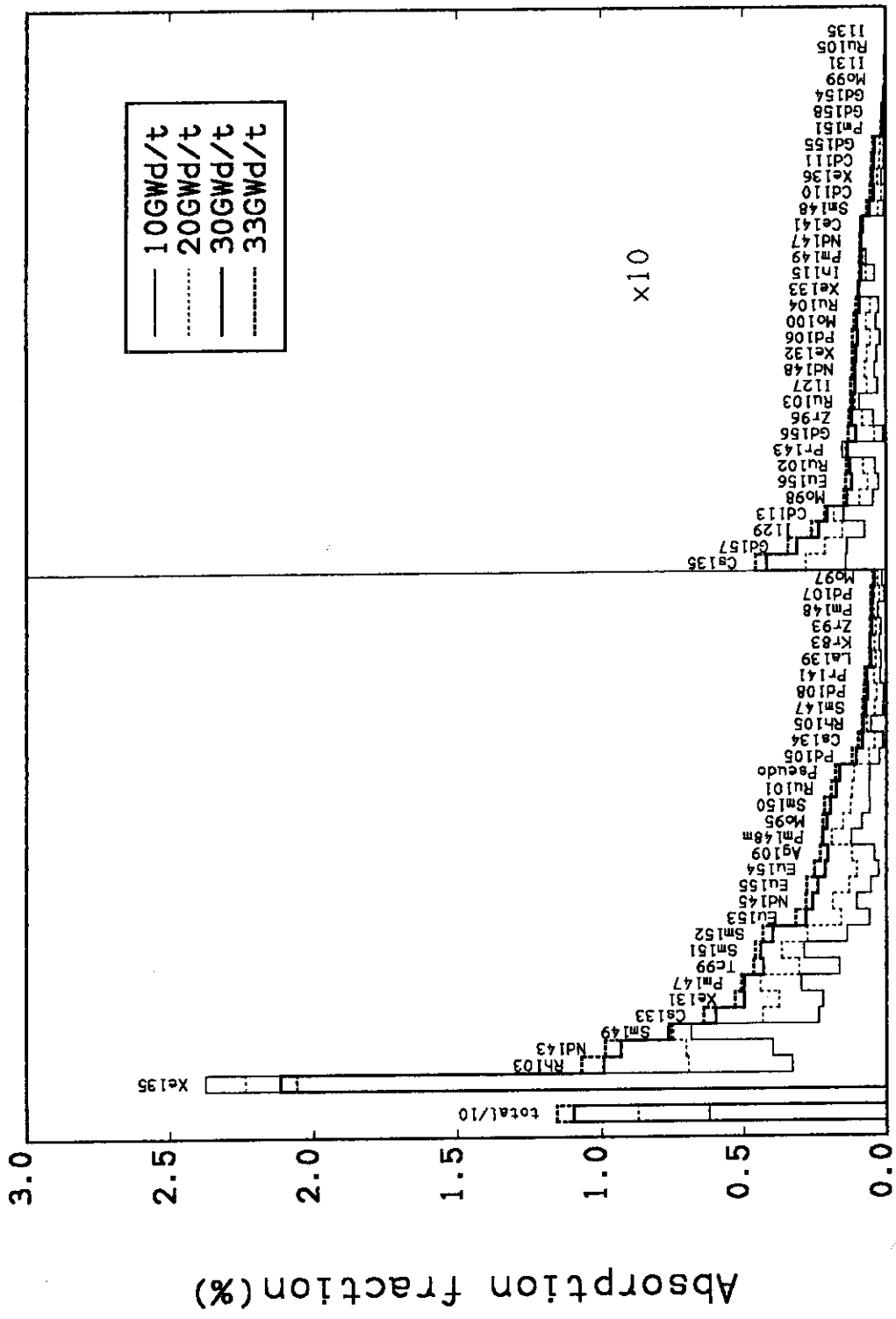

Fig. 11 Absorption fractions of FPs at each burnup in the conventional PWR.

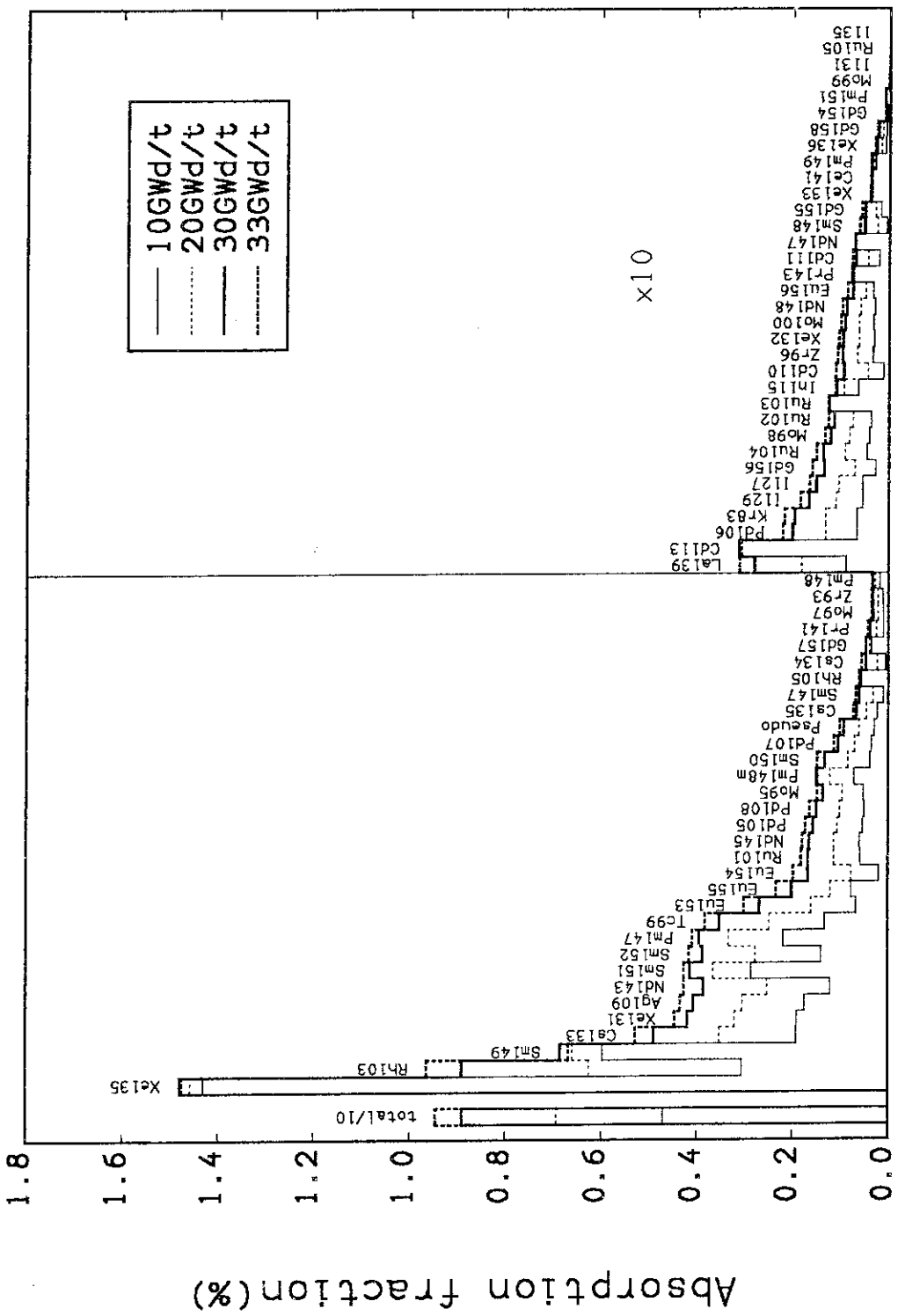

Fig. 12 Absorption fractions of FPs at each burnup in the MOX fueled PWR.

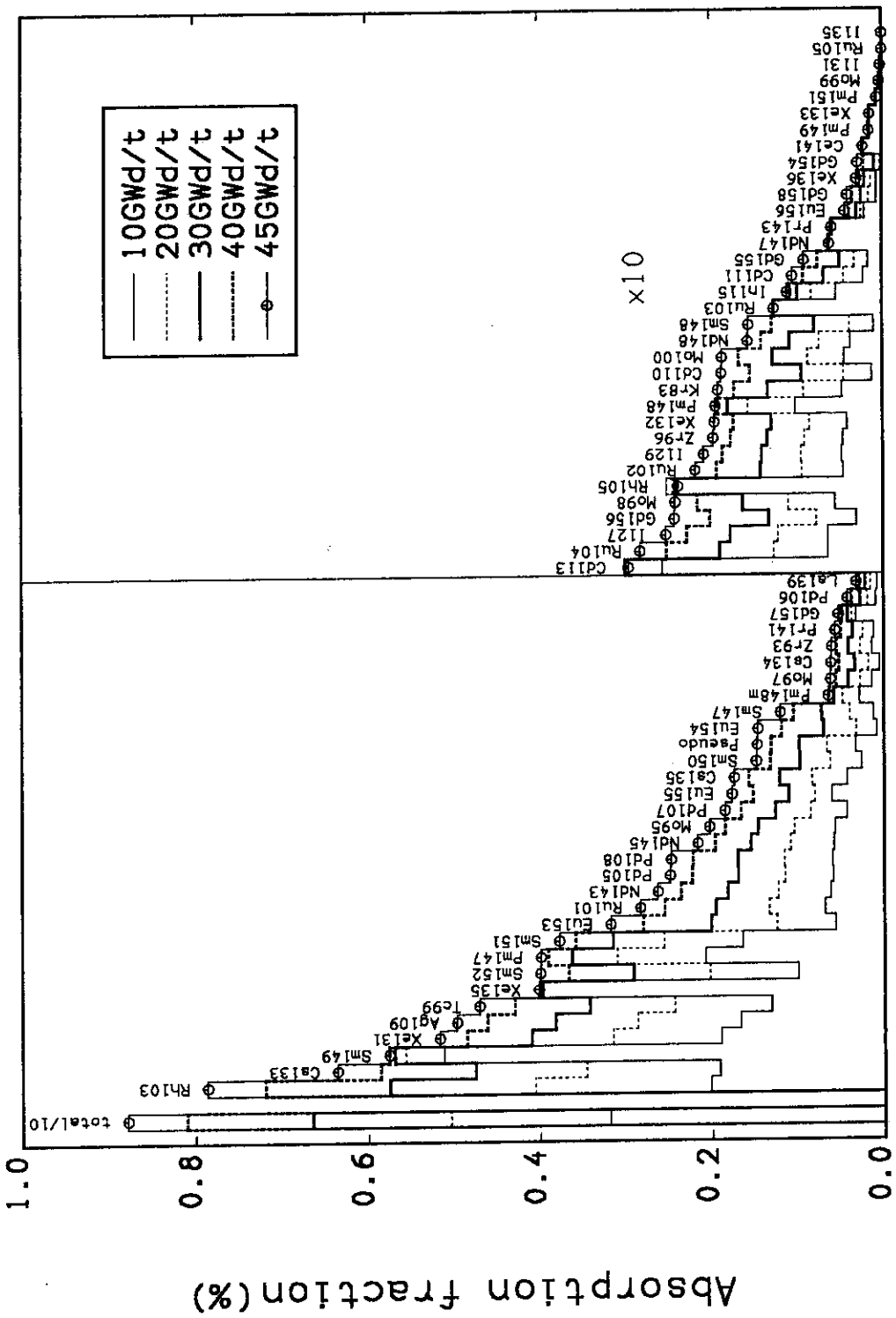

Fig. 13 Absorption fractions of FPs at each burnup in the HCLWR of Vm /Vf = 1.1.

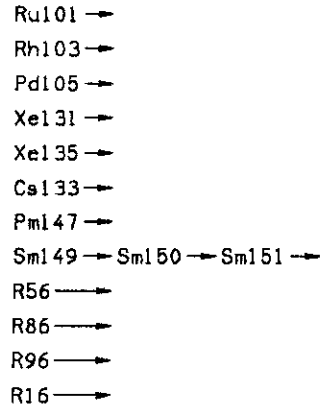

Fig. 14 Simple FP chain model for design calculations (R56, R86, R96 and R16 denote pseudo FP nuclides created by the fission reactions of U-235, U-238, Pu-239 and Pu-241, respectively).

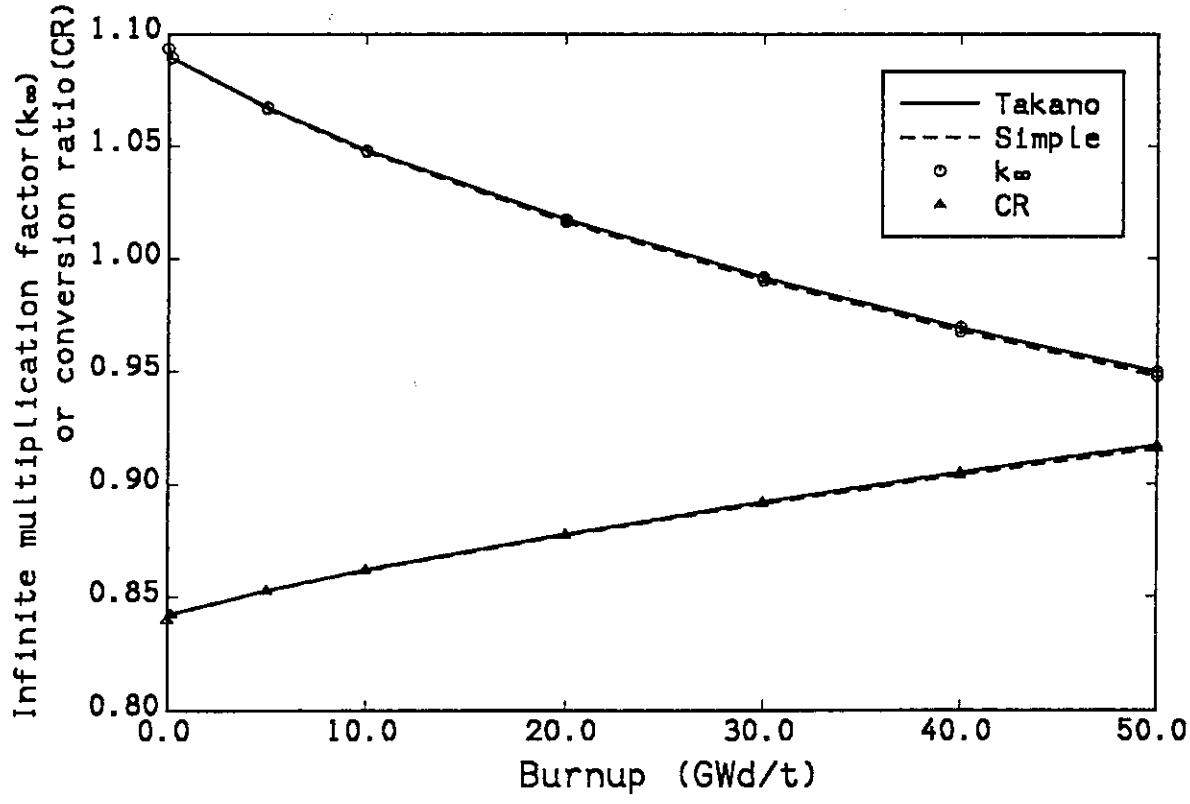

Fig. 15 Burnup dependence of infinite multiplication factor (k_∞) and conversion ratio (CR) for the cell of Vm/Vf=0.6 by Takano's and the simplified FP chains.

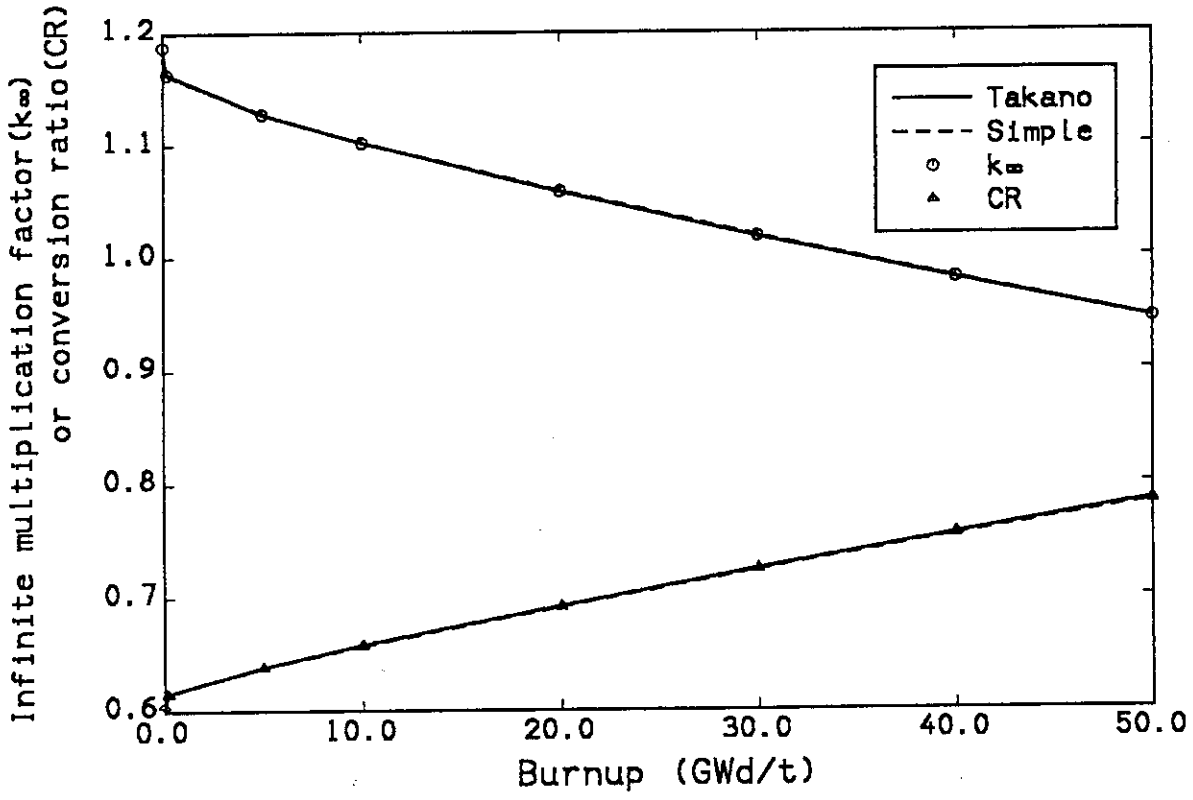

Fig. 16 Burnup dependence of infinite multiplication factor(k_∞) and conversion ratio(CR) for the cell of Vm/Vf=2.0 by Takano's and the simplified FP chains.

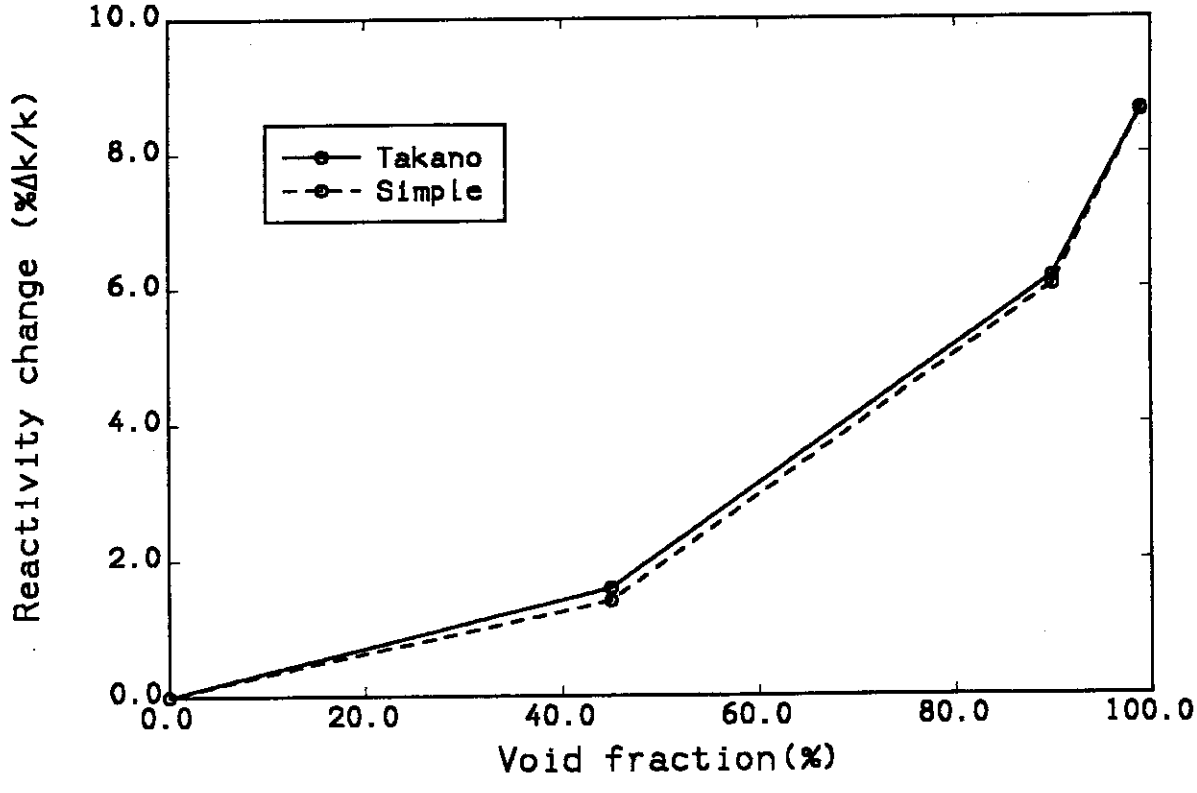

Fig. 17 Void reactivity changes at 50GWd/t by Takano's and the simplified chain for the cell of Vm/Vf=0.6.

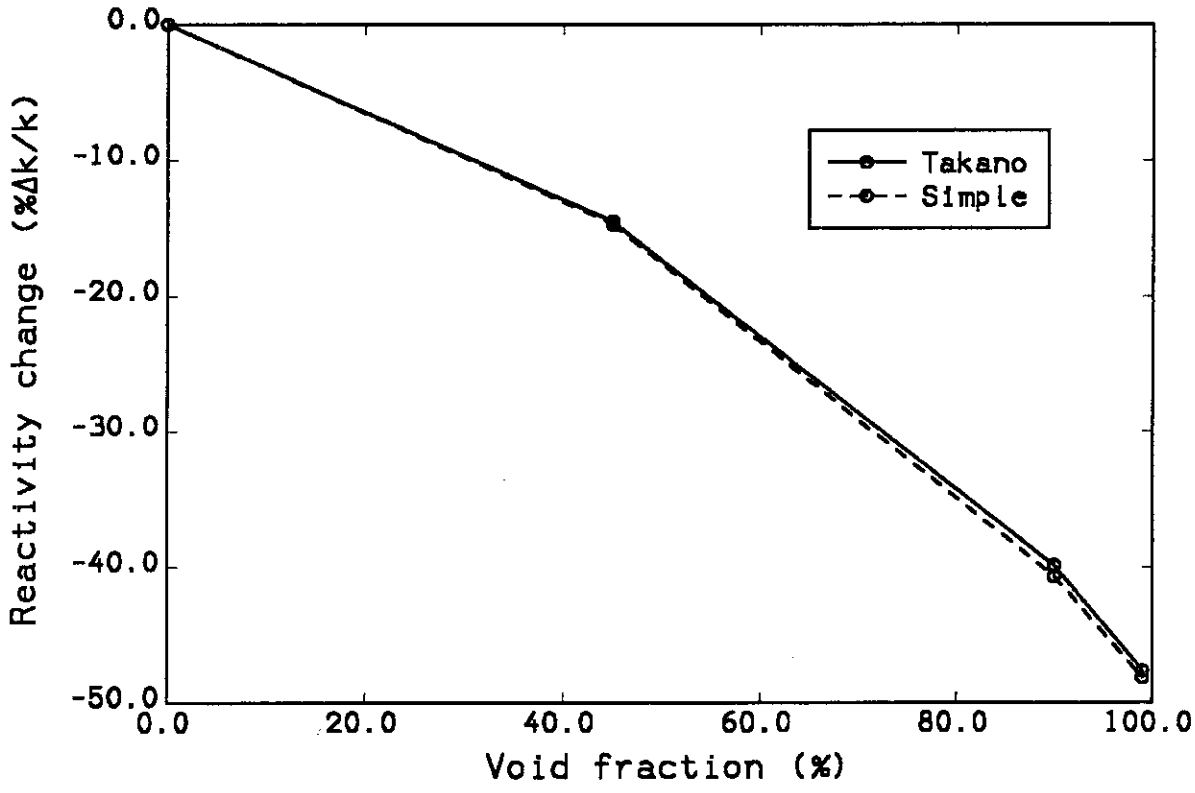

Fig. 18 Void reactivity changes at 50GWd/t by Takano's and the simplified chain for the cell of Vm/Vf=2.0.

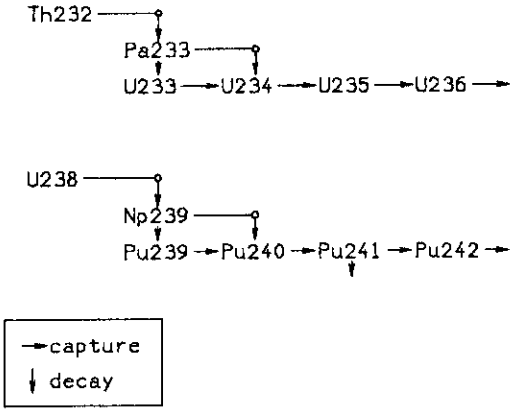

Fig. 19 Actinide burnup chain model in the original SRAC system.

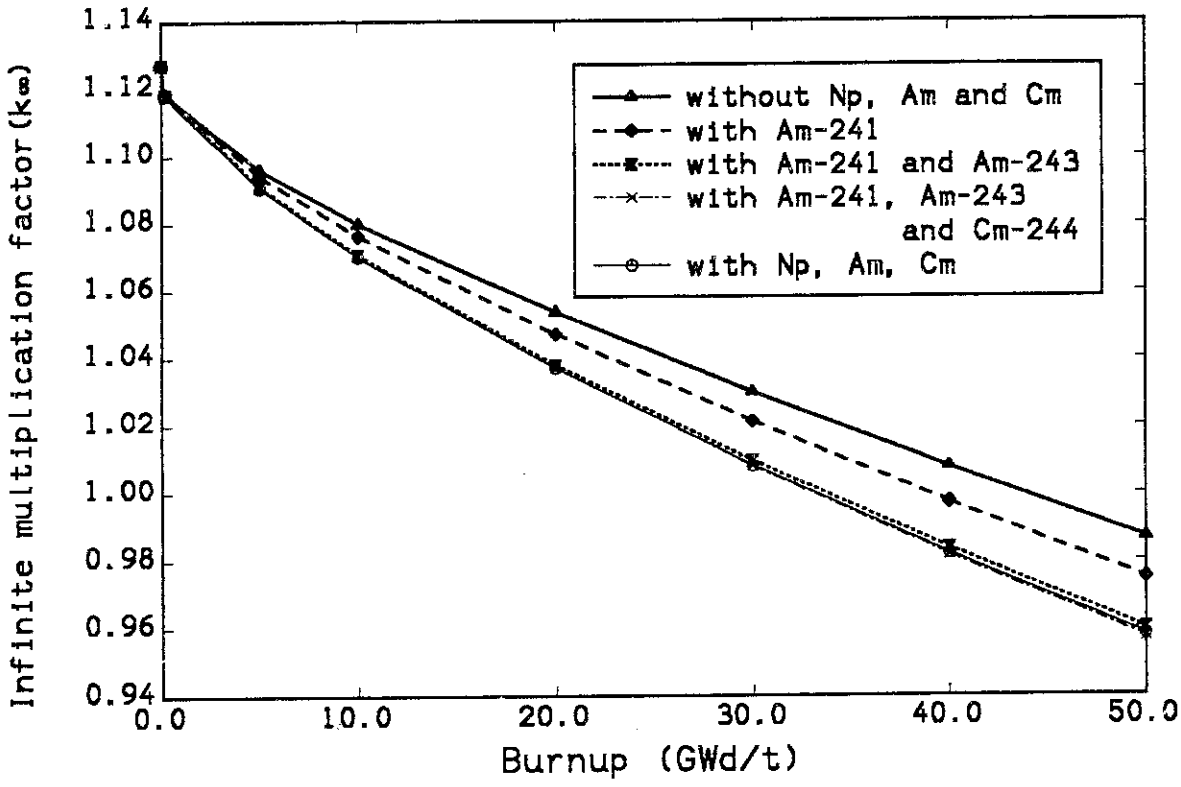

Fig. 20 Burnup reactivity changes in the cell of Vm/Vf=1.1 and the effect of higher actinides.

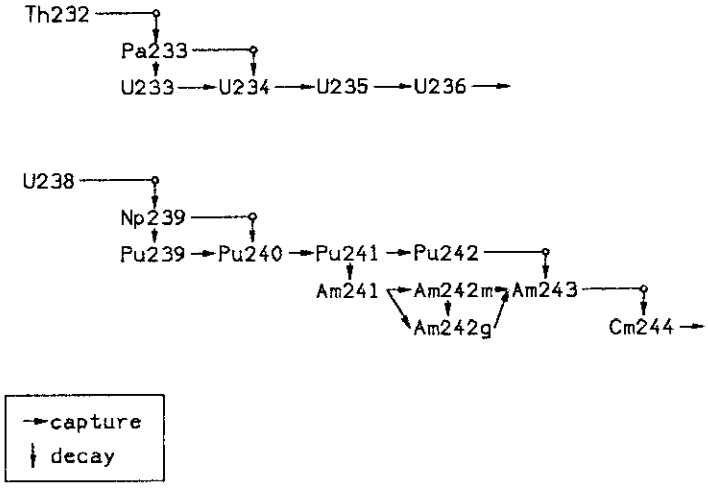

Fig. 21 Actinide chain model for HCLWR burnup calculation.

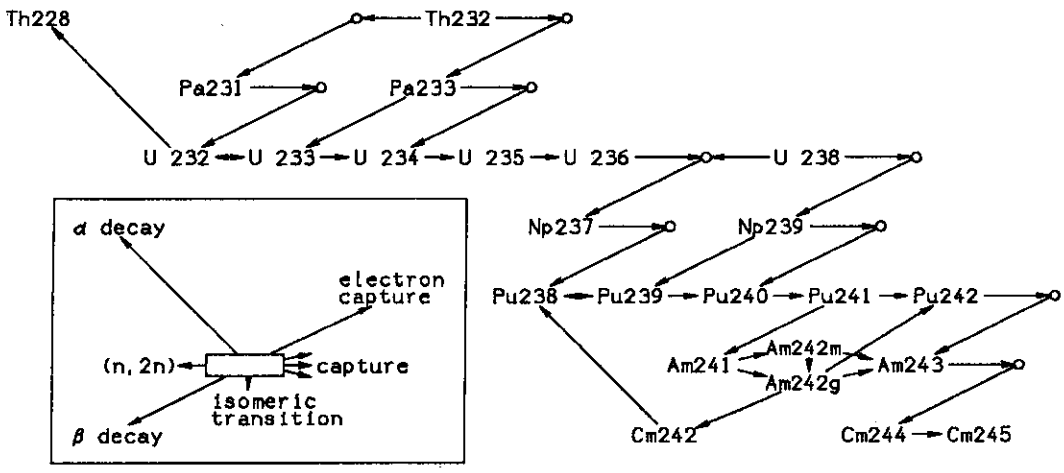

Fig. 22 Actinide chain for burnup of TRU nuclides and Th based fuel.

Table4 Fission energies of major actinides

	U-235	U-238	Pu-239	Pu-241
Original	3.108	3.108	3.220	3.220
New	3.246	3.299	3.392	3.420
(MeV/fiss.	202.6	205.9	211.7	213.5)

(unit: $\times 10^{-11}$Joule/fiss.)

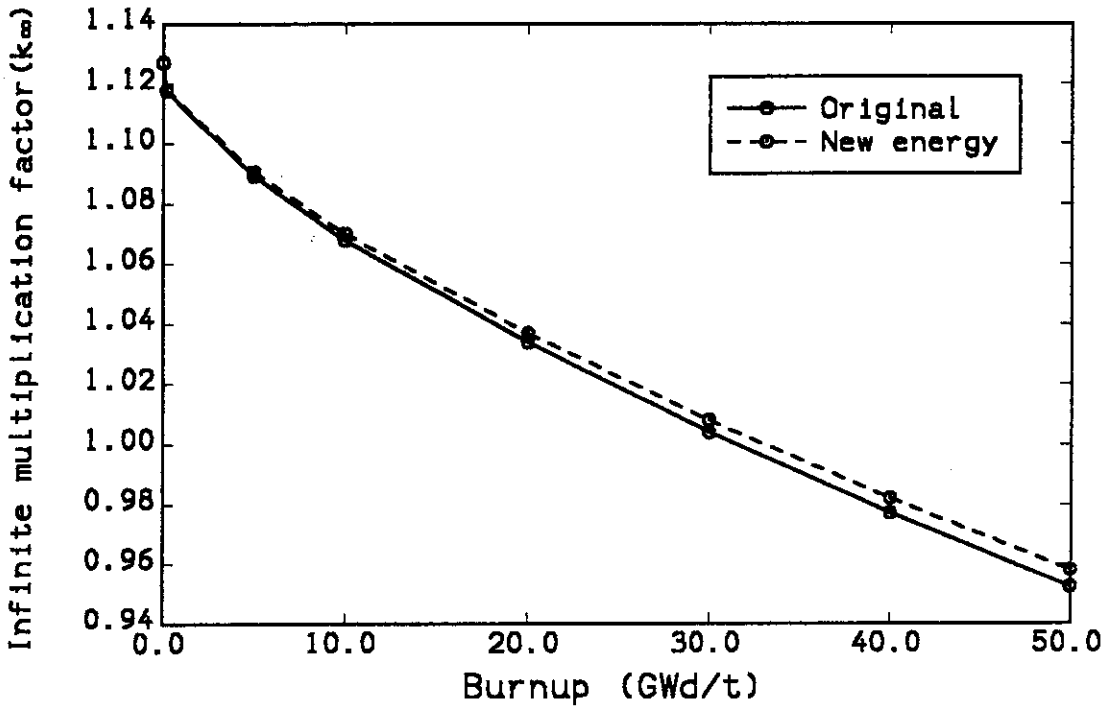

Fig. 23 Burnup reactivity changes by different fission energies (Vm/Vf= 1.1).

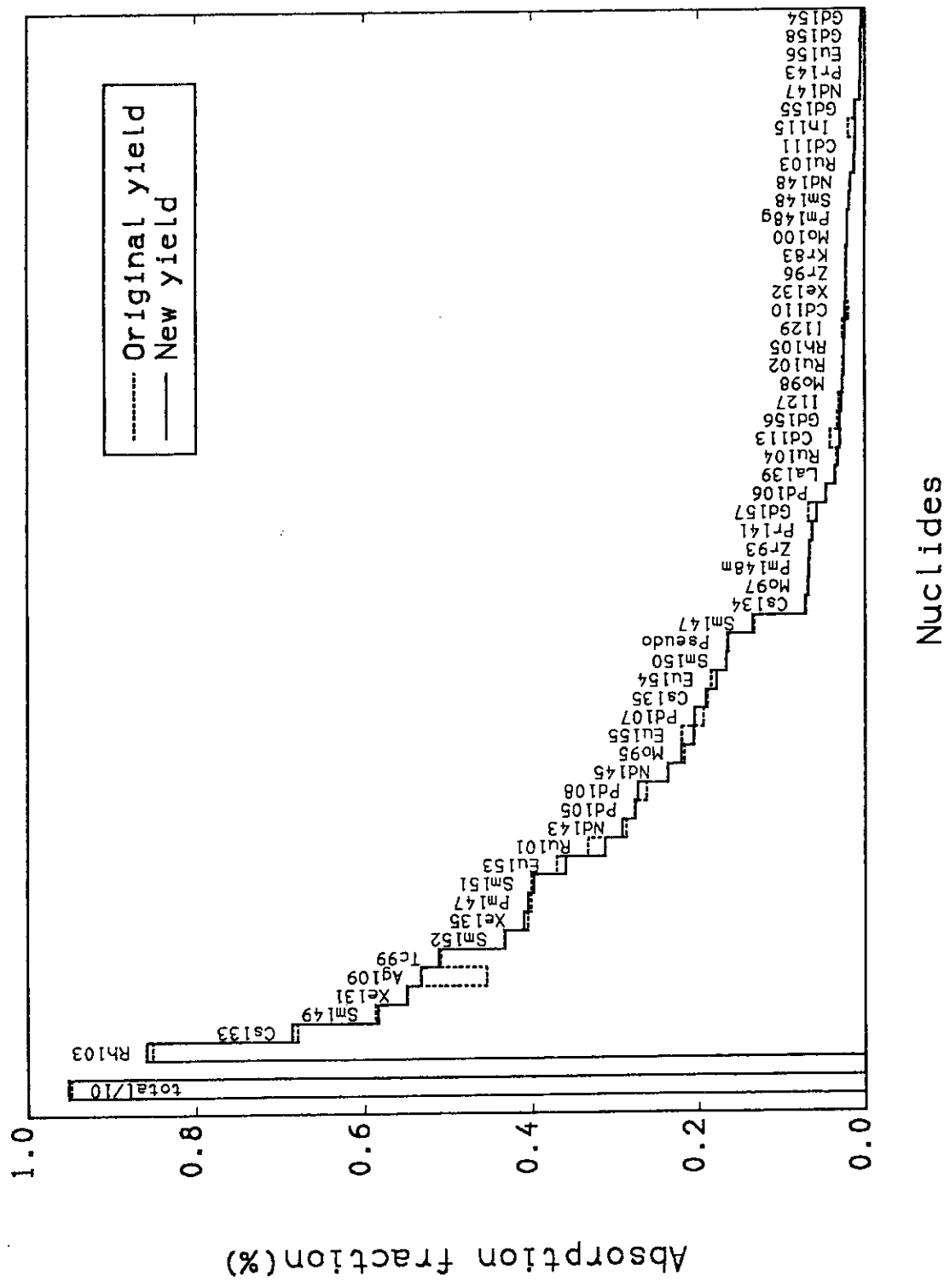

Fig. 24 Absorption fraction of FPs at 50GWd/t by new and original FP yield data (Vm/Vf = 1.1).

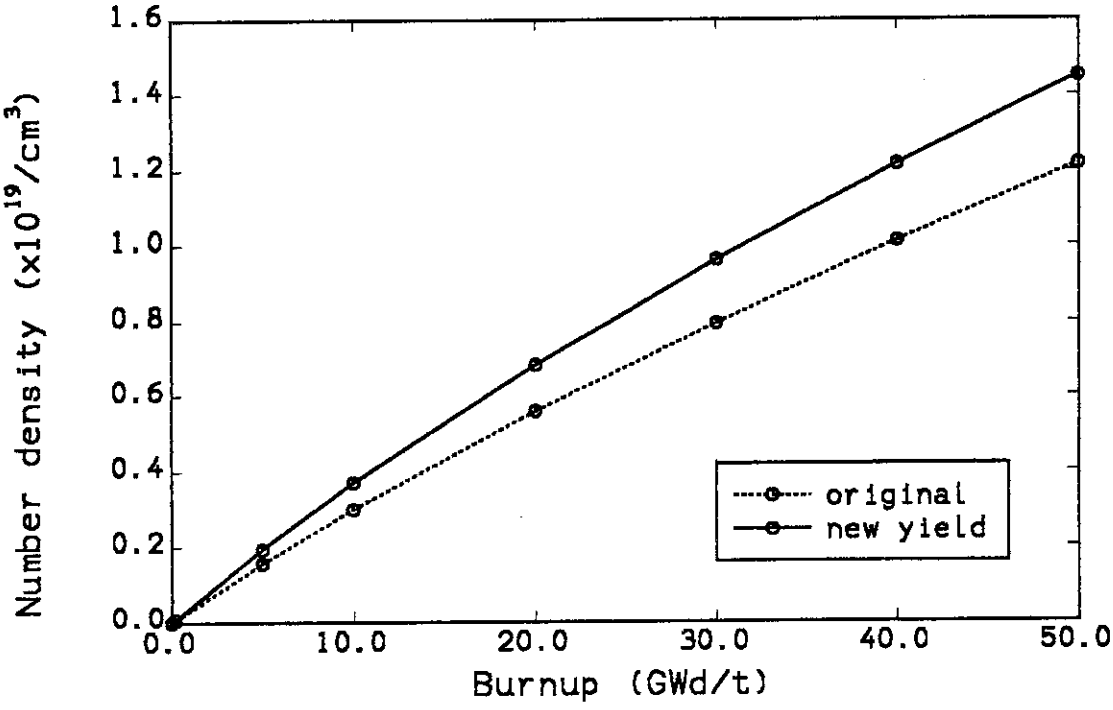

Fig. 25 Burnup dependence of Ag-109 number density calculated by new and original FP yield for the cell of Vm/Vf=1.1.

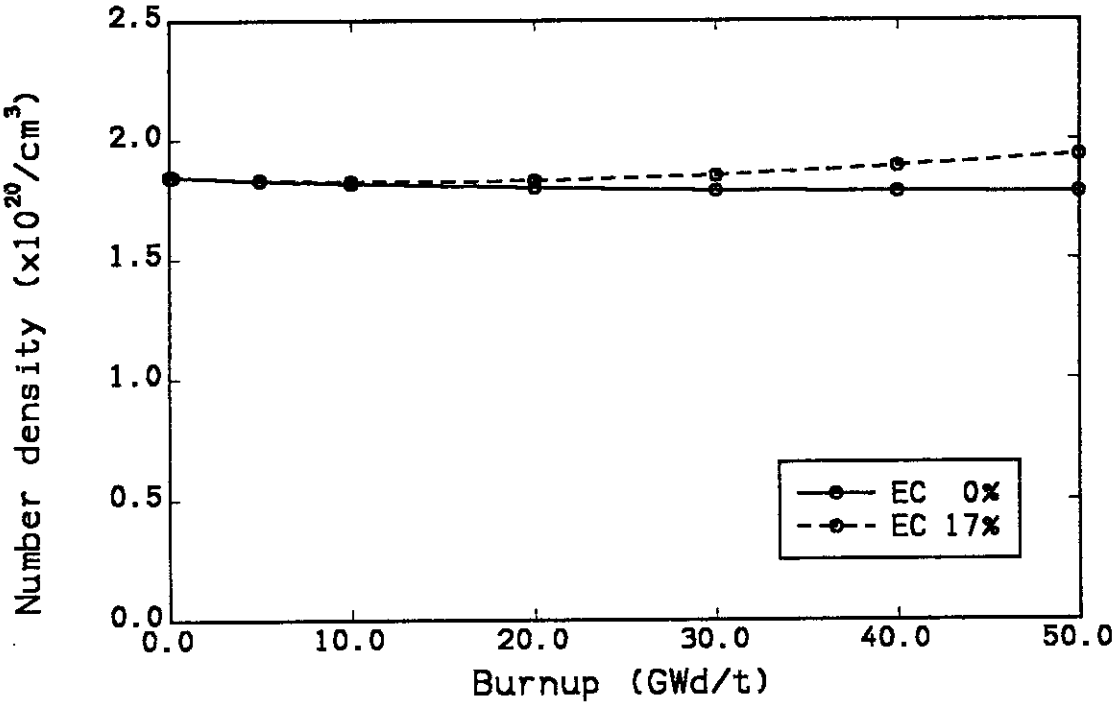

Fig. 26 Pu-242 number densities calculated with and without Am-242 EC chain (Vm/Vf=1.1, 7% fissile Pu).

4. Production of Group Cross Section Library SRACLIB-JENDL2

The group cross section libraries originally used in the SRAC system were generated on the basis of ENDF/B-IV and JENDL-1/JENDL-2 nuclear data files[14]. These are called SRACLIB-ENDFB4 and SRACLIB-JENDL1/2, respectively. In these libraries, however, all the necessary cross section data for FPs and minor actinides are not contained. For example, in SRACLIB-JENDL1/2, group cross sections of only 17 FP nuclides were generated on the basis of the JENDL-1 file. There is only Am-241 data for minor actinides both in SRACLIB-ENDFB4 and SRACLIB-JENDL1/2. Furthermore, discrepancies of nuclear data for FPs and minor actinides are remarkable among different evaluated data files such as JENDL-2, ENDF/B-V, JEF-1, etc.[9]. It was needed to examine the effect of the nuclear data uncertainty on burnup characteristics.

For these reasons, in order to investigate the behavior of minor actinides and FPs in HCLWRs, new group cross sections were produced based on JENDL-2 and ENDF/B-V nuclear data files, and the resulting libraties are called SRACLIB-JENDL2[15] and SRACLIB-ENDFB5, respectively. The library SRACLIB-ENDFB5 contains only the data of minor actinides and FPs, while SRACLIB-JENDL2 does those of more than 100 isotopes that include not only FPs and actinides, but also structural and absorber nuclides (Appendix Ⅲ).

4.1 Production of Group Cross Section Library

In the fast energy range (10MeV~0.414eV), it is important to consider resonance self shielding effect of FPs and minor actinides in a high burnup condition. For this reason, the infinite dilute cross sections and self shielding factors for these nuclides were calculated with the TIMS-PGG system[16]. The calculated self shielding factors were tabulated as a function of background cross section and temperature.

In the TIMS-PGG system, the group cross sections of light and medium weight nuclides, and also of smooth cross section of heavy nuclides, are calculated with the PROF-GROUCH-GⅡR code[16]. In this code, the weighting function assumed to produce group cross sections is

$$\phi\ (E,\ \sigma_0,\ T)\ =\phi_0\ (E)\ /\ (\sigma_t\ (E,\ T)\ +\sigma_0)$$

where $\phi_0\ (E)$ stands for the broad energy dependence of the neutron spectrum, $\sigma_t\ (E,T)$ the total cross section of the nuclide under consideration at neutron energy E and temperature T, and σ_0 the background cross section. The background cross section for nuclide i is defined as

$$\sigma_{0,\,i}=\frac{1}{N_i}\sum_{j\neq i}N_j\sigma_{t,\,j},$$

and $\phi_0\ (E)$ is assumed to be a fission spectrum (Watt spectrum[16]) above 1MeV and $1/E$ spectrum from 0.414eV to 1MeV.

The group cross sections for heavy nuclides in the resolved and unresolved resonance energy region are calculated with the TIMS-1 code[17]. In the unresolved region, TIMS-1 generates resonance parameters (resonance levels and widths) by using a Monte Carlo method. The resonance widths and level spacings in the unresolved resonance region are distributed around their mean values according to the χ^2 and the Wigner distributions, respectively, and TIMS-1 searches a series of the resonance parameters which satisfy these distributions. With these resonance parameters generated and the resonance param-

eters in the resolved resonance region, ultra fine energy mesh group cross sections are calculated. These cross sections are used in the spectrum calculation by numerically solving the neutron slowing down equation. This is the same method as used in the PEACO method, but performed for infinite homogeneous medium. The group cross sections are produced weighted by this neutron spectrum.

The resonance shielding factors for reaction x at temperture T in energy group g are defined by

$$f_x^g(\sigma_0, T) = \sigma_x^g(\sigma_0, T) / \sigma_{x,\infty}^g(T_0),$$

where $\sigma_{x,\infty}^g$ is the infinite dilute cross section and $T_0 = 300$ K.

When the PEACO method is used in the SRAC system, another group cross section library is needed in the resolved resonance energy region of 131eV~0.414eV with 4600 energy groups (MCROSS library). The PEACO calculation is essential for the analysis of HCLWRs, where the reactions in the resonance energy region is dominant. The MCROSS library has been produced by the MCROSS-2 code[18] for the uranium and plutonium isotopes, Am-241, Am-243 and Cm-244. The hyperfine energy group cross sections for 20 FPs were also produced in order to investigate the mutual resonance interference effect between the actinides and FPs. The result of this investigation (Ref.20, see also Section 4.4) showed that the interference effect of the total FPs is not so large.

The group cross sections and self shielding factors in the thermal energy range (3.93eV~0.01meV) were generated by the SRACTLIB data processing code, which is described in Ref.14. In this calculation, the weighting spectrum was assumed as the Maxwellian distribution of neutron temperature T_n (taken as $T_m + 50$ K in the SRACTLIB processing code, where T_m is the material temperature), and $1/E$ spectrum in the energy region above $5 \times kT_m$. The self shielding factor tables were generated for the nuclides that have important resonances in the thermal energy range such as the 2.67eV resonance of Pu-242. On producing thermal cross section libraries of SRACLIB-JENDL2, the original SRACTLIB code was improved as follows:

- In the Cd-113 data of SRACLIB-ENDFB4, two times larger capture cross section than the total cross section was found in the thermal energy range. The reason is as follows: When there is the cross section data of MT = 101 (absorption) of MF = 3 in the basic data file, the cross sections of MT = 101 and 102 ((n,γ)) in FM = 3 were doubly added in the SRACTLIB code to produce the capture (= absorption without fission) cross section. The SRACTLIB code was improved to create the capture cross section excluding MT = 101 data.
- The original SRACTLIB code could treat only the cross section data expressed on the energy points given in the nuclear data file. In this situation, if there are only a few points in the thermal energy range, the code might generate group cross sections of insufficient accuracy, particularly near a resonance level. This situation is shown in Fig.27 for the Xe-131 case. In this figure, the group cross section obtained by the original SRACTLIB code is compared with the energy pointwise cross section generated by the RECENT code[19] within the error of 0.1%. An improvement was made to generate at least 10 energy points by the SRACTLIB code, according to the interpolation scheme given in the original nuclear data file. The revised group cross section is also shown in Fig.27.

4.2 Nuclear Data Uncertainties of FPs and Minor Actinides

Nuclear data uncertainties of FPs and minor actinides are more remarkable than those for major nuclides such as U-238 and Pu-239. Table 5 shows the comparison of the cross sections at 2200m/s, and resonance integrals for FPs and minor actinides obtained from the evaluated nuclear data files JENDL-2, ENDF/B-V and JEF-1[20]. Large discrepancies for these cross section data are observed from this table. As typical examples, the group cross sections for Ru-103, Eu-155 and Am-243 are compared between the evaluated data files in Figs.28~30. From these figures, it can be seen that the discrepancies between the evaluated data files are large for these nuclides.

To examine the effect of these nuclear data uncertainties on burnup reactivity loss, the cell burnup calculations were performed for the HCLWR cell model of Vm/Vf=0.74[20),11)]. The contributions of fractional absorption rates of the individual FPs were calculated for the three evaluated files, JENDL-2, ENDF/B-V and JEF-1. They are compared in Fig.31. The remarkable differences of fractional absorption between the three files are observed for Tc-99, Ru-103, Pd-108, Xe-131, Cs-135 and Eu-155. The burnup reactivity losses were calculated by using these different evaluated files. The relevant values of multiplication factors calculated with the other files to that obtained with JENDL-2 are shown in Fig. 32. Significant discrepancy is found between the reactivity losses obtained with JENDL-2 and ENDF/B -V, while the discrepancy is very small between those for JENDL-2 and JEF-1. This is caused from an accidental cancellation as seen from Fig.31.

Figure 33 shows the comparison of the fractional absorptions calculated by using the different cross sections only for the minor actinides[11)]. Here, the JENDL-2 data were used for the other nuclides such as uranium and plutonium isotopes. The difference between the absorptions of Am-243 obtained with JENDL-2 and ENDF/B-IV is larger than 0.2%. However, the results obtained with JENDL-2, ENDF /B-V and JEF-1 are in good agreement with one another. The multiplication factor calculated with the minor actinide data of ENDF/B-IV is observed to become larger than those obtained with the other data[9)].

4.3 Self Shielding Effect of FPs

The fission product absorptions are calculated by using infinitely dilute cross sections without taking into account the resonance shielding effect in the analyses of conventional LWRs and FBRs. However, the resonance shielding effect of FPs is thought to be important in HCLWRs, because of the large absorption fraction of FPs and the importance of resonance energy region in the HCLWR neutronics calculations. In this and the next Sections, resonance self and mutual shielding effects of FPs[20)] are described respectively. The HCLWR cell model of Vm/Vf=0.74 is mainly considered in this study.

The contribution of individual FP to the total absorption rate is shown in Fig. 34 at the burnup stage of 50GWd/t. The effective cross sections of the 65 FPs were calculated considering the self shielding factors. The self shielding effect of Xe-131 and Cs-133 is remarkable in comparison with the other nuclides. Figures 35 and 36 show the comparison of the group capture cross sections for Xe-131 and Cs -133 calculated with and without the self shielding effect at 50 GWd/t. A noticeable shielding effect is observed for Xe-131 at the giant 14.4eV resonance. As for Cs-133, the effect is seen for several resonances. The reactivity loss by burnup is remarkably reduced by taking into account the self shielding effect of FPs as seen in Fig. 37. The effect causes a difference of about 0.7%Δk/k at the burnup stage of 50GWd/t.

4.4 Resonance Interference Effect Between FPs and Actinides

The resonance interference effect between FPs and actinides (mainly U-238) was studied[20)]. The effective cross sections for the 20 major FPs were calculated with the PEACO method, and those for the other FPs were obtained by using the table-look-up method. The effective cross sections calculated with the PEACO method accurately include both the self shielding and the mutual resonance overlapping effect.

The resonance cross sections of U-238 and Sm-150 are shown in Fig.38, as an example of the resonance overlapping. It is seen from the figure that the resonances of U-238 and Sm-150 are strongly overlapped near 21eV. Figure 39 shows the neutron flux in the fuel region of the cell near 21eV. Furthermore, the capture reaction rate of Sm-150 in this energy region is shown in Fig.40. In these figures, the vertical lines at 17.6 and 22.6eV show the energy boundaries of the SRAC group structure. It

is seen from these figures that the capture rate of Sm–150 is reduced considerably because of the flux depression by the 20.87eV resonance of U–238. Thus the effective cross section averaged by the depressed neutron spectrum over the energy range from 17.6 to 22.6eV becomes 195 barns and is far smaller than that calculated with the table–look–up (964 barns). These reductions of capture rate and group cross section in this energy region are due to the effect of the mutual resonance shielding.

In contrast with the case of Sm–150, the resonance interference effect can sometimes give a larger effective group cross section than the infinite dilution cross section. For instance, Fig.41 shows the resonance cross sections of Ag–109 and U–238, where the resonances of Ag–109 at 5.19eV overlaps with the 6.67eV resonance of U–238. By the 6.67eV resonance, neutron spectrum is largely depressed around this resonance. This neutron spectrum is illustrated in Fig.42 with the capture cross section of Ag–109 near the energy group from 5.04 to 6.48eV. The cross section of Ag–109 weighted by the depressed energy spectrum, σ_{eff}, is compared in Fig. 43 with the original infinite dilution cross section, σ_{∞}. The group cross sections in the energy range of 5.04～6.48eV averaged by the 1/E spectrum are 4300 barns for σ_{∞} and 5100 barns for σ_{eff}.

Figure 44 compares the fractional absorption for the FPs calculated with the table–look–up and the PEACO methods. The resonance interference effects are observed for several nuclides. The table–look–up method overestimates the absorption rates of Sm–151 and Sm–150, and underestimates the absorptions of Cs–133, Xe–131, Ag–109, Eu–153 and Mo–95. However, the difference between the total fractional absorptions for all FPs is very small because of an accidental cancellation between the contributions of individual FPs. For this reason, the PEACO method is not applied to FPs in the latest SRAC system.

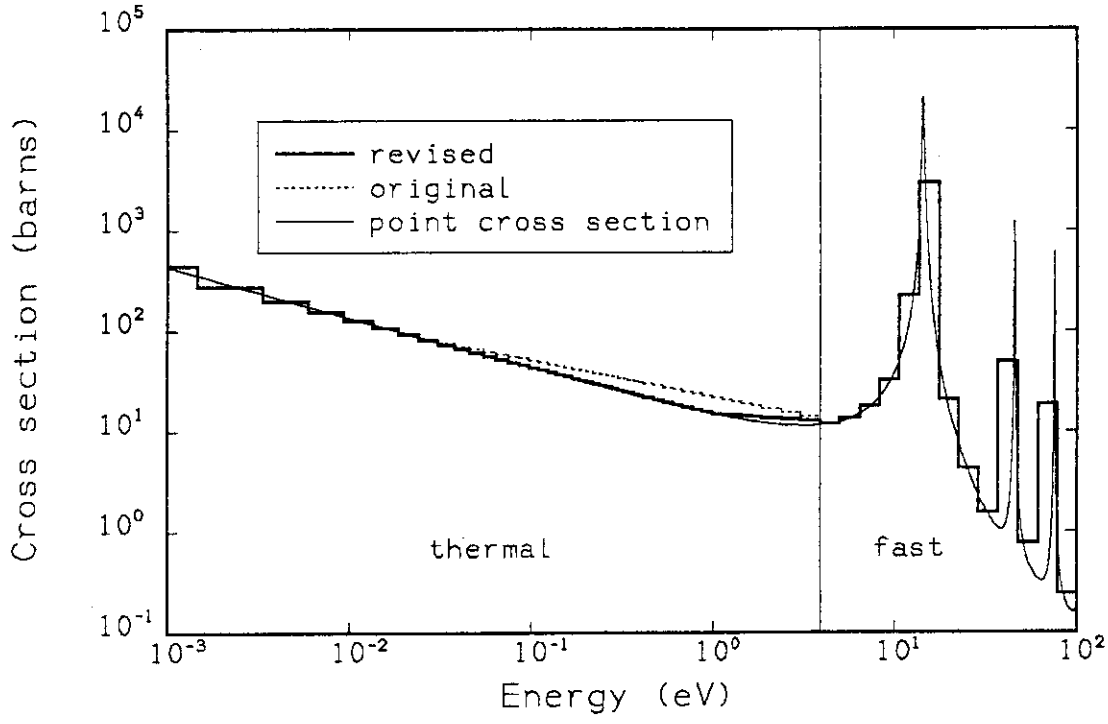

Fig. 27 Capture cross sections of Xe-131 in the thermal energy range calculated with original and new SRACTLIB code ('point cross section' denotes energy pointwise cross section).

Table5 Comparison of thermal capture cross sections and capture resonance integrals (barns)

Nuclide		JENDL-2	ENDF/B-V	JEF-1
Ru-103	2200m/s	5.0	7.7	66.8
	RI*	92.0	70.0	595.0
Pd-108	2200m/s	8.5	12.2	7.4
	RI	252.4	226.0	188.0
Eu-155	2200g/s	4046.0	4040.0	3647.0
	RI	18840.0	1857.0	2178.0
Am-241	2200m/s	600.0	576.0	610.0
	RI	1299.0	1424.0	1449.0
Am-243	2200m/s	131.3	58.0	134.0
	RI	404.5	248.4	429.0
Cm-244	2200m/s	14.4	10.4	14.4
	RI	593.7	593.5	637.3

*Resonance integral in the 0.5eV ~ 10MeV energy range

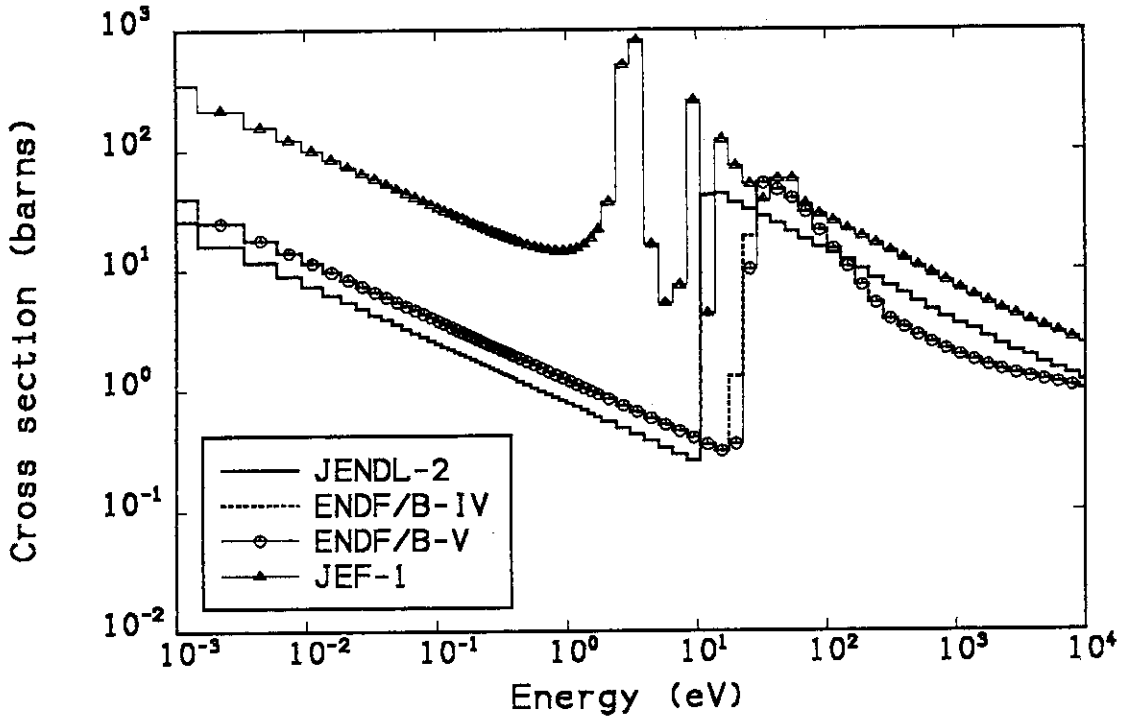

Fig. 28 Comparison of capture cross sections of Ru-103 among the four nuclear data files.

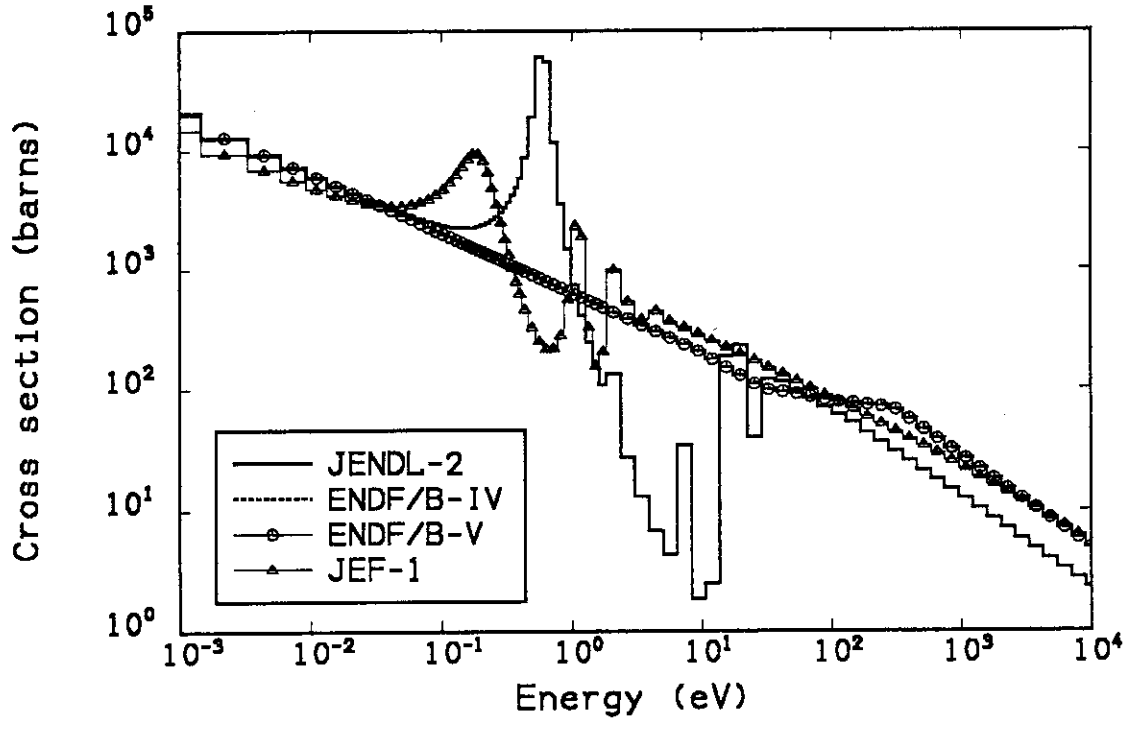

Fig. 29 Comparison of capture cross sections of Eu-155 among the four nuclear data files.

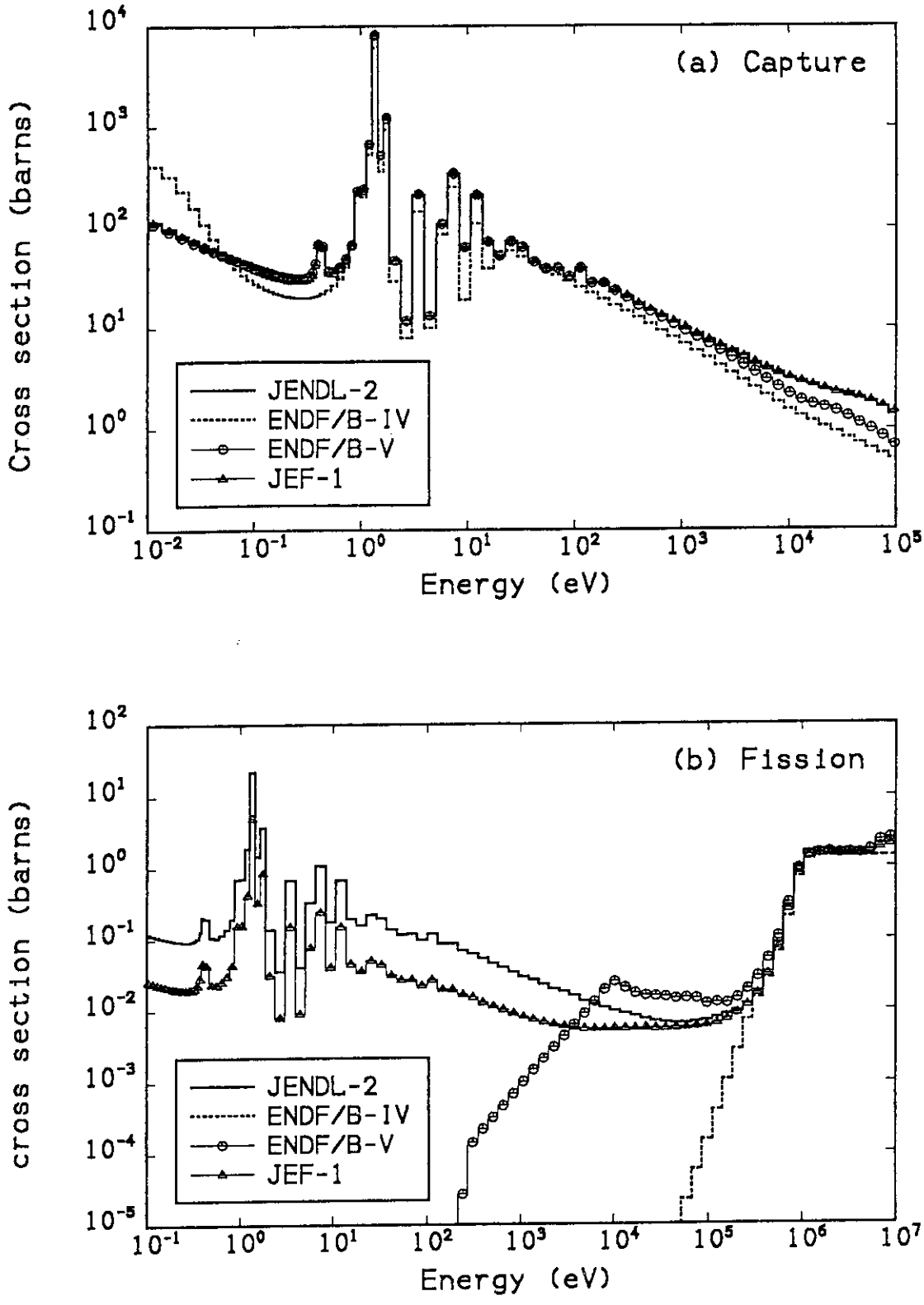

Fig. 30 Comparison of (a) capture and (b) fission cross sections of Am-243 among the nuclear data files.

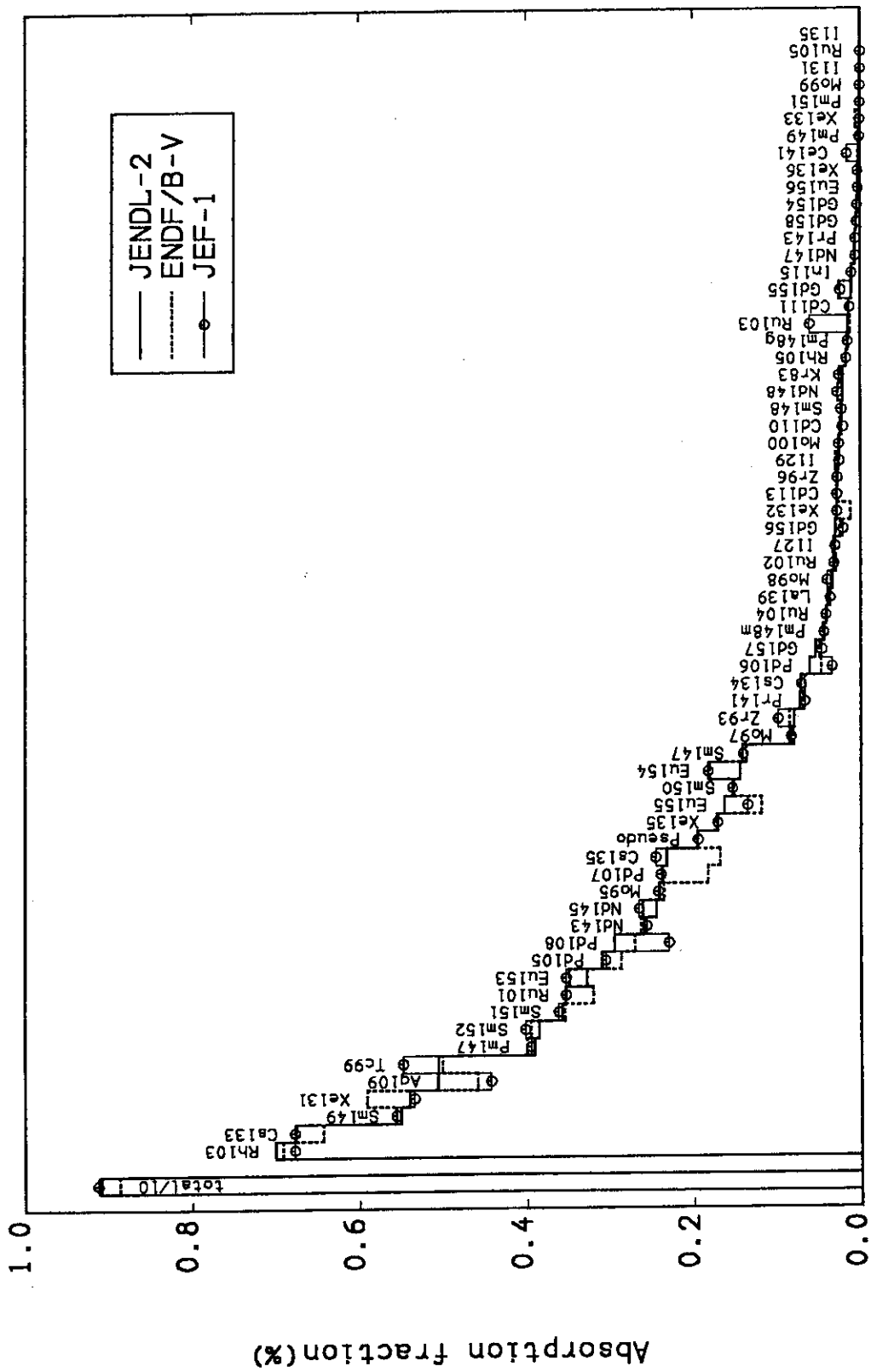

Fig. 31 Contribution of individual nuclides to total absorption at the burnup state of 50GWd/t.

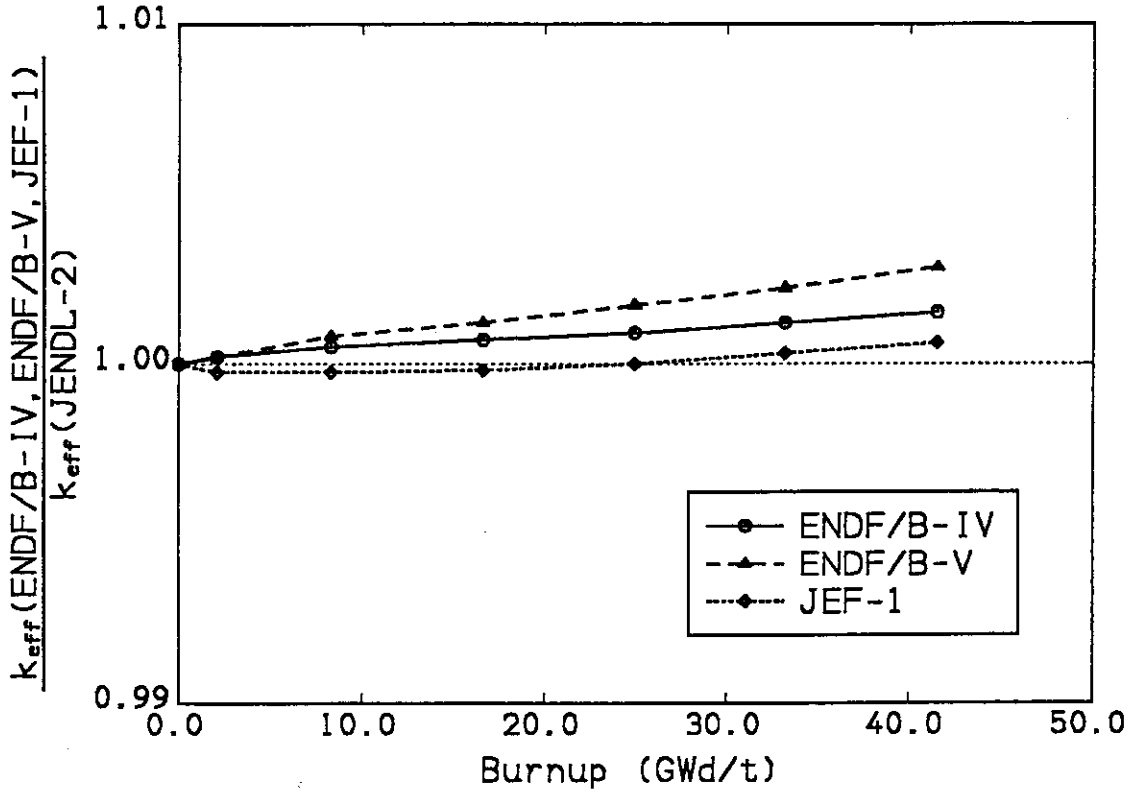

Fig. 32 Burnup dependence of the ratios of the multiplication factors calculated with the other files compared to those with JENDL-2.

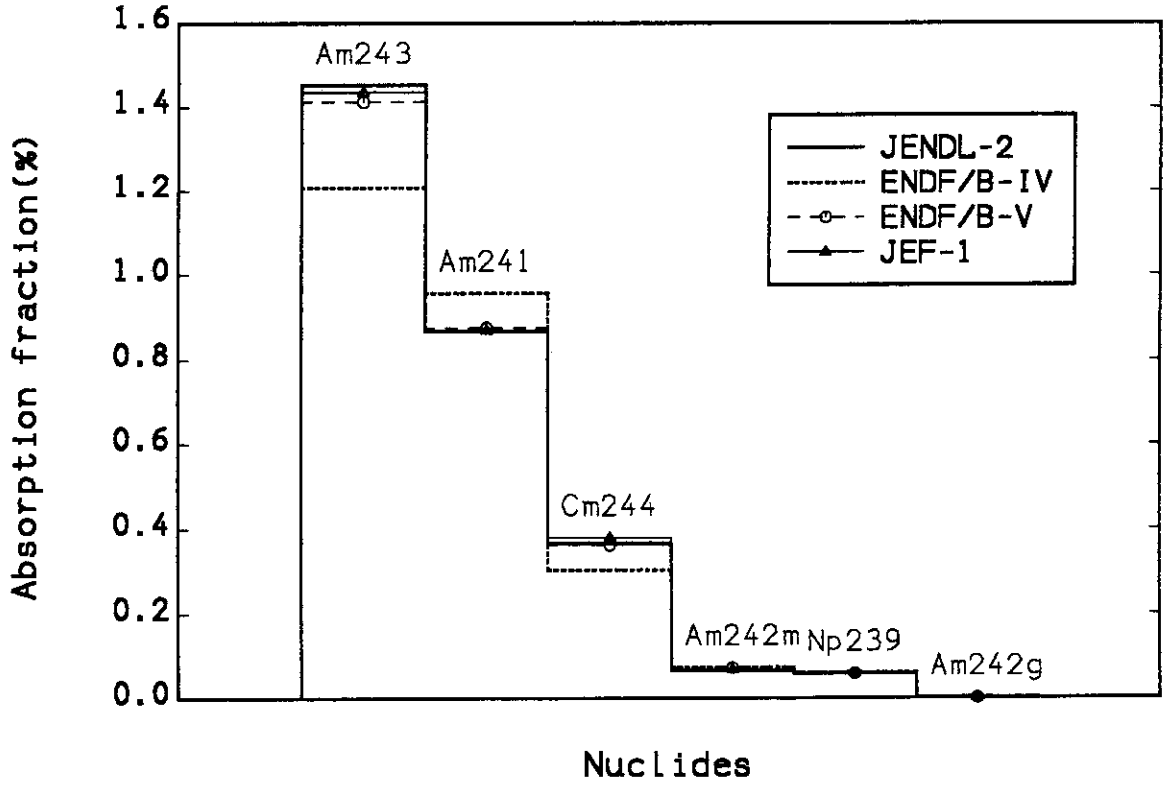

Fig. 33 Comparison of fractional absorptions for minor actinides at burnup state of 50GWd/t.

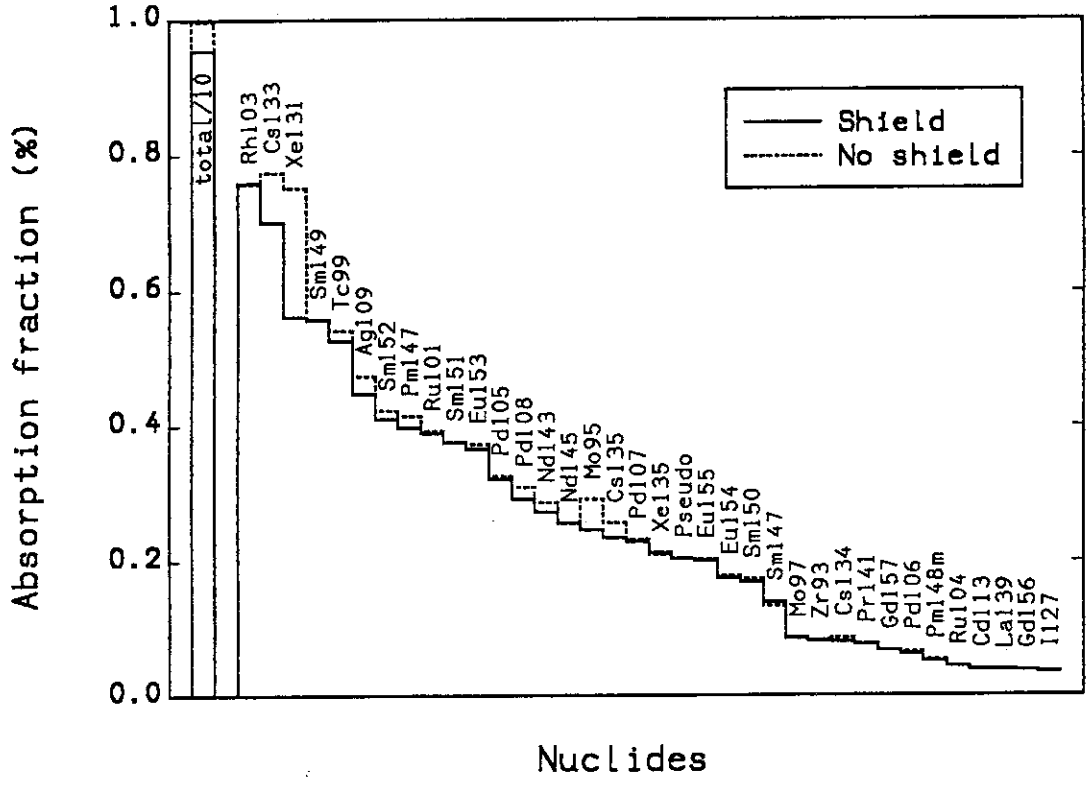

Fig. 34 Contributions of fission products to the total absorption rate with and without self shielding effect (Vm/Vf=0.74, 50GWd/t).

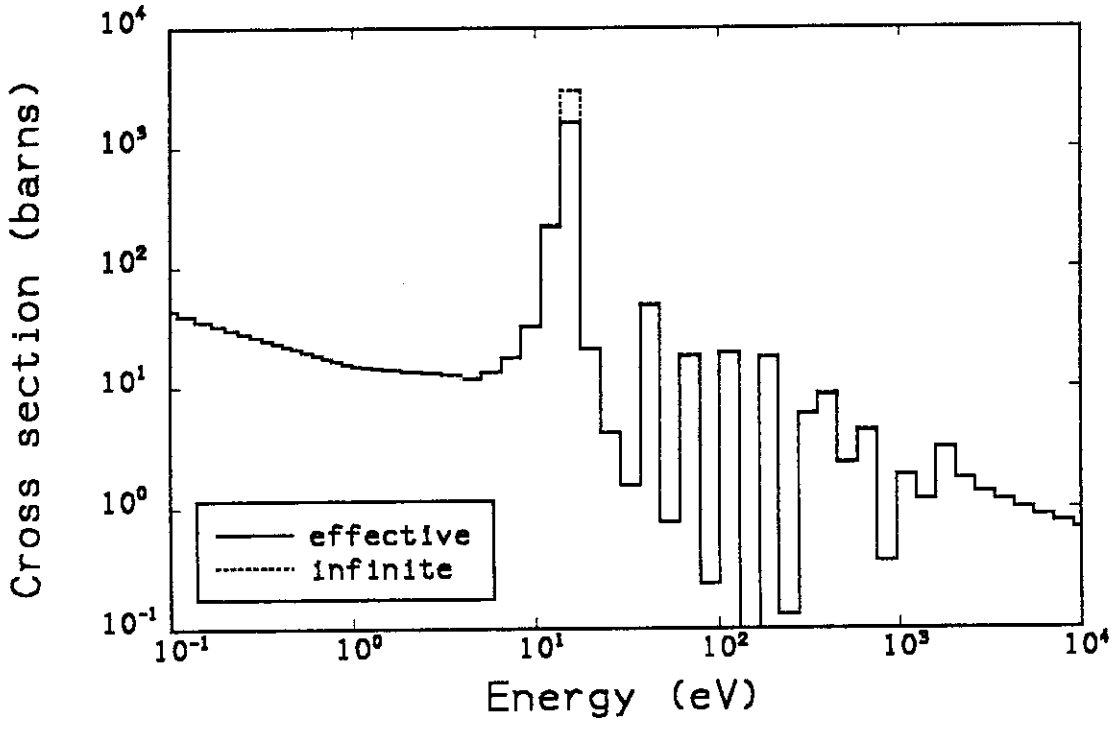

Fig. 35 Comparison of inifinite dilute and shielded group cross sections of Xe-131 for the cell of Vm/Vf=0.74 at 50GWd/t.

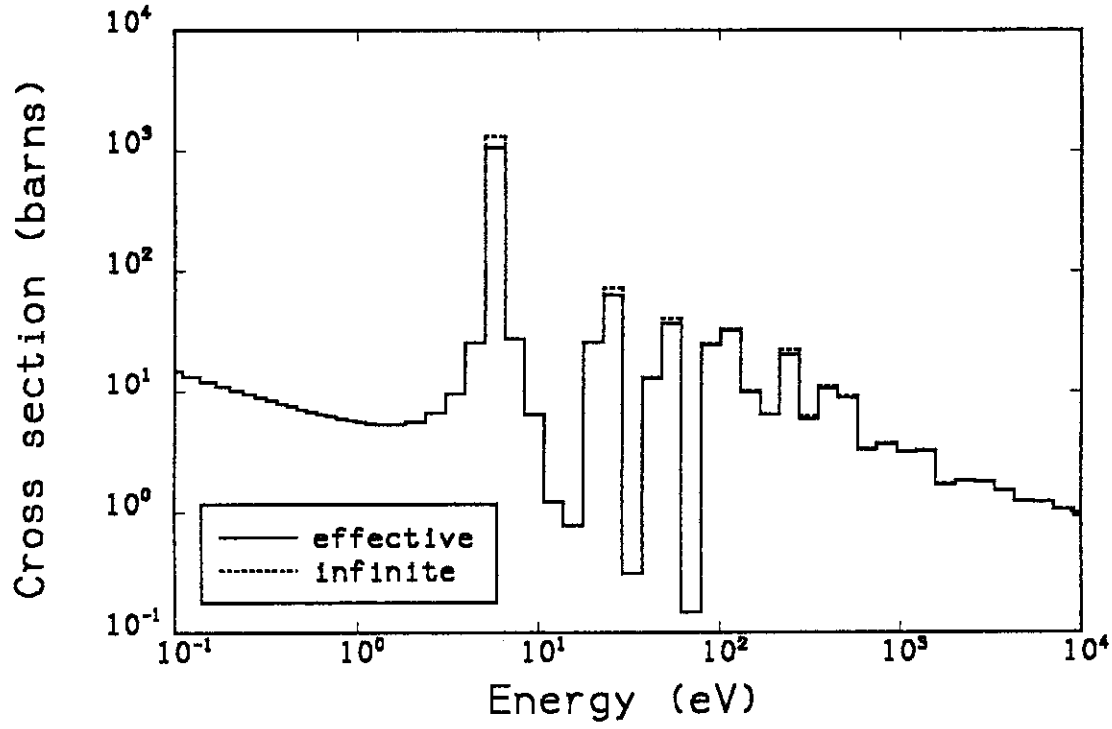

Fig. 36 Comparison of inifinite dilute and shielded group cross sections of Cs-133 for the cell of Vm/Vf=0.74 at 50GWd/t.

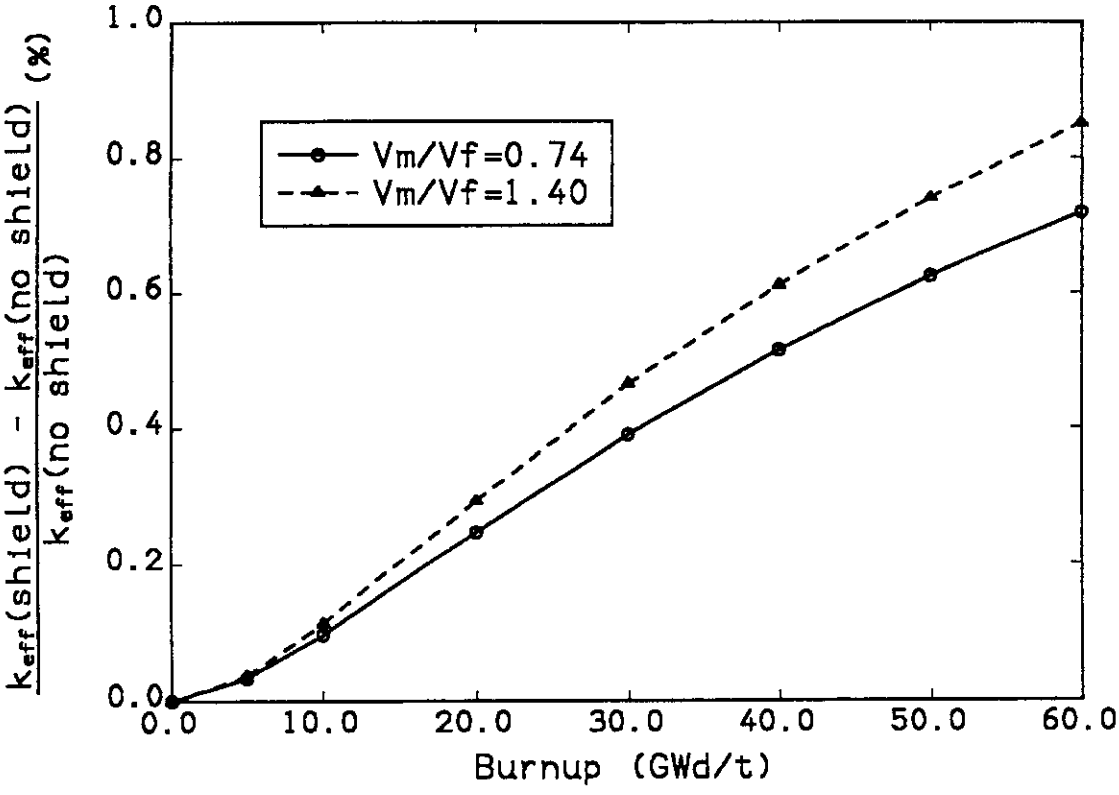

Fig. 37 The effect of resonance shielding for fission products on the multiplication factors.

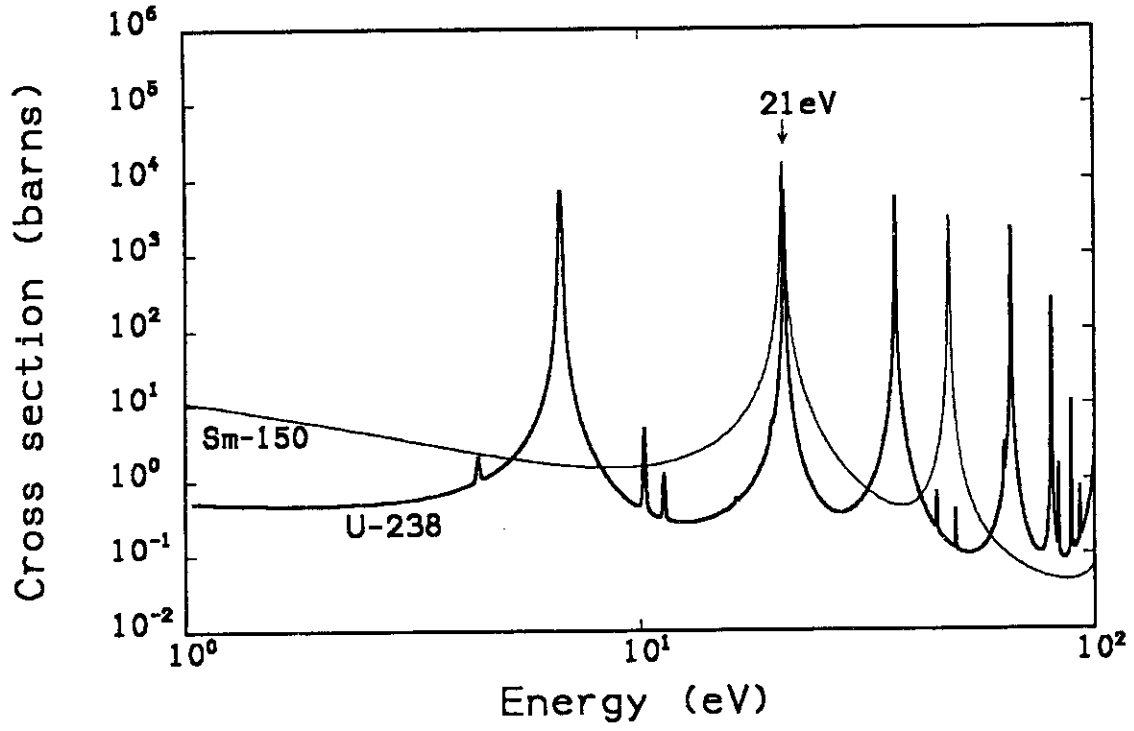

Fig. 38 Comparison of resonance capture cross sections for U-238 and Sm-150.

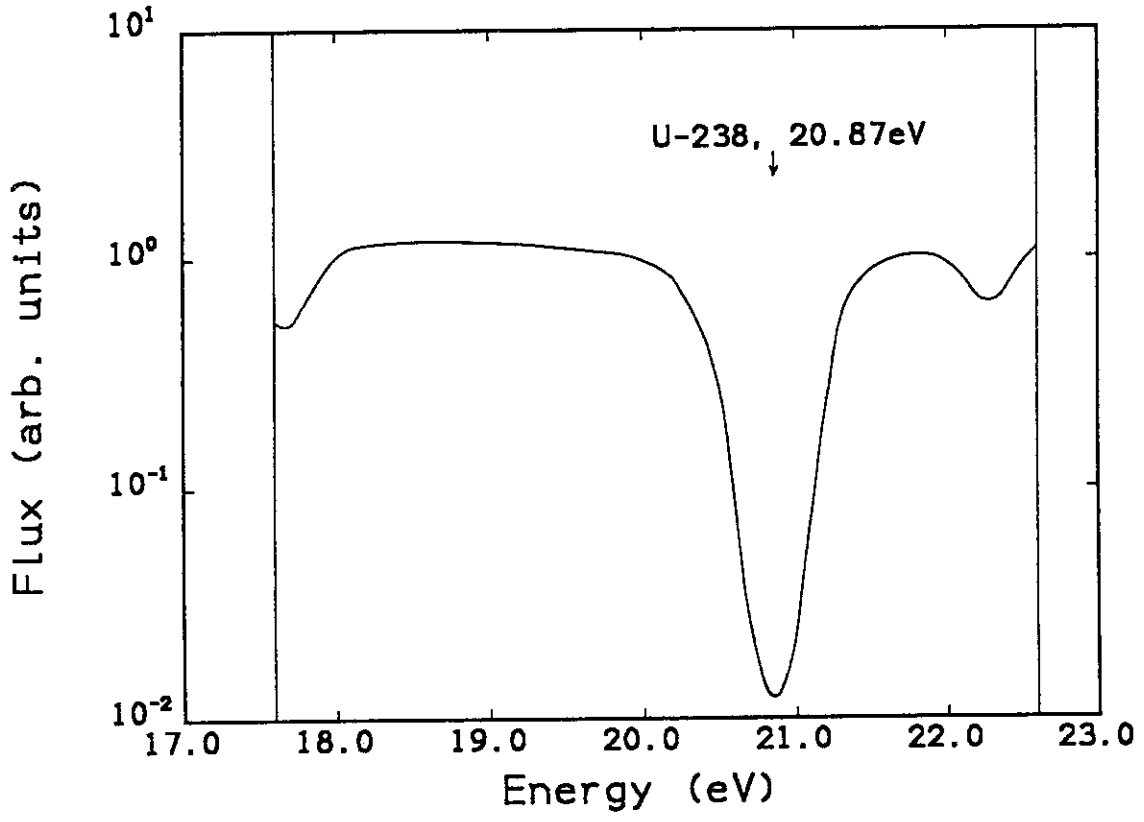

Fig. 39 Neutron flux calculated with PEACO at the burnup state of 50 GWd/t.

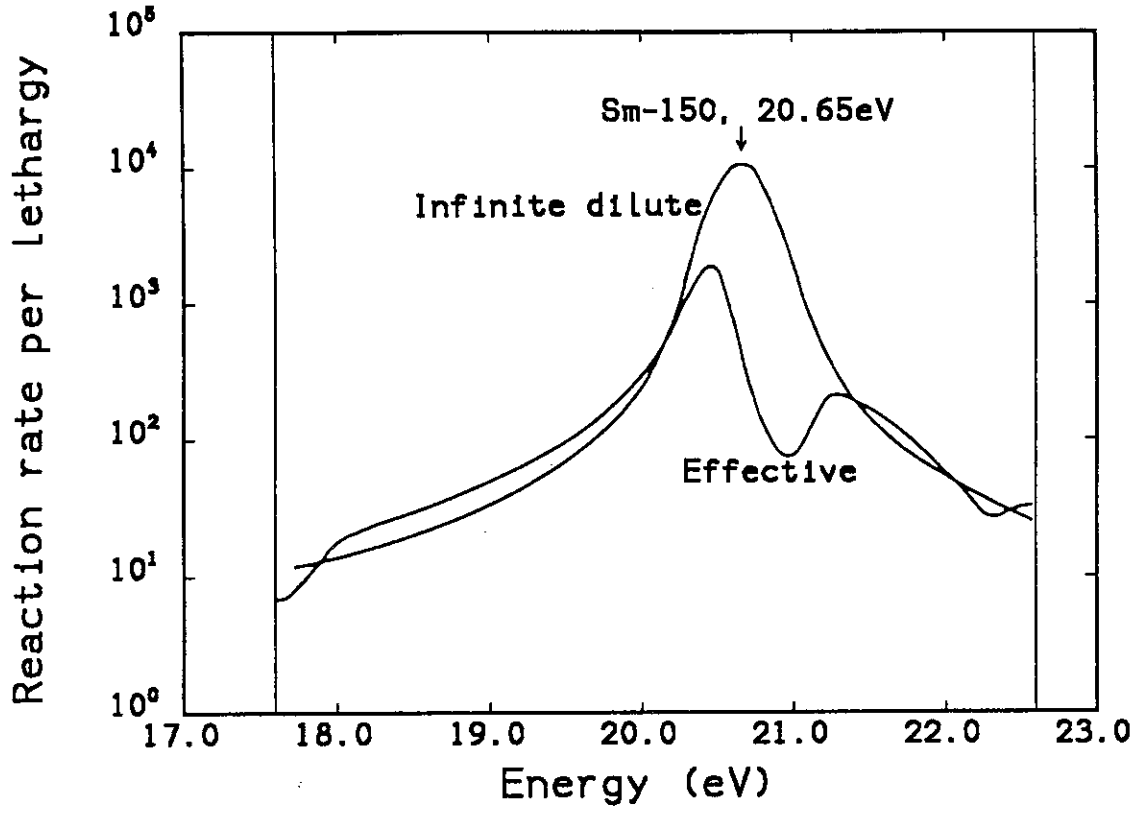

Fig. 40 Capture reaction rate of Sm-150 calculated with the ultra fine group method at 50GWd/t in the 17.6 to 22.6eV energy group.

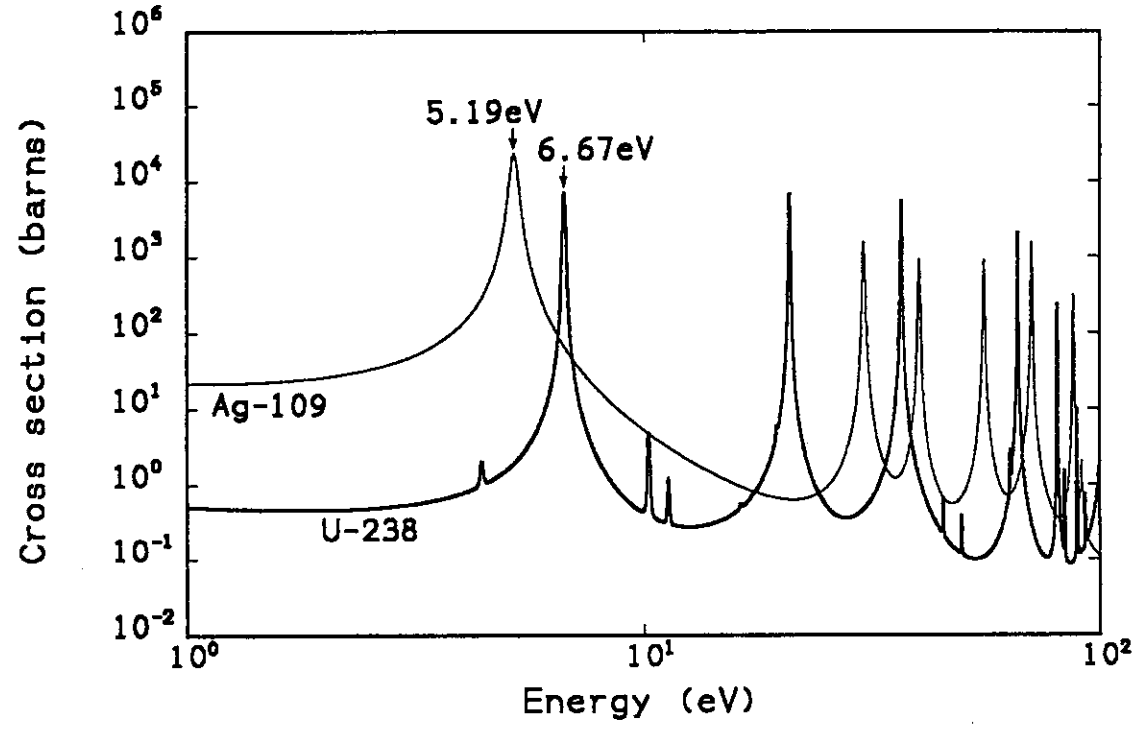

Fig. 41 Comparison of resonance capture cross sections for U-238 and Ag -109.

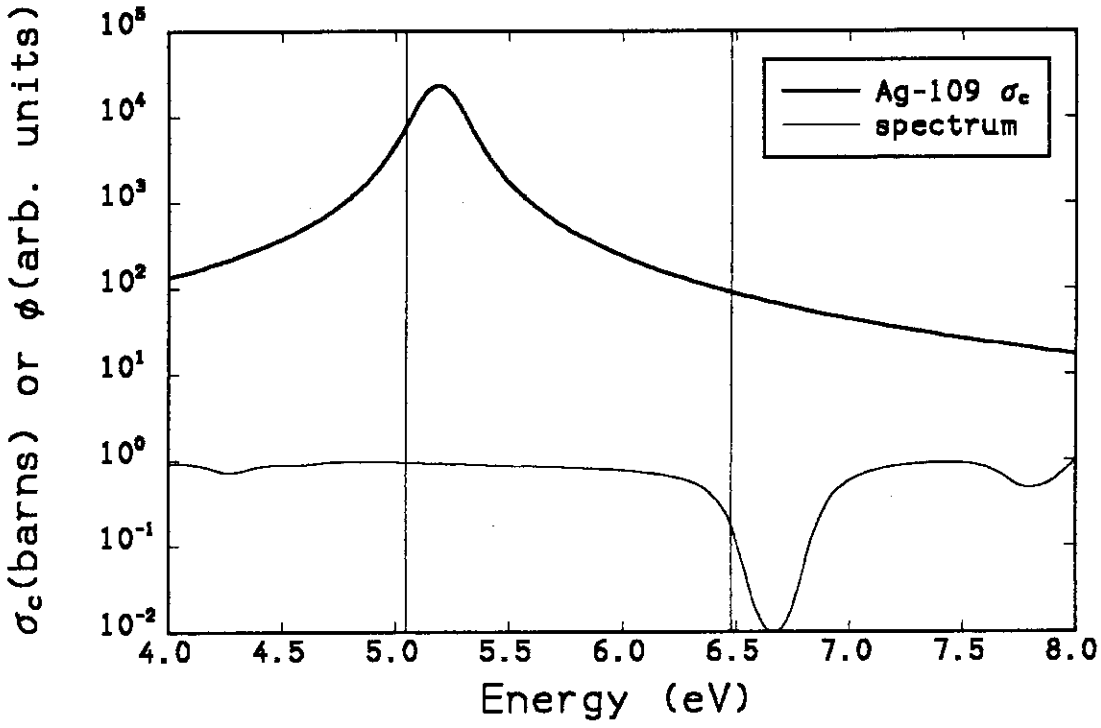

Fig. 42 Capture cross section of Ag-109 and neutron spectrum calculated by the ultra fine group method.

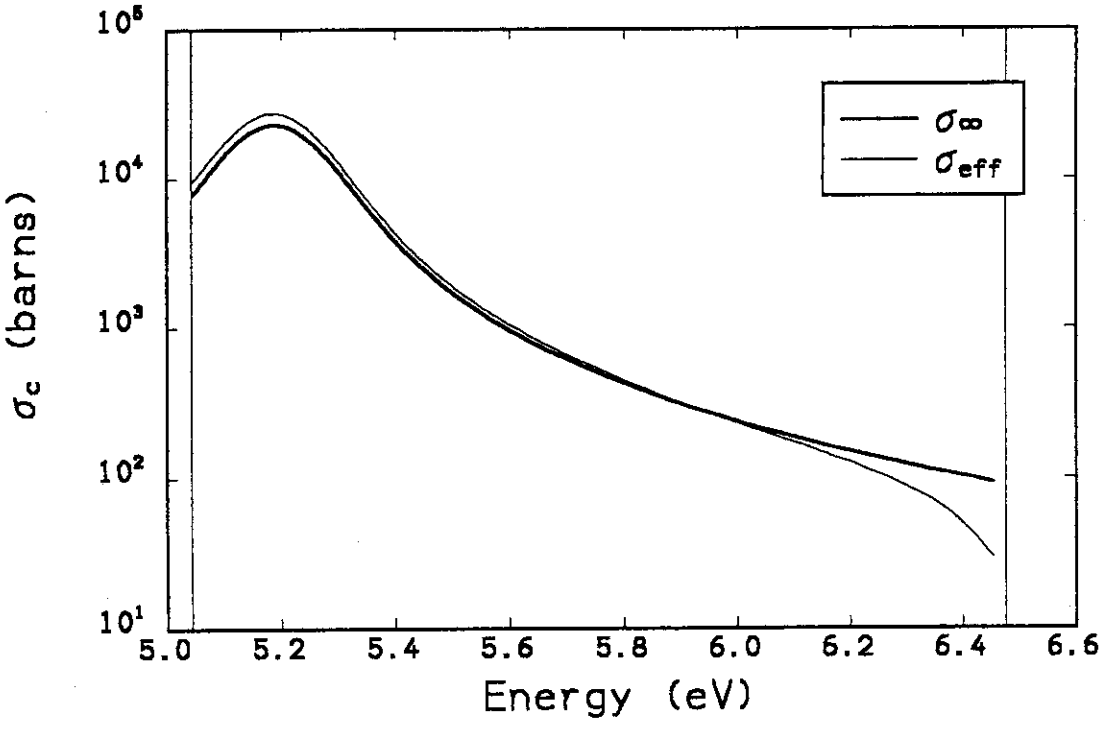

Fig. 43 Infinite dilute cross section and effective cross section weighted by the ultra fine group neutron spectrum for Ag-109.

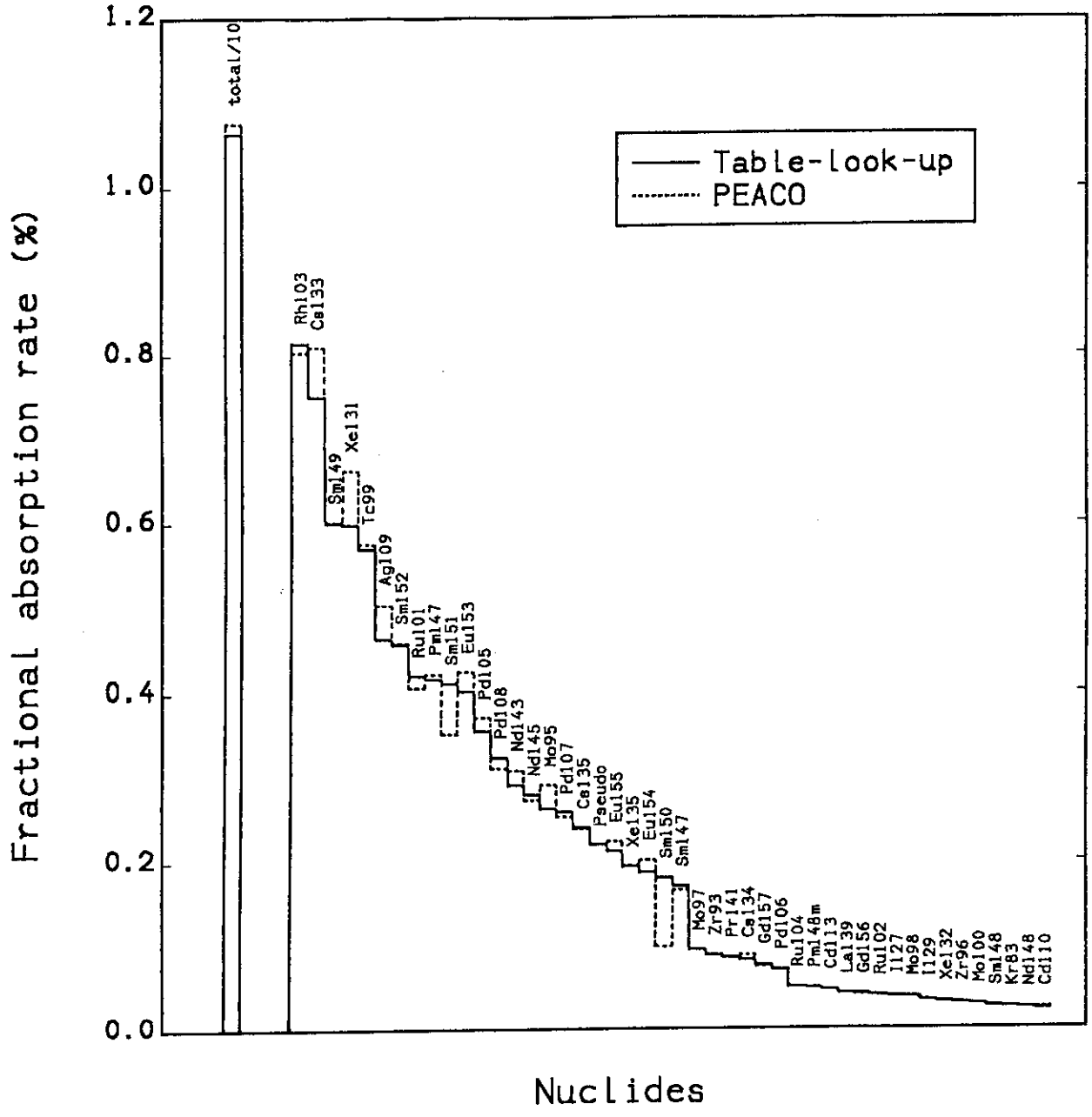

Fig. 44 Fractional absorption rate of FPs calculated with the table-look-up method and ultra fine group method (PEACO) for the cell of Vm/Vf=0.74 at 50GWd/t.

5. Burnup Analysis of PWR Spent Fuel

The accuracy of the SRAC burnup routine and the new burnup data was examined by performing burnup analysis of PWR spent fuels. The calculated results were compared with the results of experimental analysis. The experimental analysis of nuclide composition of PWR spent fuels was made at Department of Chemistry in JAERI[21),22)]. In this measurement, uranium, trans-uranium and FP isotopes were quantitatively analysed for 11 spent fuels of different burnup history. The SRAC calculation was made with Takano's FP chain, the actinide chain of 24 nuclides and the library SRACLIB-JENDL2. The calculations by the widely used burnup code ORIGEN2[23)] and by SRAC-FPGS[24)] were also made for comparison. In the SRAC-FPGS calculation, depletion calculation is made by the burnup code FPGS-3[25)] with the effective cross sections prepared by SRAC. The burnup code FPGS-3 is based on the DCHAIN code. The FPGS-3 code treats generation and transmutation of more than 1000 nuclides. Furthermore, in FPGS-3, the cyclic chain such as

Pu-239→Pu-240→Pu-241→Am-241→Am-242→Cm-242→Pu-238→Pu-239

can be precisely treated. It is therefore possible to directly compare the accuracy of the SRAC burnup calculation with the SRAC-FPGS calculation because the same effective cross sections are used in the both calculations. In the SRAC-FPGS calculation, both the libraries based on JENDL-2 and JENDL-3 were used.

The ORIGEN2 code uses spectrum weighted cross sections calculated for about 230 nuclides. This weighting spectrum should be prepared by the other neutronics calculation code for different reactor and fuel combinations. In the ORIGEN2 code, the cross section data are already prepared for the major reactor types such as PWR, BWR and LMFBR. The fission yield data were available for about 850 FPs. In the ORIGEN2 calculation here, the nuclear data of ENDF/B-IV were used together with the ENDF/B-V data.

Figures 45～47 show the Calculation/Experiment (C/E) values of the fraction of each nuclide to the quantity of initial uranium. In these figures, similar burnup dependence of C/E values is found for almost all nuclides. This dependence is presumably caused by the difference of the position of the spent fuel samples loaded in the core. This difference of loaded position may lead to the difference of neutron spectrum in which fuel samples were irradiated. The burnup calculations were made for the infinite PWR lattice, where the spectrum is an ideal PWR one. If the burnup calculations are needed to be made accurately, the spectrum difference should be taken into account in these calculations. This means that the detailed information about the fuel loading and shuffling patterns is necessary.

In Figs.45-9, 46-4 and 46-6, the amounts predicted with the SRAC burnup calculation are observed larger for the higher isotopes of Pu-242, Am-243 and Cm-244 than those with SRAC-FPGS and ORIGEN. This is caused from the larger depletion rate of U-238 and thus larger production rate of Pu-239 calculated with the SRAC code. As shown in the Figs.45-4 and 45-6, the amounts of U-238 by SRAC are slightly smaller and those of Pu-239 are larger than the SRAC-FPGS results. It should be necessary to further investigate the cause of the discrepancy between SRAC and SRAC-FPGS for the amounts of U-238 and Pu-239.

SRAC seems to well estimate the concentration of FPs evenly for the five nuclides in Figs.47-1～47-5 in comparison with the results by SRAC-FPGS and ORIGEN. It should be noted, however, that SRAC can treat only 65 FPs in the burnup calculation.

In general, the SRAC system is found to predict the amount of the burnup related isotopes in a comparable accuracies with those by the burnup codes, SRAC-FPGS and ORIGEN2.

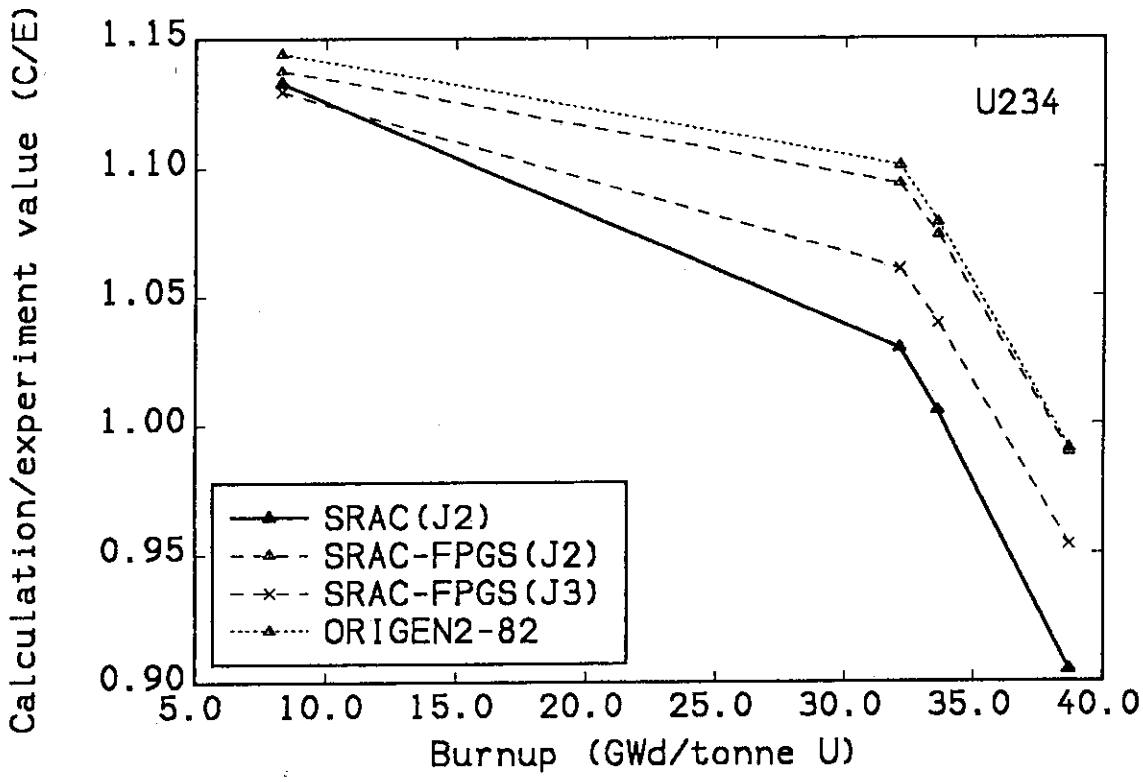

Fig. 45–1 Fractions of U–234 to initial uranium atoms in the PWR spent fuels (Calculation/Experiment (C/E) values).

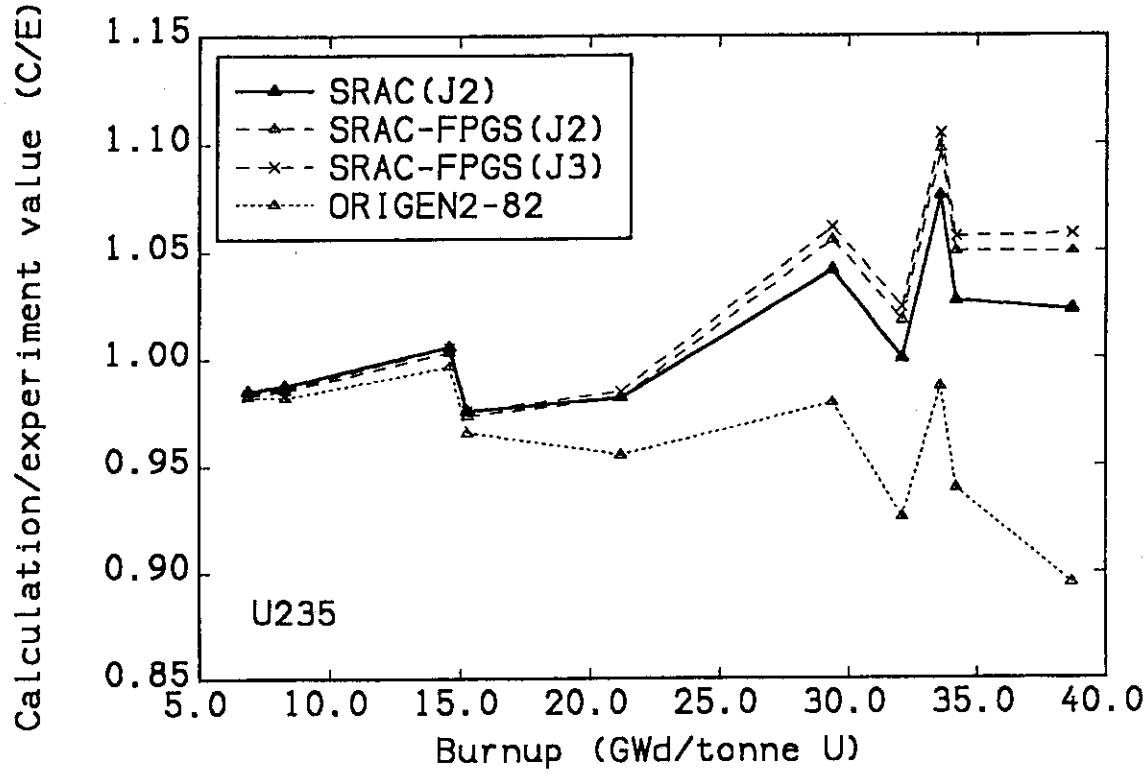

Fig. 45–2 Fractions of U–235 to initial uranium atoms in the PWR spent fuels (C/E values).

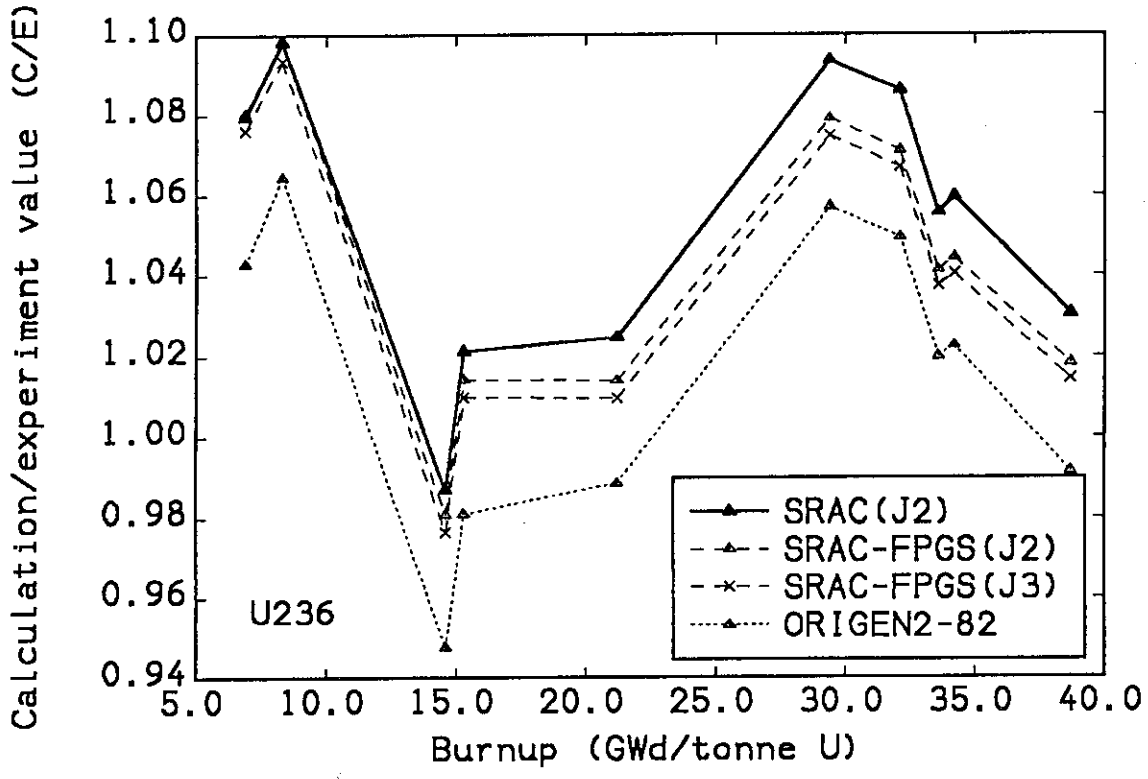

Fig. 45–3 Fractions of U–236 to initial uranium atoms in the PWR spent fuels (C/E values).

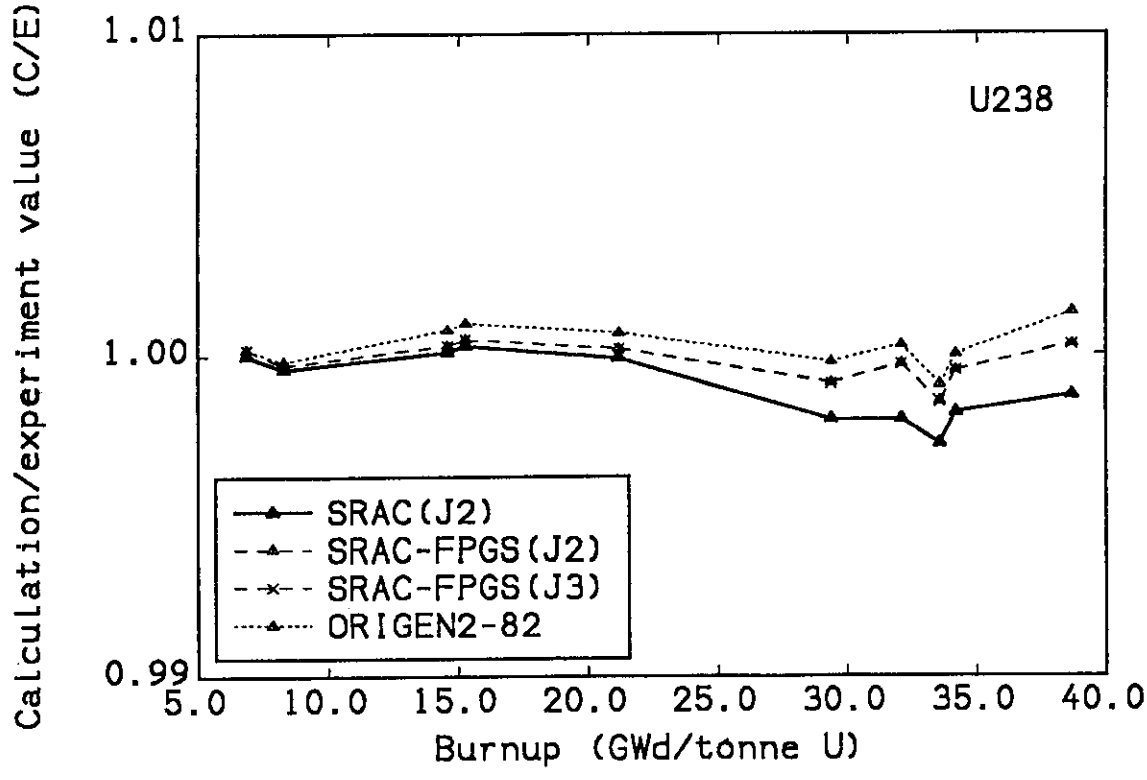

Fig. 45–4 Fractions of U–238 to initial uranium atoms in the PWR spent fuels (C/E values).

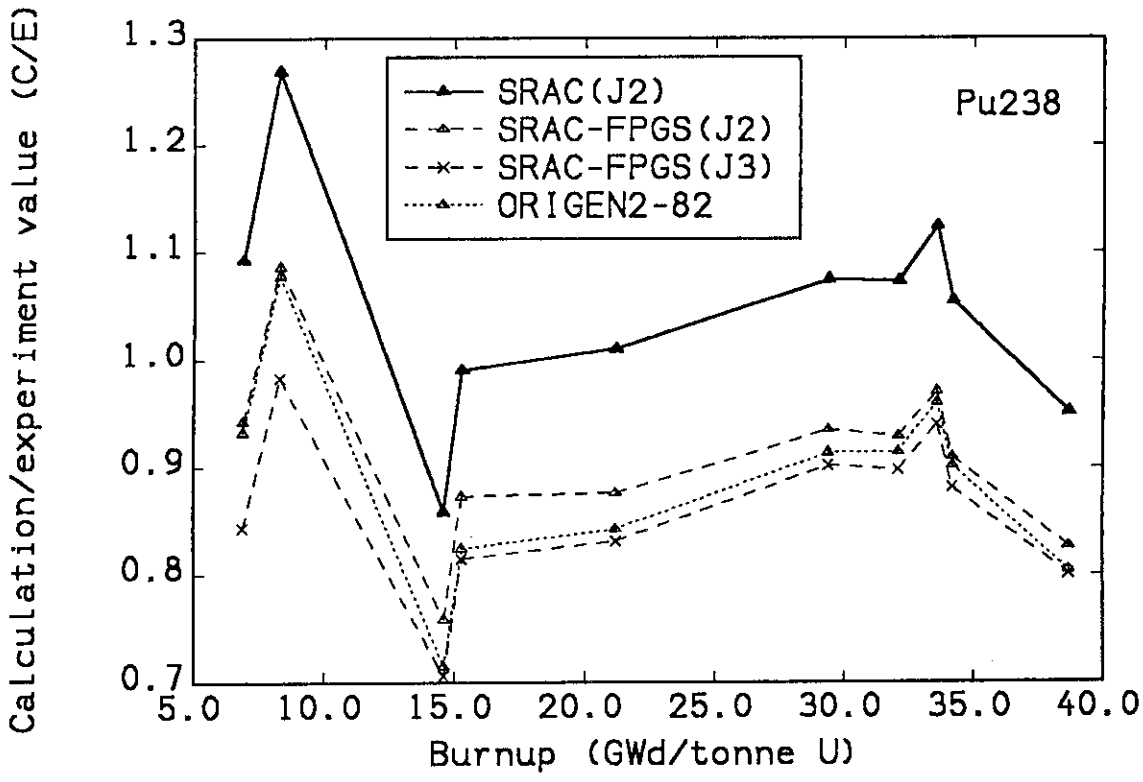

Fig. 45-5 Fractions of Pu-238 to initial uranium atoms in the PWR spent fuels (C/E values).

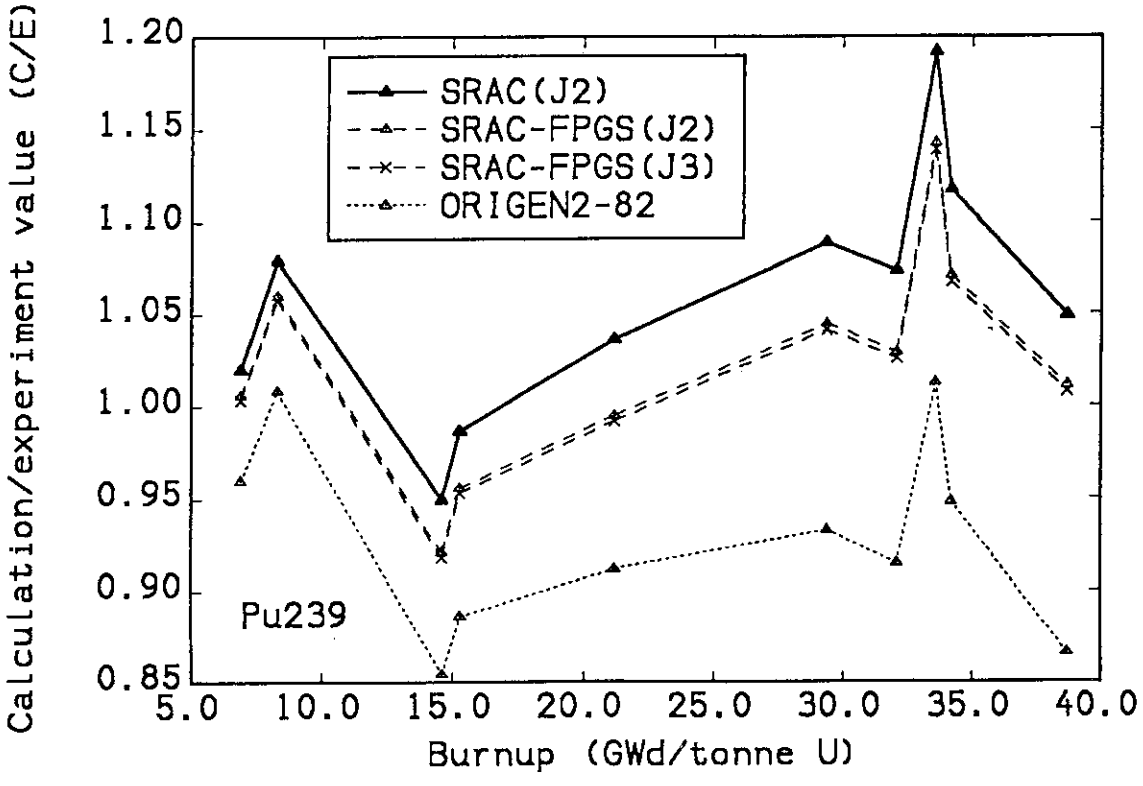

Fig. 45-6 Fractions of Pu-239 to initial uranium atoms in the PWR spent fuels (C/E values).

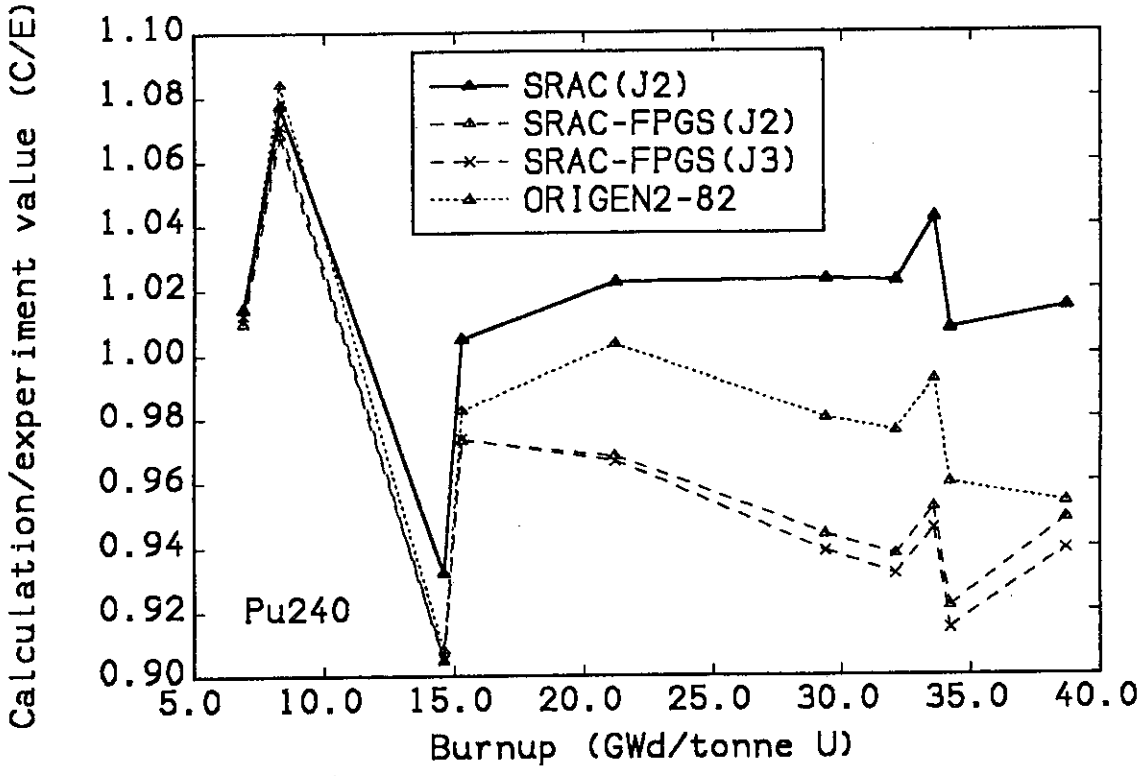

Fig. 45–7 Fractions of Pu–240 to initial uranium atoms in the PWR spent fuels (C/E values).

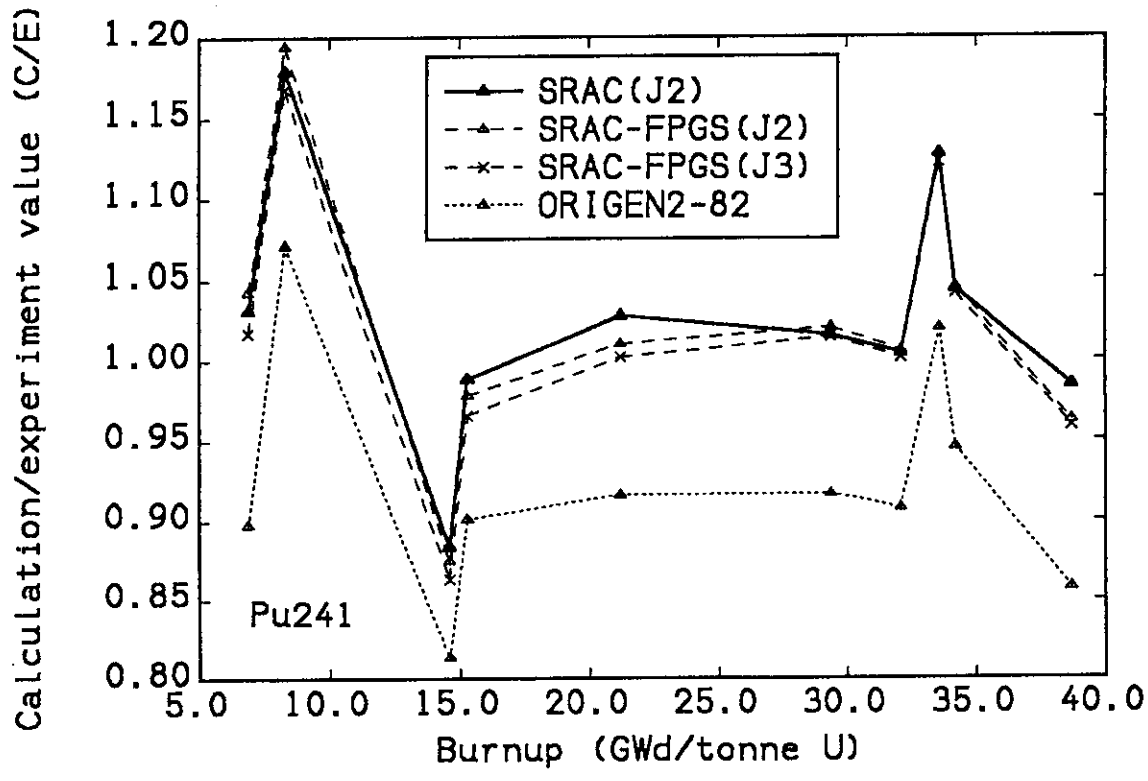

Fig. 45–8 Fractions of Pu–241 to initial uranium atoms in the PWR spent fuels (C/E values).

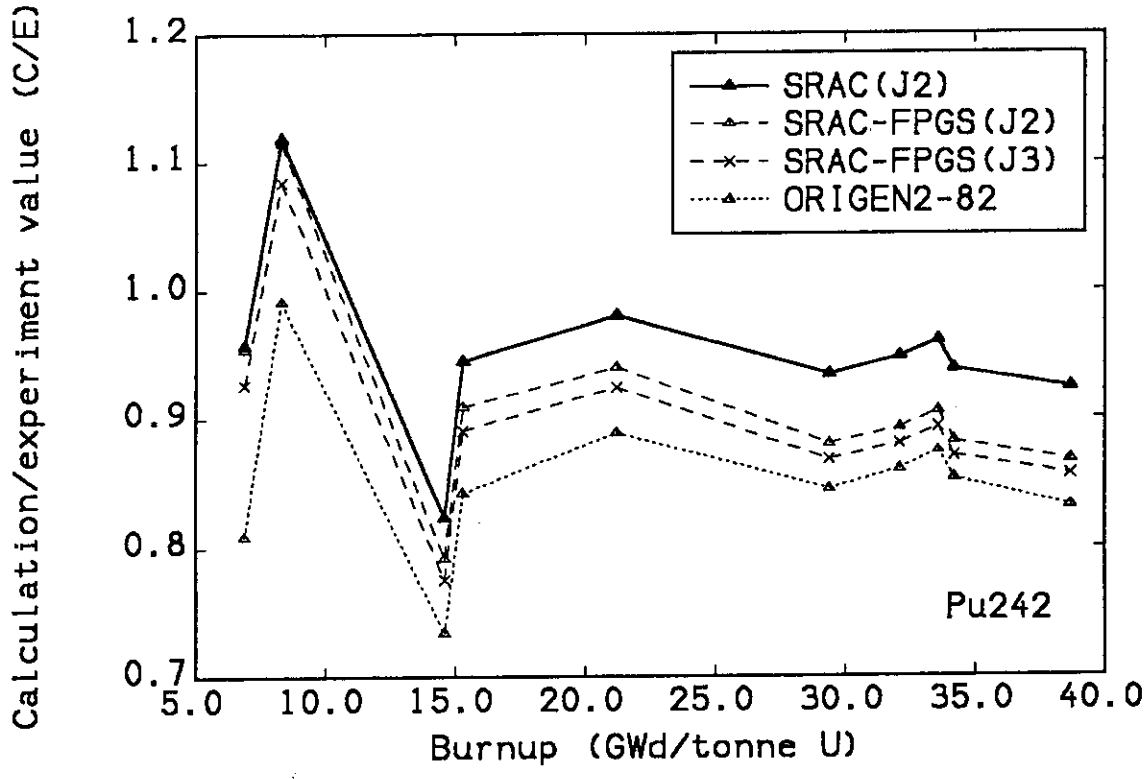

Fig. 45–9 Fractions of Pu–242 to initial uranium atoms in the PWR spent fuels (C/E values).

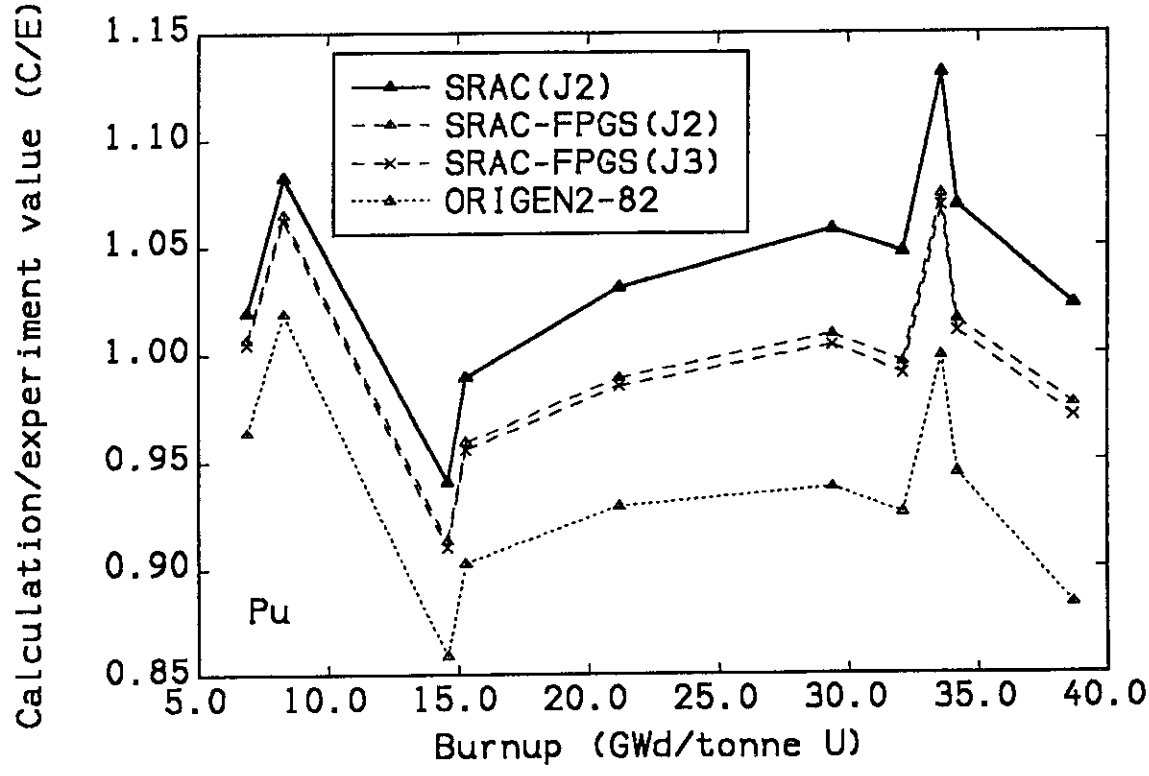

Fig. 45–10 Fractions of Pu to initial uranium atoms in the PWR spent fuels (C/E values).

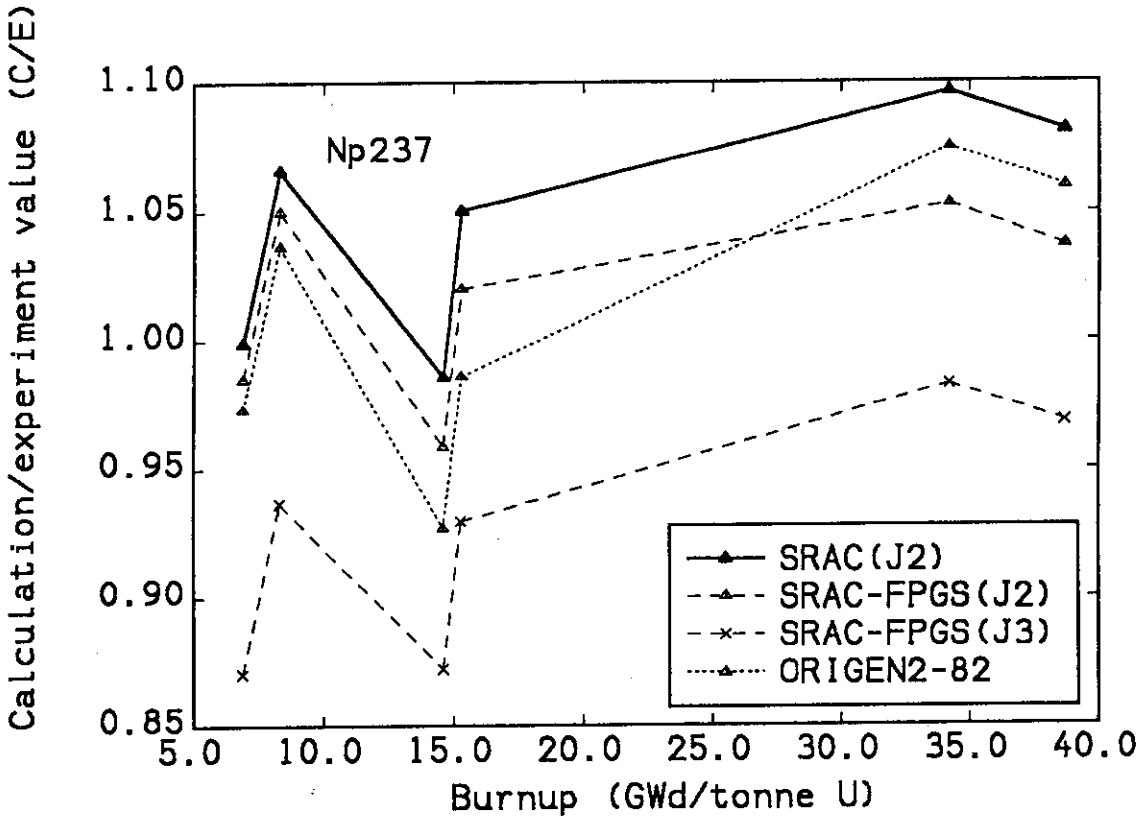

Fig. 46-1 Weight ratios of Np-237/initial uranium in the PWR spent fuels (C/E values).

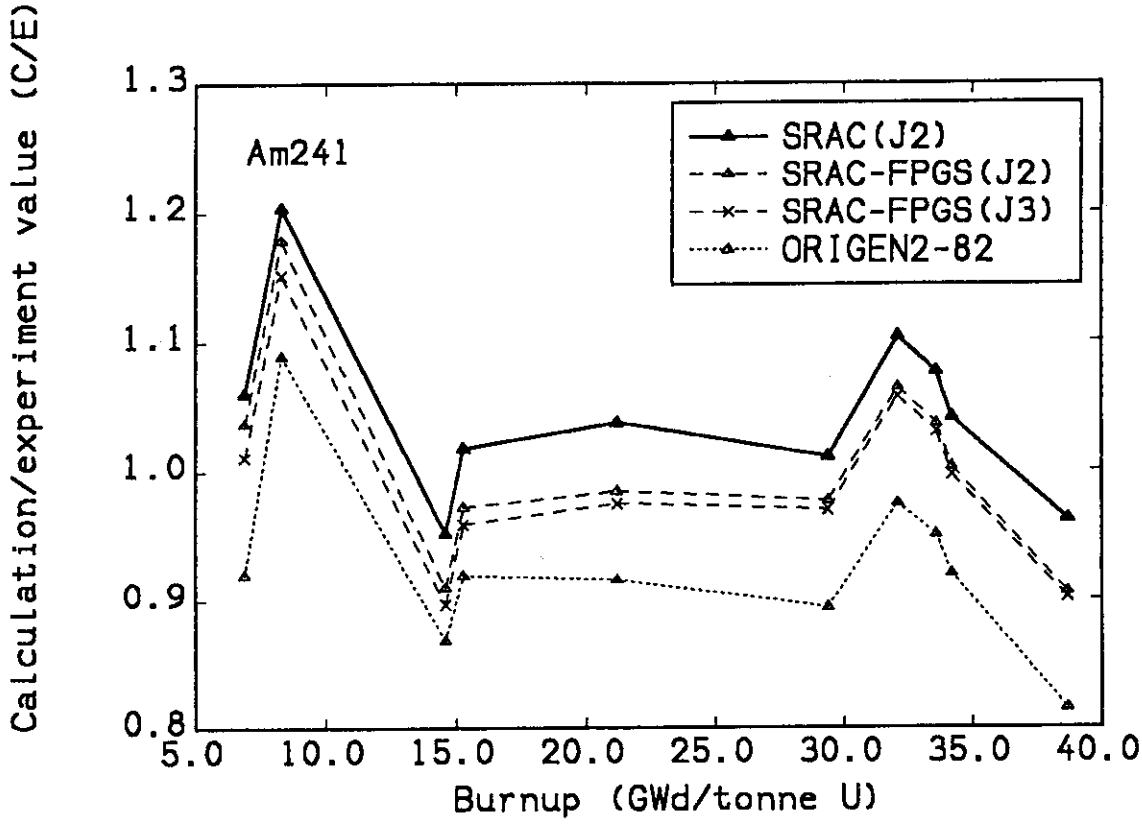

Fig. 46-2 Weight ratios of Am-241/initial uranium in the PWR spent fuels (C/E values).

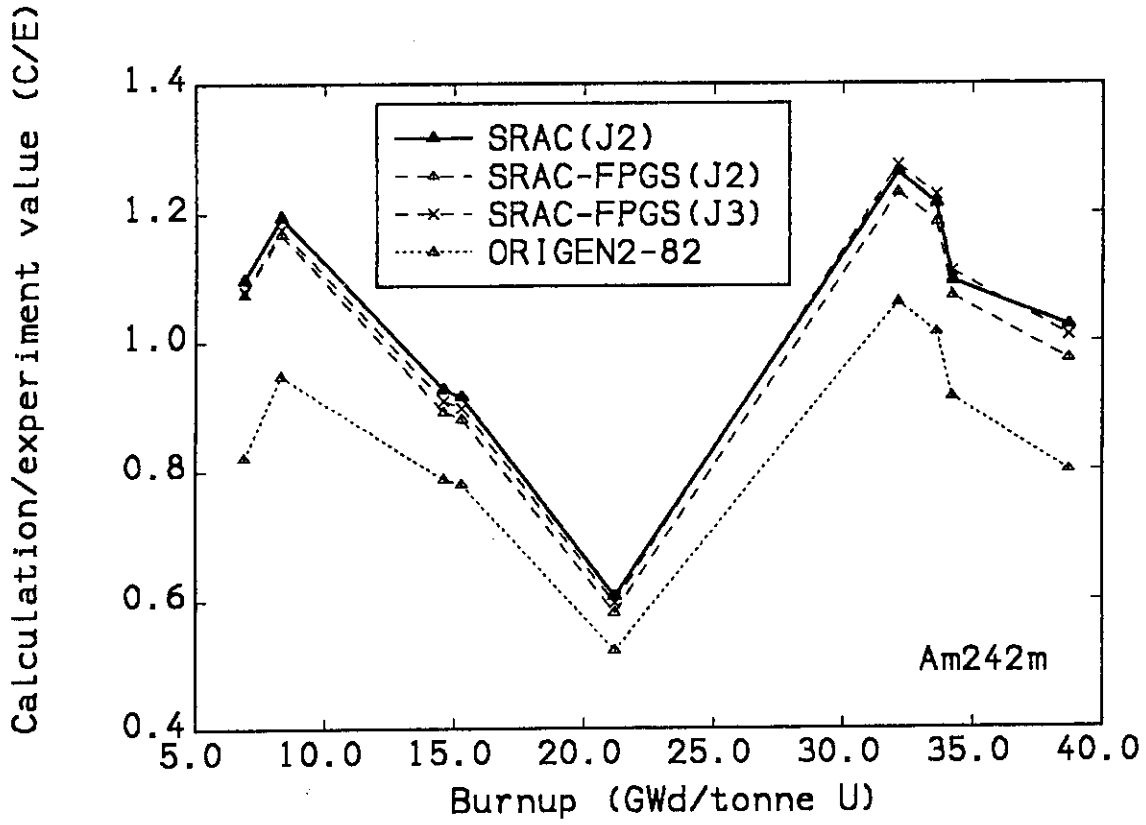

Fig. 46-3 Weight ratios of Am-242m/initial uranium in the PWR spent fuels (C/E values).

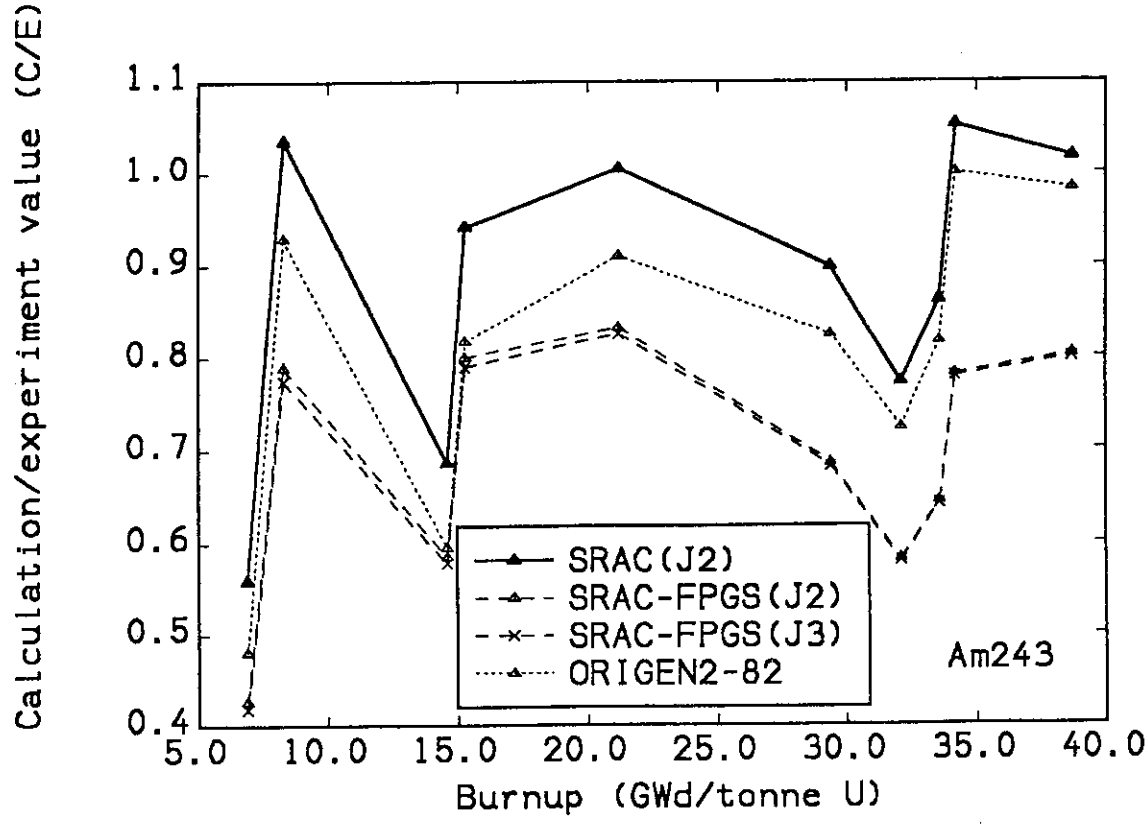

Fig. 46-4 Weight ratios of Am-243/initial uranium in the PWR spent fuels (C/E values).

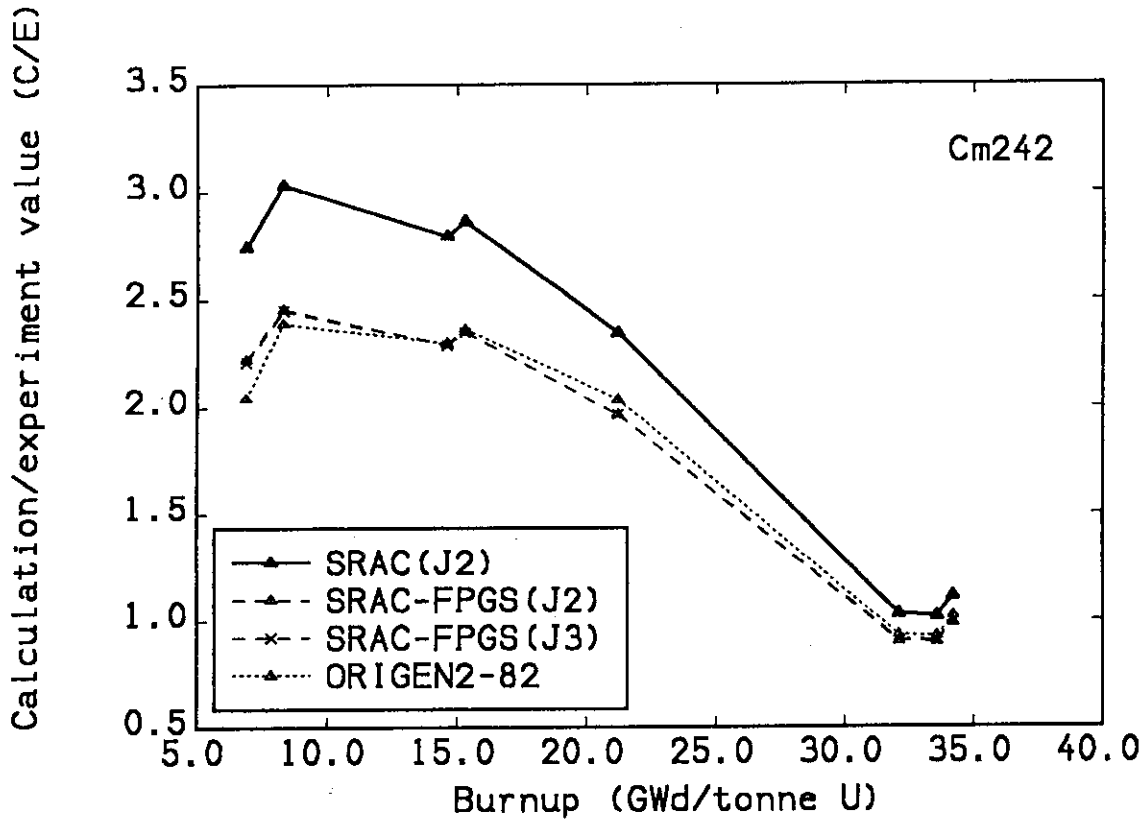

Fig. 46-5 Weight ratios of Cm-242/initial uranium in the PWR spent fuels (C/E values).

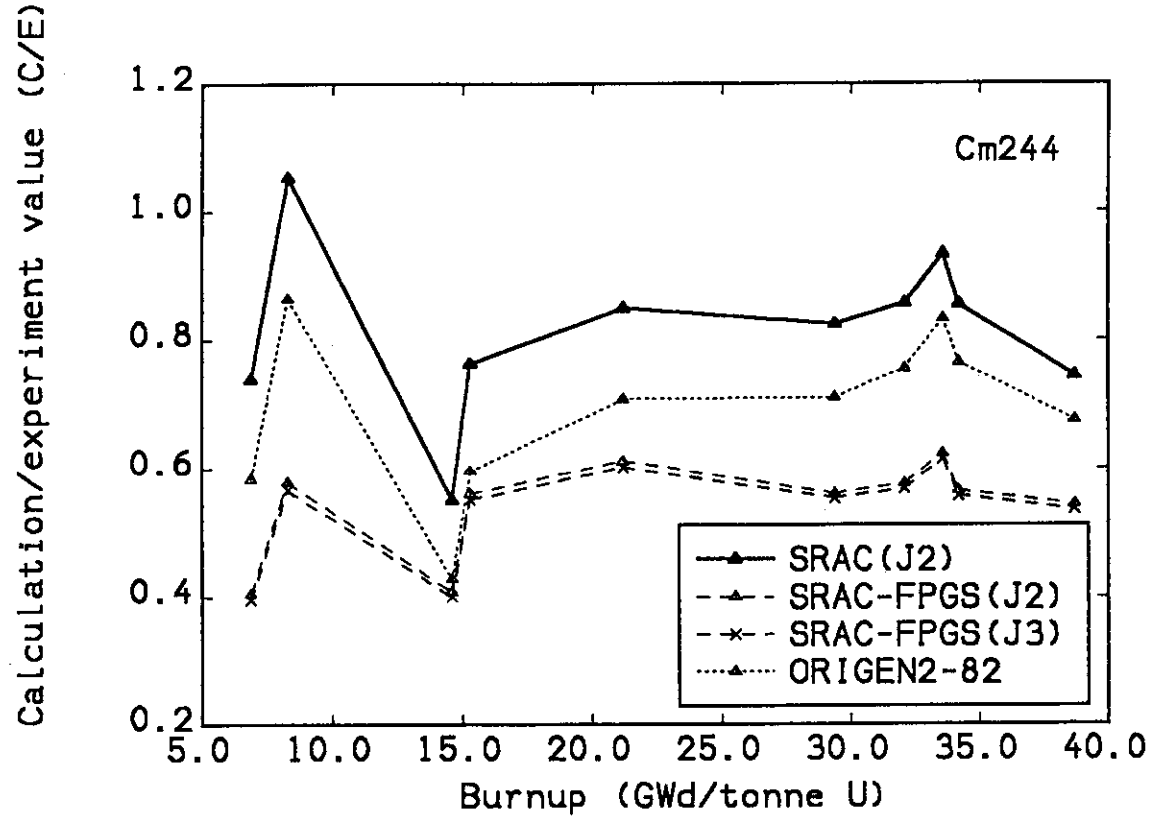

Fig. 46-6 Weight ratios of Cm-244/initial uranium in the PWR spent fuels (C/E values).

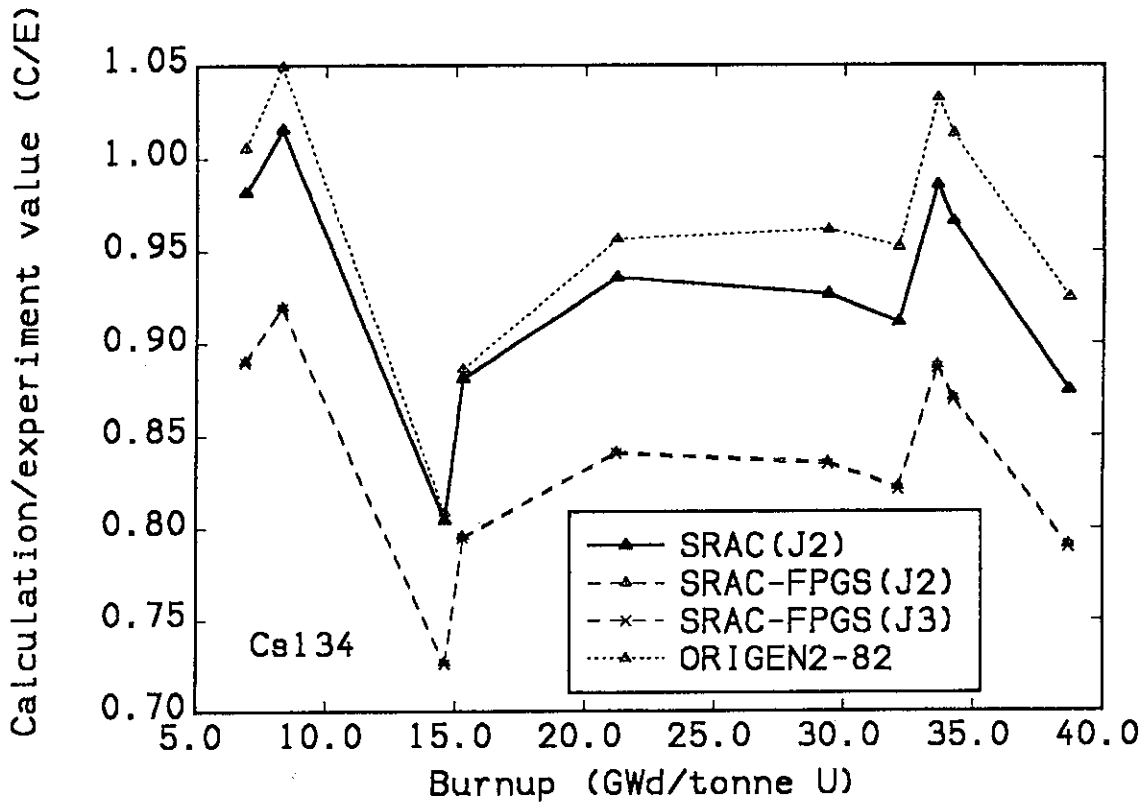

Fig. 47-1 Cs-134 atoms/initial uranium in the spent fuels of PWR (C/E values).

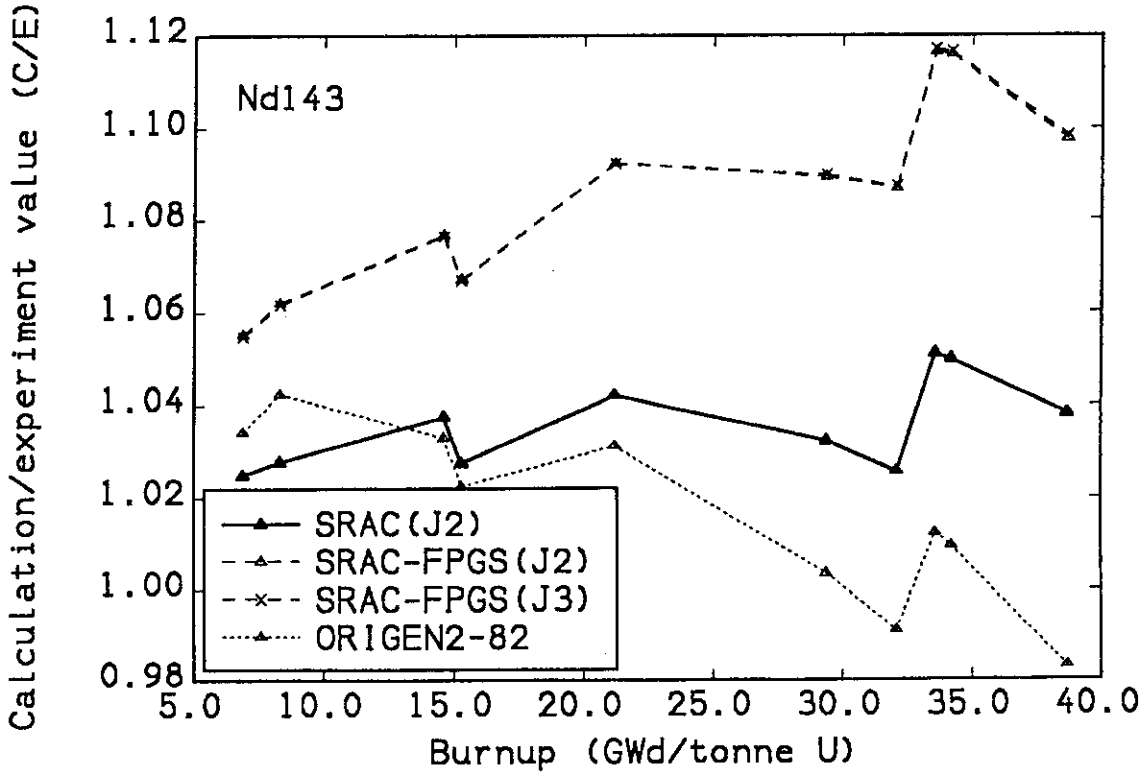

Fig. 47-2 Nd-143 atoms/initial uranium in the spent fuels of PWR (C/E values).

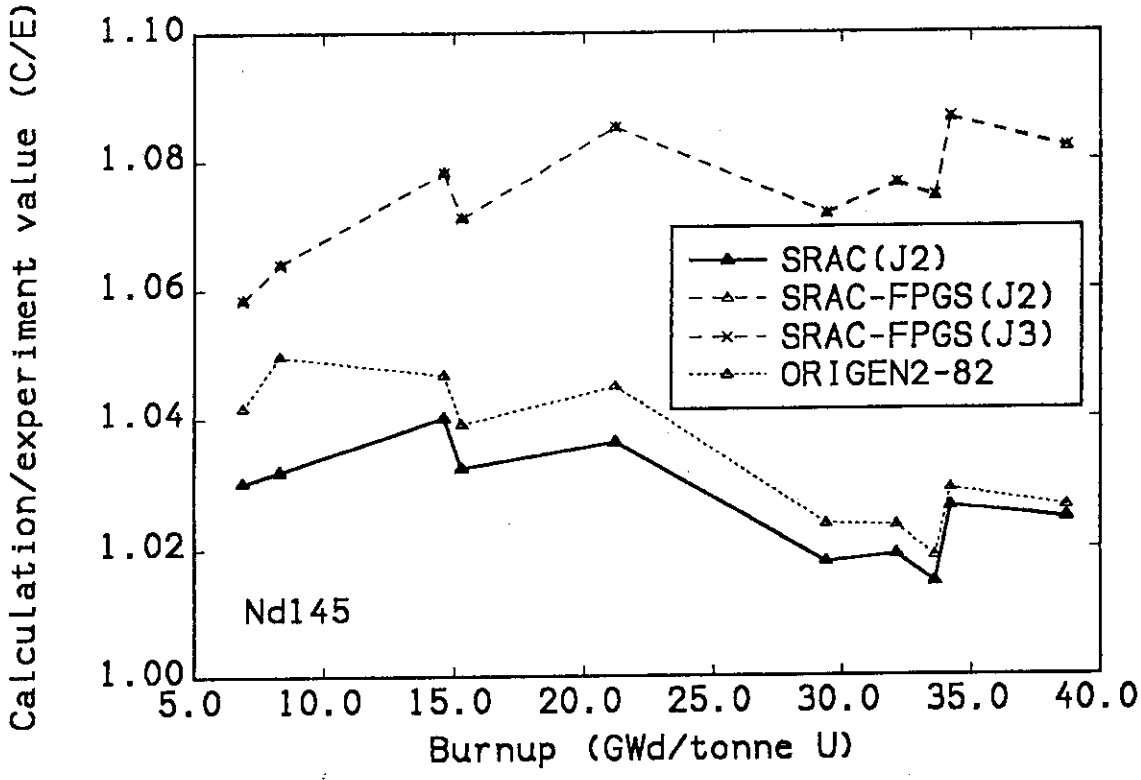

Fig. 47-3 Nd-145 atoms/initial uranium in the spent fuels of PWR (C/E values).

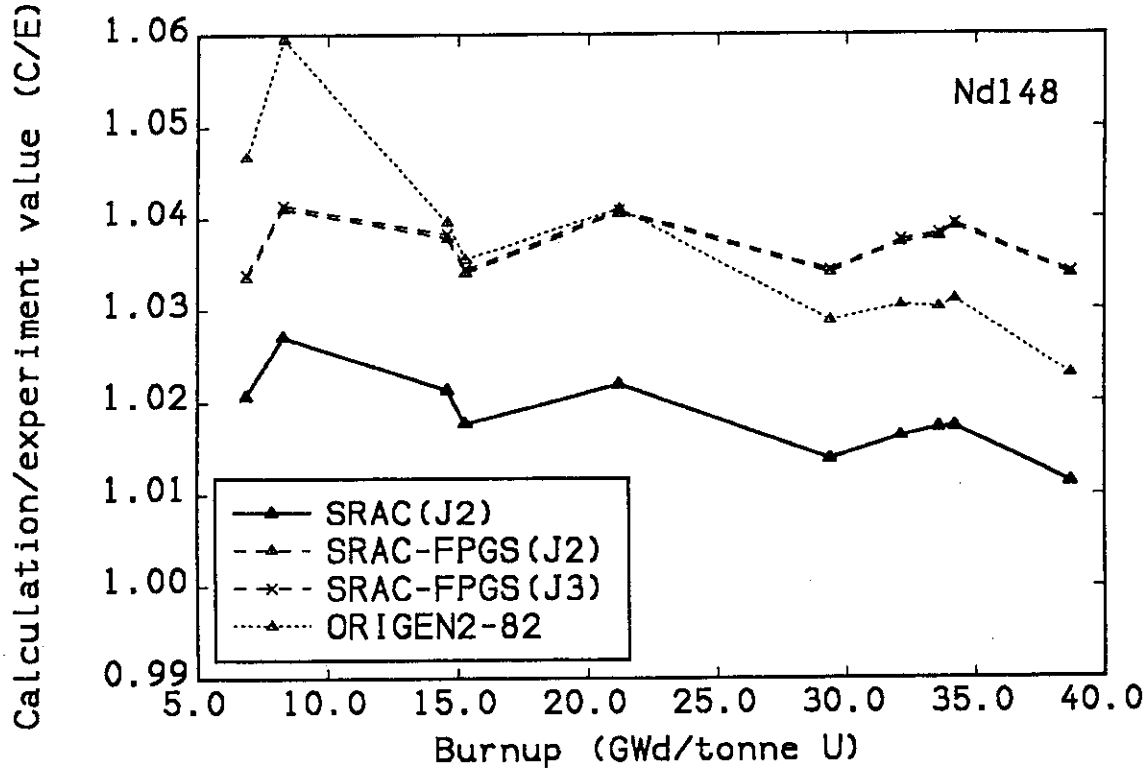

Fig. 47-4 Nd-148 atoms/initial uranium in the spent fuels of PWR (C/E values).

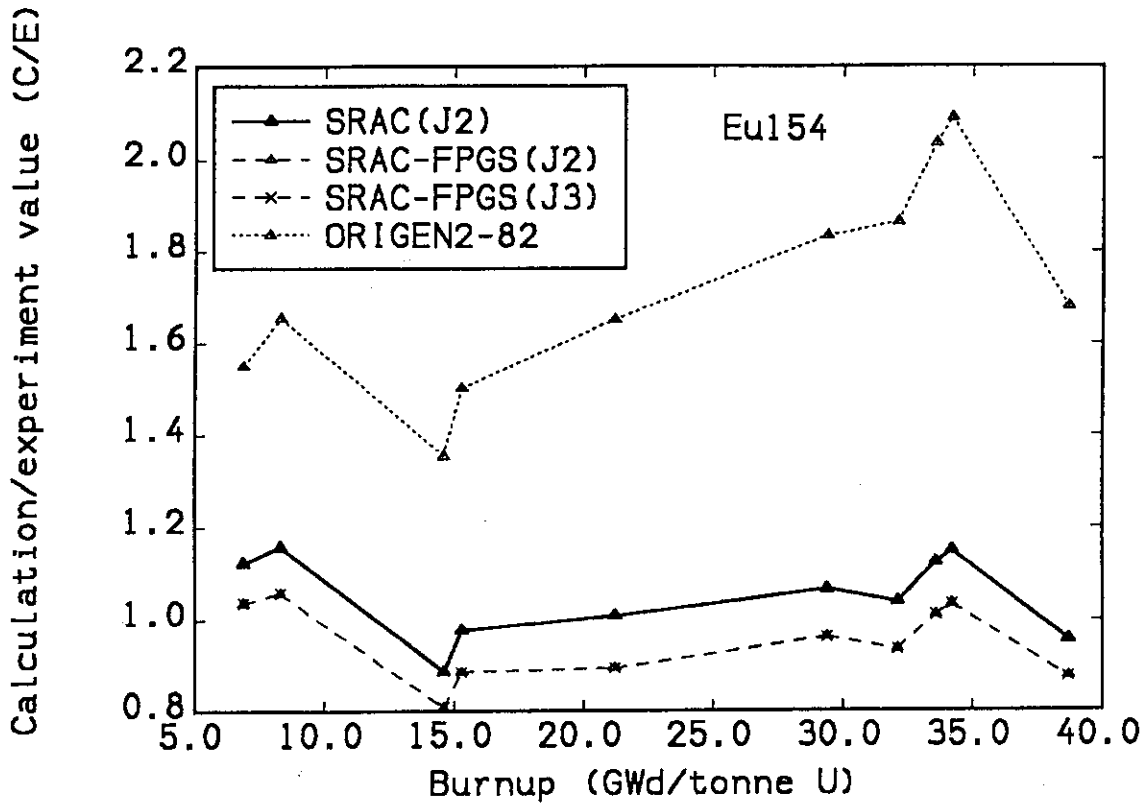

Fig. 47-5 Eu-154 atoms/initial uranium in the spent fuels of PWR (C/E values).

6. New Functions of the Burnup Calculation

6.1 Fission Gas Release

As frequently described in this report, the treatment of FP nuclides is one of the most important problems in the burnup calculation of HCLWRs. Some parts of fission gas products of these FPs, such as noble gases are known to be released from fuel pellet to gas plenum. This release may lead to important contributions on burnup characteristics of HCLWLRs especially at high burnup stage.

In order to investigate this contribution, a new function to treat fission gas release was added to the burnup routine of the SRAC system[26]. In this gas release option, atomic number densities of fission gas product nuclides are controlled to simulate gas release in each burnup step. The nuclides to be released during burnup are the isotopes of Kr, Xe and I. According to the previously calculated fraction of released fission gas, two different number densities, released and remaining, are considered for these fission gas nuclides at each burnup step. Number densities remained in the fuel are used for cell calculation. The released fission gases never react with neutrons. Both released and remained gas products decay into daughter nuclides.

By the fission gas release option of the SRAC system and Takano's FP chain, the effect of gas release on burnup characteristics of HCLWRs was examined[26]. In this study, it was assumed that the burnup and temperature dependence of the gas release fraction in HCLWR oxide fuel was the same as that recommended by the Nuclear Regulatory Commission of USA for safety analysis in LWRs and LMFBRs in 1978[27]. The release fraction is given by

$$F(Bu,\ T)=f(T)+\frac{1-\exp[-0.436\times10^{-4}\ (Bu-20000)\ ]}{1+\frac{0.665}{f(T)}\exp[-1.107\times10^{-4}\ (Bu-20000)\ ]}\cdot[1-f(T)\ ],$$

where $F(Bu,\ T)$ is the fission gas release fraction, $f(T)$ the release fraction at 20000 MWd/t, T the volume-averaged fuel temperature (℃) and Bu the local burnup in megawatt-days per tonne of fuel nuclides.

Figure 48 shows the difference of effective multiplication factors (k_{eff}s) between the cases with and without fission gas release for different values of Vm/Vf. Here, an average fuel temperature of 800℃ is assumed. For Vm/Vf=1.1, contribution of gas release is less than 0.1% Δk/k up to 40GWd/t, and is about 0.3% at 50GWd/t. In harder neutron spectrum, i.e. in tighter lattice or in higher moderator voidage condition, the effect of FP gas release becomes smaller. For this reason, the fission gas release option is removed in the latest SRAC system.

6.2 Constant Flux Burnup

In the SRAC system, a burnup calculation is performed under the condition of constant (time independent) power (see Chapter 2). But, this assumption may not be valid, for example, in the situation to create burnup dependent macroscopic cross section table of a blanket region. In this situation, the power actually increases with the accumulation of fissile Pu. Hence, a model using the power level proportional to $\Sigma_f=\sum N_n\sigma_{f,n}$ (i.e. constant flux condition) was newly incorporated into the SRAC system as a better approximation for the blanket cell calculation.

Production of each Pu isotope in a blanket cell was investigated with two different conditions of constant power and constant flux[28]. Based on the experience of HCLWR burnup analyses, three different

initial linear heat ratings for a blanket fuel pin were assumed, i.e., 17W/cm, 8.5W/cm and 3.4W/cm. Cell burnup calculations were performed up to 10GWd/t for a depleted UO_2 blanket pin cell. Figure 49 shows the burnup dependence of production of each Pu isotope in the case where Vm/Vf is 1.1. Productions of Pu–239 and Pu–240 depend on neither the power models (i.e., constant power and constant flux) nor linear heat rate at all. Those of Pu–241 and Pu–242 considerably depend on them. These are caused by competition of β–decay of Pu–241 (half life time of 14 years) and neutron capture reaction of Pu–240 under the lower flux level in the blanket region. In spite of the large discrepancy on the production of Pu –241 and Pu–242, overall conversion ratio can be accurately evaluated, because the production of Pu–239 and Pu–240 occupy about 90% of total Pu and the fractional production rate in blanket region is relatively small compared to core region.

6.3 Cell Parameter Change during Burnup

For evaluation of void reactivity, temperature coefficient, reactivity control, etc., the COREBN code requires the burnup dependent macroscopic cross section sets for the various cell conditions including normal operating condition. These cross section sets are prepared by the SRAC cell calculations by changing the cell parameter such as moderator void fraction. It is needed in the original SRAC system to prepare as many input data as the number of burnup steps $\times$ the number of cell conditions, in addition to a cell burnup calculation for a normal operating condition.

The burnup dependent fuel compositions in such calculations are the same as a normal operating condition. It is therefore possible to sequentially perform the calculations of the same cell condition for different burnup steps. A new burnup calculation option was installed in the SRAC system for the purpose of performing such a sequence of cell calculations. Depletion calculations are not actually performed in this calculation process. In place of depletion calculation, the atomic number densities of depleting nuclides at each 'burnup step' are automatically fed, and only a series of cell calculations for these steps are made. The atomic number densities are usually calculated by the SRAC cell burnup under a normal operating condition, but any other density set can be used. This new calculation option is therefore effective not only for the core burnup calculations by the COREBN code, but also for cell parametric survey calculations such as fuel enrichment and composition survey.

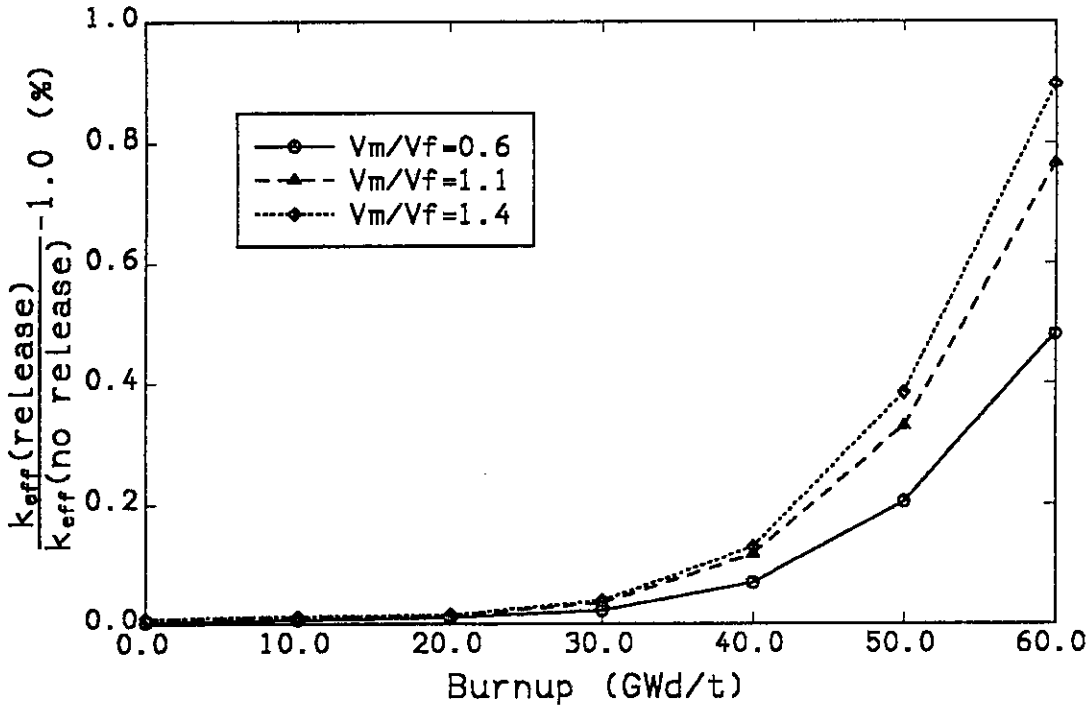

Fig. 48 Difference of effective multiplication factors (k_{eff}s) with and without fission gas release effect.

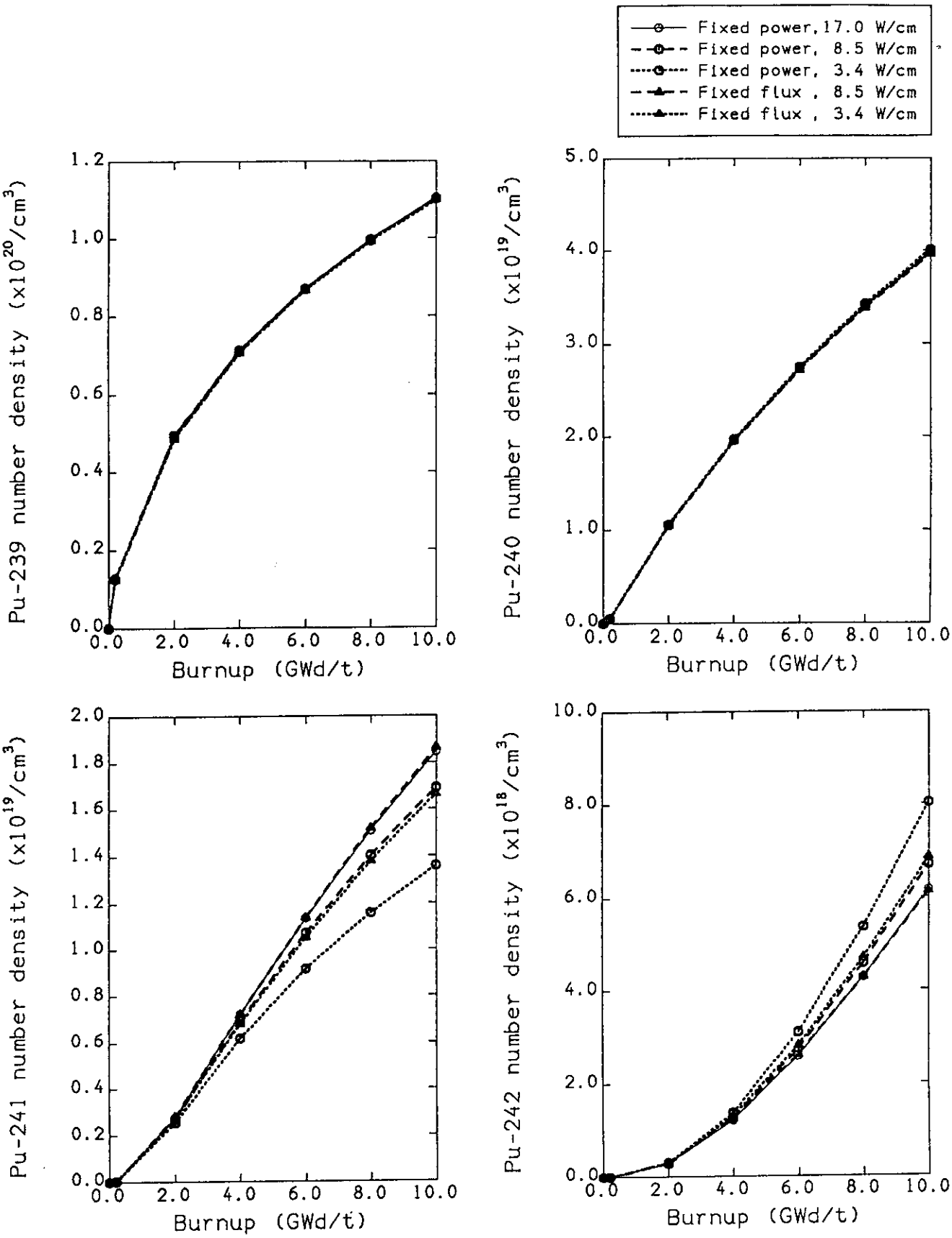

Fig. 49 Production of Pu isotopes in the blanket cell calculated with fixed power and fixed flux conditions (Vm/Vf=1.1). For the fixed flux cases, linear heat rating is an initial value.

7. Conclusion

In HCLWR neutronics calculations, prediction of burnup characterstics is one of the most important problems. Particularly, FPs and minor actinides must be treated in detail as compared with the conventional LWR calculations. New burnup chain models were developed to treat FP and actinide nuclides accurately. Burnup data, such as fission energies and FP yield, were also revised, based on the latest data evaluated by JNDC working group.

The chain model of 65 FPs and 17 actinides (Takano's model, Figs.8 and 21) is used in our burnup study of HCLWR cells. These chains have been tested in the HCLWR burnup calculations. Additionally, the simple FP chain was also proposed for design calculation of HCLWRs. The results calculated by this chain model agree very well with Takano's model. A detailed actinide chain with 24 nuclides has been implemented in the SRAC code for the burnup calculations of various types of reactors.

The group cross section library, SRACLIB–JENDL2, was generated based on the JENDL–2 nuclear data file. For burnup calculations, group cross sections for FPs and actinides were produced, including the group cross sections of pseudo FPs for several burnup chain models. The self shielding factors were tabulated in the SRACLIB–JENDL2 library for the investigation of the resonance self shielding effect of FPs. Furthermore, the resonance interference effect between FPs and actinides was investigated by using the ultra fine energy group method (PEACO method). The importance of the self shielding effect of FPs was pointed out by these investigations.

A burnup analysis of PWR spent fuels was performed with the new group cross section library and the chain models. In this analysis, it was shown that prediction accuracy obtained by the SRAC system was comparable to those by the burnup codes, SRAC–FPGS and ORIGEN2. It should be further investigated, however, the cause of the discrepancy between SRAC and SRAC–FPGS for the amounts of U–238 and Pu–239.

New functions, such as the constant flux burnup, were added to the SRAC system, mainly for the convenience to yield macroscopic cross sections used in the core burnup calculation. These functions are useful, for example, in the burnup calculation of the core with blankets, and in the evaluation of core void reactivity characteristics at higher burnup stages.

By these revisions and improvements, the SRAC system becomes more reliable and also effective for burnup calculations of HCLWRs and advanced LWRs with high burnup rate.

Acknowledgements

The authors would like to express their thanks to Mr. Hitoshi Ihara of JAERI, who gave them a lot of useful comments on JNDC FP library and also on DCHAIN and FPGS codes. They also would like to thank Dr. Takeo Adachi and the other members of Dissolution Study Group in the Department of Chemistry, JAERI, who gave them information about the PWR spent fuel analysis.

7. Conclusion

In HCLWR neutronics calculations, prediction of burnup characterstics is one of the most important problems. Particularly, FPs and minor actinides must be treated in detail as compared with the conventional LWR calculations. New burnup chain models were developed to treat FP and actinide nuclides accurately. Burnup data, such as fission energies and FP yield, were also revised, based on the latest data evaluated by JNDC working group.

The chain model of 65 FPs and 17 actinides (Takano's model, Figs.8 and 21) is used in our burnup study of HCLWR cells. These chains have been tested in the HCLWR burnup calculations. Additionally, the simple FP chain was also proposed for design calculation of HCLWRs. The results calculated by this chain model agree very well with Takano's model. A detailed actinide chain with 24 nuclides has been implemented in the SRAC code for the burnup calculations of various types of reactors.

The group cross section library, SRACLIB–JENDL2, was generated based on the JENDL–2 nuclear data file. For burnup calculations, group cross sections for FPs and actinides were produced, including the group cross sections of pseudo FPs for several burnup chain models. The self shielding factors were tabulated in the SRACLIB–JENDL2 library for the investigation of the resonance self shielding effect of FPs. Furthermore, the resonance interference effect between FPs and actinides was investigated by using the ultra fine energy group method (PEACO method). The importance of the self shielding effect of FPs was pointed out by these investigations.

A burnup analysis of PWR spent fuels was performed with the new group cross section library and the chain models. In this analysis, it was shown that prediction accuracy obtained by the SRAC system was comparable to those by the burnup codes, SRAC–FPGS and ORIGEN2. It should be further investigated, however, the cause of the discrepancy between SRAC and SRAC–FPGS for the amounts of U–238 and Pu–239.

New functions, such as the constant flux burnup, were added to the SRAC system, mainly for the convenience to yield macroscopic cross sections used in the core burnup calculation. These functions are useful, for example, in the burnup calculation of the core with blankets, and in the evaluation of core void reactivity characteristics at higher burnup stages.

By these revisions and improvements, the SRAC system becomes more reliable and also effective for burnup calculations of HCLWRs and advanced LWRs with high burnup rate.

Acknowledgements

The authors would like to express their thanks to Mr. Hitoshi Ihara of JAERI, who gave them a lot of useful comments on JNDC FP library and also on DCHAIN and FPGS codes. They also would like to thank Dr. Takeo Adachi and the other members of Dissolution Study Group in the Department of Chemistry, JAERI, who gave them information about the PWR spent fuel analysis.

References

1) Tsuchihashi K., Ishiguro Y., Kaneko K. and Ido M.: "Revised SRAC Code System", JAERI 1302 (1986).
2) Ishiguro Y., Tsuchihashi K. and Sasaki M.: "Physics Problems on Analysis of High Conversion Pressurized Water Reactor (HCPWR) with Tighter Pitch Lattices (An Analysis of PROTEUS-LWHCR Cores by SRAC System)", JAERI-M 84-180 (1984) (in Japanese).
3) Ishiguro Y.: "PEACO-II: A Code for Calculation of Effective Cross Section in Heterogeneous Systems", JAERI-M 5527 (1974).
4) Fowler T.B. and Vondy D.R.: "Nuclear Reactor Core Analysis Code: CITATION", ORNL-TM-2496 (1969).
5) Akie H., Ishiguro Y. and Takano H.: "Summary Report on the International Comparison of NEACRP Burnup Benchmark Calculations for High Conversion Light Water Reactor Lattices", JAERI-M 88-200 (NEACRP L-309) (1988).
6) Vallée A., Millot J.P. and Bruna G.: "The FRAMATOME RCVS Concept and Physics", Proc. ENC '86, Geneva, 2, 477 (1986).
7) Garrison J.D. and Roos B.W.: "Fission-Product Capture Cross Sections", Nucl. Sci. Eng., 12, 115 (1962).
8) Iijima S., Yoshida T. and Yamamoto T.: "Fission Product Model for BWR Lattice Calculation Code", J. Nucl. Sci. Technol., 19, 96 (1982).
9) Takano H., Ihara H. and Akie H.: "Group Cross Sections of Fission Products and Minor Actinides", Proc. 1986 Seminar on Nuclear Data, p.121, JAERI-M 87-025 (NEANDC(J)-123/U, INDC (JPN)-109/L) (1987).
10) Tasaka K.: "DCHAIN: Code for Analysis of Build-up and Decay of Nuclides", JAERI 1250 (1977).
11) Takano H. and Akie H.: "Effect of Transplutonium Nuclides on Burnup Reactivity Changes in HCLWRs", J. Nucl. Sci. Technol., 24, 501 (1987).
12) Tasaka K., Ihara H., Akiyama M., Yoshida T., Matsumoto Z. and Nakasima R.: "JNDC Nuclear Data Library of Fission Products", JAERI 1287 (1983).
13) Ihara H. (Ed.) : "Tables and Figures from JNDC Nuclear Data Library of Fission Products, Version 2", JAERI-M 89-204 (NEANDC (J) -145/U, INDC (JPN) -132/1) (1989).
14) Tsuchihashi K., Takano H., Horikami K., Ishiguro Y., Kaneko K. and Hara T.: "SRAC: JAERI Thermal Reactor Standard Code System for Reactor Design and Analysis", JAERI 1285 (1983).
15) Takano H., Kaneko K. and Akie H.: "SRACLIB-JENDL2: Group Constants Library for Thermal Reactor Analysis Code System SRAC", Reactor Engineering Department Annual Report (April 1, 1986 - March 31, 1987), p.5, JAERI-M 87-126 (1987).
16) Takano H., Hasegawa A. and Kaneko K.: "TIMS-PGG: A Code System for Producing Group Constants in Fast Neutron Energy Region", JAERI-M 82-072 (1982) (in Japanese).
17) Takano H., Ishiguro Y. and Matsui Y.: "TIMS-1: A Processing Code for Production of Group Constants of Heavy Resonant Nuclei", JAERI 1267 (1980).
18) Takano H.: "MCROSS-2: A Code for Calculation of Effective Cross Sections", JAERI-M 4721 (1972).
19) Cullen D.E.: UCRL-50400, 17, Part A-C (1979).
20) Takano H., Kaneko K., Akie H. and Ishiguro Y.: "The Effect of Fission Products on Burnup Characteristics in High Conversion Light Water Reactors", Nucl. Technol., 80, 250 (1988).
21) Nakahara Y. et al.: "Amount of Nuclides Constituting PWR Spent Fuels, Comparison of Observed

with Calculated Values", Radiochimica Acta, 50, 141 (1990).

22) Adachi T. et al.: "Dissolution Studies of Spent Nuclear Fuels", JAERI-M 91-010 (1991) (in Japanese).

23) Croff A.G.: "ORIGEN2 - A Revised and Updated Version of the Oak Ridge Isotope Generation and Depletion Code", ORNL-5621, ORNL (1980).

24) Takano H. et al.: Private communication (1988).

25) Ihara H. et al.: Private communication (1988).

26) Akie H. and Takano H.: "Effect of Fission Gas Release on Burnup Characteristics and Void Reactivity in HCLWRs", J. Nucl. Sci. Technol., 24, 668 (1987).

27) Meyer R.O., Beyer C.E. and Voglewede J.C.: "Fission-Gas Release from Fuel at High Burnup", Nucl. Safety, 19, 699 (1978).

28) Okumura K. and Ishiguro Y.: "Note on Burnup Calculation of Pu Isotopes in Blanket Used in HCLWR", Reactor Engineering Department Annual Report (April 1, 1987 - March 31, 1988), p.74, JAERI-M 88-221 (1988).

Appendix I Input Instructions for SRAC Cell Burnup Calculation

Input instructions for SRAC cell burnup are shown here. Although the instructions specified in Ref. 1 are still valid, several new functions described in Chapter 6 become available.

The input for cell burnup calculation is minimized because the information such as chain scheme, yield, decay constant, power per fission, etc. is compiled in the burnup library. The user can still choose the chain schemes which are stored in separate libraries (see Appendix II).

Following input data are required if IC20>0 in the general control input of the case.

BLOCK 1 Control integers /3/

NEP Number of burnup steps to modify the effective microscopic cross sections for burnable nuclides ($\leqq$15). Remind that the cell calculation of the final step is skipped.

New: When a negative NEP value is specified, constant flux burnup process will be perfo-rmed.

Note: If NMAT in material specification is specified by a negative number, the atomic number densities at the final step will be stored on FT07F001 so as to be used in the material specification in a restart run for the succeeding burnup step. At the end of each burnup step, an automated judgement is added to check whether or not the next cell burnup steps will terminate within the specified I/O limit.

IBUNIT Burnup unit to control exposure time
=0 MWD (megawatt-days)
=1 fraction of U-235 burnt

IBEDIT Edit control
=0 brief edit
=1 detailed edit
=2 edit in more detail for code testing

BLOCK 2 /2/

POWERL Whole core power in MW

CVOL The factor to yield the total amount of fuel volume in core, by multiplying it into the cell volume. For example, in a one dimensional calculation of a cell of a fuel plate, the thickness of fuel meat stands for the fuel volume, then the factor is the product of width $\times$ height of fuel plate $\times$ number of fuel plate in the core.

New: Negative CVOL value deactivates depletion calculations, but a sequential cell calculations will be performed by using the burnup dependent atomic number densities of depleting nuclides stored in MACRO file (see BLOCK 4).

The ratio of the above two items is used to get absolute neutron flux, then any common factor to the above two may be multiplied. For example, the term 'core' appearing in this item can be read as 'fuel element' or 'assembly'.

BLOCK 3 / | NEP | /

PERIOD Burnup steps in ascending order without counting the initial step, in the unit specified by IBUNIT.

BLOCK 4 Required if CVOL<0 /A4/

CASE

New: Case name to specify the member 'CASE'NDEN in MACRO file which contains atomic number densities of depleting nuclides.

Appendix II Chain Model and Data Library

Several burnup libraries are installed in the SRAC system for the optional use of chain models. The data for main models are

'J3973.BURN.DATA (ACTINID4)' ··· 17 actinides + Iijima's FP chain,
'J3973.BURN.DATA (CHAIN66Y)' ··· 17 actinides + chain of 65 FPs,
'J3973.BURN.DATA (SIMPLEE)' ··· 17 actinides + simple FP chain,

and these data are read from FT50F001. These data contain nuclide table, chain description data and FP yield data. The data for Takano's chain (CHAIN66Y) are described here (Tables II-1 and II-2).

(1) Nuclide table

This table shows the ID number, ID name, fissile indicator, resonance indicator, decay constant and fission energy of each nuclide. Heavy nuclides are tabulated first, and absorber nuclides and FP nuclides follow. The ID name P67 in the Table II-1 shows the pseudo FP nuclide for Takano's FP chain.

(2) Chain description

After the nuclide table, there are data for chain description. The data contain heavy nuclide chains, absorber chains and FP chains. Each burnup chain is expressed by a series of signed integers of three digits. The heavy nuclide and FP chains are shown in Chapter 3. The absorber chains are written as,

+003−001+026
+003+003+101+102+103
+003−001+027
+003−001+056
+003−001+028
+003−001+060
+003−001+059
+003+005+029+030+031+032+033 ,

which mean,

B-10→
Gd-155→Gd-156→Gd-157→
Ag-107→
Ag-109→
In-113→
In-115→
Cd-113→
Hf-156→Hf-157→Hf-158→Hf-159→Hf-160→.

(3) FP yield

The final data is the FP yield table. A part of the table is shown in Table II-2.

Table II-1 Nuclide table in the burnup data of Takano's chain

NO	NUC	FIS	RES	DECAY CONST. (1/SEC)	J/FISS.	NO	NUC	FIS	RES	DECAY CONST. (1/SEC)	J/FISS.
1	TH8	0	0	0.0	3.11241E-11	54	PD8	0	0	0.0E-00	0.0
2	TH0	1	0	0.0	3.11241E-11	55	PD9	0	0	1.4305E-05	0.0
3	TH2	1	2	0.0	3.11241E-11	56	AG9	0	2	0.0E-00	0.0
4	PA1	0	0	0.0	3.11241E-11	57	CD0	0	0	0.0	0.0
5	PA2	0	0	6.0777E-06	3.11241E-11	58	CD1	0	0	0.0	0.0
6	PA3	1	2	2.9713E-07	3.11241E-11	59	CD3	0	0	2.3618E-24	0.0
7	U02	0	0	3.0506E-10	3.20950E-11	60	IN5	0	0	4.3069E-23	0.0
8	U03	1	2	0.0	3.20950E-11	61	I07	0	0	0.0	0.0
9	U04	1	2	0.0	3.20950E-11	62	I09	0	0	1.3991E-15	0.0
10	U05	1	2	0.0	3.24635E-11	63	I01	0	0	9.9782E-07	0.0
11	U06	1	2	0.0	3.24635E-11	64	I03	0	0	9.2568E-06	0.0
12	U08	1	2	0.0	3.29922E-11	65	I05	0	0	2.9129E-05	0.0
13	PU8	1	0	0.0	3.29922E-11	66	XE1	0	0	0.0E-00	0.0
14	PU9	1	2	0.0	3.39167E-11	67	XE2	0	0	0.0E-00	0.0
15	PU0	1	2	0.0	3.39167E-11	68	XE3	0	0	1.5165E-06	0.0
16	PU1	1	2	1.49421E-09	3.42003E-11	69	XE5	0	2	2.1205E-05	0.0
17	PU2	1	2	5.84174E-14	3.42003E-11	70	XE6	0	0	0.0	0.0
18	NP7	0	0	0.0	0.0	71	CS3	0	0	0.0E-00	0.0
19	NP8	0	0	3.7842E-06	0.0	72	CS4	0	0	1.0652E-08	0.0
20	NP9	1	2	3.40659E-06	3.29922E-11	73	CS5	0	0	9.5500E-15	0.0
21	AM1	1	2	0.0	3.42003E-11	74	LA9	0	0	0.0	0.0
22	AMM	1	2	1.44506E-10	3.42003E-11	75	CE1	0	0	2.4776E-07	0.0
23	AMG	1	2	1.20262E-05	3.42003E-11	76	PR1	0	0	0.0	0.0
24	AM3	1	2	0.0	3.42003E-11	77	PR3	0	0	5.9077E-07	0.0
25	CM4	1	2	1.21286E-09	3.42003E-11	78	ND3	0	0	0.0E-00	0.0
26	B00	0	0	0.0	0.0	79	ND4	0	0	0.0	0.0
27	AG7	0	2	0.0	0.0	80	ND5	0	0	0.0E-00	0.0
28	IN3	0	2	0.0	0.0	81	ND6	0	0	0.0	0.0
29	HF6	0	2	0.0	0.0	82	ND7	0	0	7.2537E-07	0.0
30	HF7	0	2	0.0	0.0	83	ND8	0	0	0.0	0.0
31	HF8	0	2	0.0	0.0	84	PM7	0	0	8.3740E-09	0.0
32	HF9	0	2	0.0	0.0	85	PMM	0	0	1.9425E-07	0.0
33	HF0	0	2	0.0	0.0	86	PMG	0	0	1.4939E-06	0.0
34	KR3	0	0	0.0E-00	0.0	87	PM9	0	0	3.6273E-06	0.0
35	ZR3	0	0	1.4356E-14	0.0	88	PM0	0	0	7.1364E-05	0.0
36	ZR5	0	0	1.2525E-07	0.0	89	PM1	0	0	6.7796E-06	0.0
37	ZR6	0	0	0.0	0.0	90	SM7	0	0	0.0E-00	0.0
38	M05	0	0	0.0	0.0	91	SM8	0	0	0.0E-00	0.0
39	M07	0	0	0.0	0.0	92	SM9	0	2	0.0E-00	0.0
40	M08	0	0	0.0	0.0	93	SM0	0	0	0.0E-00	0.0
41	M09	0	0	2.9164E-06	0.0	94	SM1	0	0	2.4406E-10	0.0
42	M00	0	0	0.0	0.0	95	SM2	0	0	0.0E-00	0.0
43	TC9	0	0	1.0264E-13	0.0	96	EU3	0	0	0.0E-00	0.0
44	RU1	0	0	0.0E-00	0.0	97	EU4	0	0	2.5541E-09	0.0
45	RU2	0	0	0.0E-00	0.0	98	EU5	0	0	4.4285E-09	0.0
46	RU3	0	0	2.0347E-07	0.0	99	EU6	0	0	5.2815E-07	0.0
47	RU4	0	0	0.0	0.0	100	GD4	0	0	0.0E-00	0.0
48	RU5	0	0	4.3365E-05	0.0	101	GD5	0	2	0.0E-00	0.0
49	RH3	0	0	0.0E-00	0.0	102	GD6	0	0	0.0E-00	0.0
50	RH5	0	0	5.4450E-06	0.0	103	GD7	0	2	0.0E-00	0.0
51	PD5	0	0	0.0E-00	0.0	104	GD8	0	0	0.0E-00	0.0
52	PD6	0	0	0.0E-00	0.0	105	P67	0	0	0.0E-00	0.0
53	PD7	0	0	3.3792E-15	0.0						

Table II-2 FP yield data of Takano's chain (CHAIN66Y)

	TH2	U03	U05	U06	U08	PU9	PU0	PU1	PU2
KR3	2.1953-2	1.0175-2	5.3805-3	5.2213-3	3.8660-3	2.9500-3	3.0268-3	2.1189-3	2.3952-3
ZR3	6.7555-2	7.0151-2	6.3902-2	5.6995-2	5.0009-2	3.8963-2	3.7797-2	3.0940-2	3.1366-2
ZR5	0.0	0.0	0.0	0.0	0.0	0.0	0.0	0.0	0.0
ZR6	4.3891-2	5.6500-2	6.2641-2	5.7342-2	5.9091-2	5.0665-2	4.9142-2	4.5935-2	4.4747-2
MO5	5.3751-2	6.1907-2	6.4962-2	6.4114-2	5.1068-2	4.8948-2	4.3966-2	4.0745-2	4.0226-2
MO7	4.4922-2	5.4955-2	6.0082-2	5.1439-2	5.5746-2	5.4452-2	5.1983-2	4.9117-2	4.8829-2
MO8	3.6643-2	5.1283-2	5.7083-2	5.7390-2	5.7467-2	5.7885-2	5.4285-2	5.0864-2	5.1347-2
MO9	2.8730-2	4.8663-2	6.1105-2	5.8731-2	6.1957-2	6.1403-2	5.9743-2	6.2335-2	5.3617-2
MOO	1.3926-2	4.4162-2	6.2323-2	5.6126-2	6.6998-2	6.8263-2	6.0689-2	6.1738-2	5.6562-2
TC9	9.272-11	1.3934-7	1.4447-8	2.5410-9	9.972-11	1.0473-7	1.6512-8	2.8408-9	1.3010-9
RU1	7.2941-3	3.2306-2	5.0814-2	5.2910-2	6.0822-2	5.8979-2	6.0517-2	6.0042-2	5.8836-2
RU2	3.7256-3	2.4497-2	4.2331-2	4.9273-2	6.3198-2	5.9646-2	6.0806-2	6.3827-2	5.8254-2
RU3	1.5246-3	1.6696-2	3.0274-2	4.2030-2	6.2096-2	6.9500-2	6.7119-2	6.1440-2	5.8768-2
RU4	9.1023-4	1.0305-2	1.8397-2	3.3781-2	5.0233-2	5.9263-2	5.9193-2	6.9098-2	5.8423-2
RU5	4.5722-4	4.8220-3	9.6384-3	2.4569-2	3.9393-2	5.3513-2	5.5327-2	6.1073-2	5.6422-2
RH3	8.205-15	3.240-10	3.321-11	5.897-12	1.787-13	8.373-10	1.647-10	1.056-11	5.046-12
RH5	1.005-11	8.5665-8	1.7006-8	9.2299-9	7.053-10	5.2317-7	2.1032-7	2.5867-8	1.2950-8
PD5	1.694-16	1.180-11	9.998-13	2.800-13	3.2638-9	5.752-11	1.730-11	9.263-13	5.030-13
PD6	4.4586-4	2.5881-3	4.0232-3	1.0185-2	2.5311-2	4.2856-2	4.9763-2	6.2505-2	5.3331-2
PD7	5.1679-4	1.1734-3	1.4028-3	9.2282-3	1.2961-2	3.3610-2	4.1507-2	5.2011-2	5.0132-2
PD8	6.2066-4	6.3107-4	6.6938-4	3.4485-3	5.9875-3	2.1685-2	3.0307-2	3.9253-2	4.2146-2
PD9	0.0	0.0	0.0	0.0	0.0	0.0	0.0	0.0	0.0
AG9	6.0924-4	4.4238-4	3.4482-4	1.4347-3	2.6844-3	1.8795-2	1.7948-2	2.2616-2	3.2568-2
CD0	4.947-11	2.6694-8	2.5404-9	1.8476-9	8.843-11	3.8287-7	2.0799-7	2.4556-8	2.6571-8
CD1	7.0940-4	1.9207-4	2.0022-4	6.5255-4	8.0205-4	3.0360-3	5.0300-3	5.6990-3	1.2820-2
CD3	8.4926-4	1.3444-4	1.6075-4	3.7524-4	5.1827-4	6.4120-4	1.5713-3	1.4358-3	3.0292-3
IN5	6.9082-4	1.1799-4	1.0763-4	5.1106-4	3.3774-4	3.5648-4	6.6229-4	4.2137-4	1.0219-3
I07	8.9620-4	5.6175-3	1.2466-3	2.2358-3	1.2606-3	4.8955-3	4.1825-3	2.2853-3	3.0361-3
I09	3.7227-3	1.5071-2	7.1785-3	9.8263-3	9.9976-3	1.3934-2	1.0516-2	7.3582-3	8.2300-3
I01	1.6227-2	3.6061-2	2.8843-2	3.0369-2	3.2386-2	3.8466-2	3.5451-2	2.8453-2	3.1872-2
I03	0.0	0.0	0.0	0.0	0.0	0.0	0.0	0.0	0.0
I05	5.3140-2	4.9125-2	6.2897-2	5.6165-2	6.7830-2	6.4468-2	6.7436-2	7.0544-2	6.8895-2
XE1	9.552-11	1.0626-6	4.2790-8	5.5299-9	4.145-11	6.8622-7	1.2851-7	6.4018-9	1.0040-8
XE2	2.8888-2	4.9387-2	4.2999-2	4.3073-2	5.1465-2	5.3931-2	4.8070-2	4.2201-2	4.5674-2
XE3	3.9585-2	6.0224-2	6.7019-2	7.0259-2	6.6065-2	6.9756-2	7.0056-2	6.7696-2	6.5925-2
XE5	3.0888-4	1.2830-2	2.4192-3	1.5847-3	2.7948-4	1.1524-2	6.9843-3	2.3140-3	2.6443-3
XE6	5.6502-2	7.0140-2	6.3059-2	6.4034-2	6.8506-2	6.6256-2	6.7476-2	6.6645-2	6.8760-2
CS3	2.971-11	3.7285-7	8.3481-9	2.2500-9	2.543-11	2.6509-7	4.2504-8	2.5207-9	2.6400-9
CS4	4.2210-9	1.3204-5	1.2697-7	1.7100-7	3.1437-9	9.8932-6	1.8202-6	1.8505-7	1.4800-7
CS5	2.3006-7	1.8555-4	2.0825-5	4.2900-6	1.8021-7	1.5883-4	4.4124-5	6.7119-6	5.7601-6
LA9	7.0833-2	6.3324-2	6.3524-2	5.8461-2	5.9033-2	5.6176-2	5.8709-2	5.8972-2	6.0123-2
CE1	7.3355-2	6.5310-2	5.7967-2	5.5461-2	5.4832-2	5.2576-2	4.7649-2	4.9664-2	5.1098-2
PR1	1.950-14	9.506-10	1.730-11	1.180-12	4.555-15	4.041-10	3.050-11	1.790-12	1.190-12
PR3	6.5327-2	5.8921-2	5.9388-2	6.0885-2	4.5666-2	4.4286-2	4.7210-2	4.7067-2	4.6800-2
ND3	1.489-15	1.339-10	2.060-12	1.220-13	4.018-16	3.651-11	3.740-12	1.750-13	1.220-13
ND4	0.0	0.0	0.0	0.0	0.0	0.0	0.0	0.0	0.0
ND5	5.2846-2	3.3918-2	3.9175-2	3.6682-2	3.7559-2	2.9915-2	3.2772-2	3.3438-2	3.4669-2
ND6	0.0	0.0	0.0	0.0	0.0	0.0	0.0	0.0	0.0
ND7	3.0105-2	1.7499-2	2.2533-2	2.3407-2	2.5298-2	2.0428-2	2.2329-2	2.3678-2	2.4193-2
ND8	1.9789-2	1.2720-2	1.6695-2	1.7405-2	2.0816-2	1.6347-2	1.9150-2	1.9898-2	2.0633-2
PM7	2.891-12	2.0192-8	9.458-10	9.910-11	1.091-12	1.4505-8	7.886-11	1.560-10	9.640-11
PMM	1.082-10	9.0294-9	7.819-11	3.0069-9	5.904-11	2.3624-7	3.5560-8	4.6896-9	2.6865-9
PMG	3.970-11	3.8553-9	3.339-11	1.1030-9	2.166-11	1.0087-7	1.3045-8	2.0023-9	9.855-10
PM9	8.8231-3	7.7702-3	1.0664-2	1.3684-2	1.6076-2	1.2392-2	1.3692-2	1.5233-2	1.6145-2
PM0	0.0	0.0	0.0	0.0	0.0	0.0	0.0	0.0	0.0
PM1	3.1403-3	3.1525-3	4.1838-3	4.2264-3	8.0064-3	7.7195-3	8.4315-3	9.3682-3	1.0247-2
SM7	7.278-18	1.010-12	1.520-14	8.444-16	2.167-18	5.522-13	5.272-14	2.249-15	3.462-16
SM8	1.923-15	8.656-11	1.960-12	1.260-13	8.052-16	5.432-11	4.450-12	2.621-13	1.970-13
SM9	1.680-13	3.0187-9	1.110-10	1.140-11	1.392-13	2.6809-9	2.640-10	2.161-11	1.680-11
SMO	3.7017-8	2.8022-5	3.0415-7	1.2505-6	8.0108-8	1.1584-5	1.1404-5	2.7821-6	1.7912-6
SM1	3.031-10	7.1071-7	7.1984-8	9.8399-9	5.126-10	1.1204-6	2.2002-7	3.4110-8	3.1000-8
SM2	7.5904-4	2.1355-3	2.6783-3	3.8775-3	5.2075-3	5.8517-3	6.5758-3	7.4659-3	8.3476-3
EU3	3.3245-4	1.0478-3	1.6135-3	2.5533-3	4.1095-3	3.6369-3	5.7967-3	5.4816-3	6.5542-3
EU4	2.111-11	2.2791-7	2.6894-8	8.7299-9	3.444-10	9.2230-7	1.7402-7	3.6210-8	2.2800-8
EU5	3.8256-5	2.1792-4	3.2044-4	9.2283-4	1.3266-3	1.6547-3	2.4760-3	2.4167-3	3.6772-3
EU6	2.5623-5	1.1311-4	1.3186-4	3.3648-4	6.7481-4	1.1838-3	1.7543-3	1.7606-3	2.6566-3
GD4	9.414-16	1.629-10	6.569-12	8.950-13	1.572-14	4.912-10	5.310-11	4.751-12	4.100-12
GD5	3.711-14	1.6593-9	8.578-11	2.850-11	6.227-13	7.1523-9	1.4501-9	1.230-10	1.450-10
GD6	9.532-13	1.1295-8	7.998-10	2.930-10	1.292-11	7.1823-8	2.0402-8	2.3106-9	2.9400-9
GD7	9.5656-6	6.3270-5	6.1534-5	2.3080-4	3.8719-4	7.4098-4	1.3040-3	1.3716-3	1.8392-3
GD8	5.0393-6	2.3144-5	2.9159-5	1.1079-4	1.7299-4	4.0738-4	8.5032-4	8.6248-4	1.2261-3
P67	1.1456+0	9.4341-1	8.4951-1	8.0845-1	6.9251-1	6.1787-1	6.1070-1	5.9261-1	6.0192-1

For example, 2.1953-2 is read as 2.1953×10^{-2}.

Appendix III Table of Isotopes Contained in SRACLIB-JENDL2

Table III-1 Nuclides in SRACLIB-JENDL2

nucl.	reso.	fast	thermal	nucl.	reso.	fast	thermal
Ag-107		f	1	Gd-160		f	1
Ag-109	B	f	1	H-1		iU	9 P
Al-27		f	BP	Hf nat.	B	f	1 f
Am-241	B	f	Bf	Hf-174	B	f	1
Am-242		f	Bf	Hf-176	B	f	1
Am-242m		f	Bf	Hf-177	B	f	B f
Am-243	B	f	Bf	Hf-178	B	f	1
B-10		f	B	Hf-179	B	f	1
Be-9		f	BP	Hf-180	B	f	1
C-12		f	AP	I-127		f	1
Ca nat.		f	1	I-129		f	1
Cd-110		f	1	In-115		f	1 f
Cd-111		f	1	Kr-83		f	1
Cd-112			1	Kr-84			1
Cd-113		f	1	Kr-85			1
Cd-114			1	Kr-86			1
Cd-116			1	La-139		f	1
Ce-140			1	Li-6		f	1
Ce-142			1	Li-7		f	1
Ce-144			1	Mn-55		f	B
Cm-242		f	Bf	Mo nat.		f	B
Cm-243		f	1f	Mo-94			1
Cm-244	B	f	Bf	Mo-95		f	1
Cm-245		f	1f	Mo-96			1
Co-59		f	1	Mo-97		f	1
Cr nat.		f	B	Mo-98		f	1
Cs-133		f	1	Mo-100		f	1
Cs-135		f	1	Mo-102		f	1
Cs-137			1	Na-23		f	B
Cu nat.		f	B	Nb-93		f	1
Cu-63		f	1	Nd-142			1
Cu-65		f	1	Nd-143		f	1
D-2		f	9P	Nd-144			1
Eu-151			1	Nd-145		f	1
Eu-152			1	Nd-146			1
Eu-153		f	1f	Nd-148		f	1
Eu-154		f	1	Nd-150			1
Eu-155		f	1f	Ni nat.		f	B
F-19		f	1	Np-237	B	f	1 f
Fe nat.		f	B	Np-239		i	B f
Gd-155		f	1f	P47		i	1
Gd-156		f	1	P67		i	1
Gd-157		f	1	Pa-233		f	B f
Gd-158		f	1	Pb nat.		f	B

reso. : ultra fine energy mesh cross sections in the resonance region, f: f-table, i: no f-table, P:P_1 matrix, U: P_1～P_5 matrices, 1～9, A and B: temperature indices in Table III-2, blank: no data, P47 and P67: pseudo FP nuclides

Table III-1 (Continued)

nucl.	reso.	fast	thermal	nu	nucl.	reso.	fast	thermal
Pd-104			1		Sm-152		f	1
Pd-105		f	1		Sm-154			1
Pd-106		f	1		Sr-86			1
Pd-107		f	1		Sr-87			1
Pd-108		f	1		Sr-88			1
Pd-110			1		Sr-90			1
Pm-147		f	1		Ta-181		f	B
Pr-141		f	1		Tb-159			1
Pu-236		f	1f		Tc-99		f	1
Pu-238		f	1f		Te-128			1
Pu-239	B	f	Bf		Th-228		f	1f
Pu-240	B	f	Bf		Th-230		f	1f
Pu-241	B	f	Bf		Th-232	B	f	B
Pu-242	B	f	Bf		Th-233		f	1
R16		i	1		Th-234		f	1
R56		i	1		U-233	B	f	Bf
R86		i	1		U-234	B	f	B
R96		i	1		U-235	B	f	Bf
Rb-85			1		U-236	B	f	B
Rb-87			1		U-238	B	f	B
Rh-103		f	1		V-51		f	B
Ru-101		f	1		Xe-131		f	1
Ru-102		f	1		Xe-132		f	1
Ru-103		i	1		Xe-133		i	1
Ru-104		f	1		Xe-134			1
Ru-106			1		Xe-135		f	1
Sb-121		f	1		Xe-136		i	1
Sb-123		f	1		Y-89		f	1
Sb-124			1		Zr-90			1
Si nat.		f	B		Zr-91			1
Sm-147		i	1f		Zr-92			1
Sm-148		i	1		Zr-93		f	1
Sm-149		f	1		Zr-94			1
Sm-150		f	1		Zr-95			1
Sm-151		f	1		Zr-96		f	1

reso. : ultra fine energy mesh cross sections in the resonance region, f: f-table, i: no f-table, P: P_1 matrix, U: P_1~P_5 matrices, 1~9, A and B: temperature indices in Table III-2,
blank: no data, R16, R56, R86 and R96: pseudo FP nuclides

Table III-2 Temperature indices

index	temp.	index	temp.	index	temp.	index	temp.
1	300K	4	400K	7	550K	A	1200K
2	325K	5	450K	8	600K	B	1600K
3	350K	6	500K	9	900K		